DESIGN AND ANALYSIS OF FEEDBACK AND FEEDFORWARD CONTROL SYSTEMS FOR WEB TENSION IN ROLL-TO-ROLL MANUFACTURING

By

PRAMOD RAJARAM RAUL

Bachelor of Engineering in Mechanical Engineering
Government College of Engineering
Pune, India
2002

Master of Science in Mechanical and Aerospace Engineering
Oklahoma State University
Stillwater, Oklahoma, USA
2010

Submitted to the Faculty of the
Graduate College of the
Oklahoma State University,
in partial fulfillment of
the requirements for
the Degree of
DOCTOR OF PHILOSOPHY
May, 2015

DESIGN AND ANALYSIS OF FEEDBACK AND FEEDFORWARD CONTROL SYSTEMS FOR WEB TENSION IN ROLL-TO-ROLL MANUFACTURING

Dissertation Approved:

Dr. Prabhakar R. Pagilla

Dissertation Adviser

Dr. Karl N. Reid

Dr. Girish Chowdhary

Dr. R. Russell Rhinehart

ACKNOWLEDGMENTS

I wish to express my sincerest appreciation to my advisor, Dr. P. R. Pagilla for his valuable guidance, inspiration, intelligent supervision, and friendship during my graduate program. I am forever indebt to him for his motivation and technical insights, allowing me to broaden my horizons in advanced control system and web handling processes.

I would like to extend my warmest thanks to my doctoral committee members: Dr. K. N. Reid, Dr. Girish Chowdhary, and Dr. R. R. Rhinehart for their support and guidance in completion of this research.

I would also like to thank my research colleagues at Oklahoma State University Aravind Seshadri, Carlo Branca, Diao Yu, Mauro Cimino, Yaowei Lu, Kadhim Jabbar, Shyam Konduri, Orlando Cobos and long time friend Nilesh Siraskar for their timely support and suggestions.

Finally and most deeply, I would like to express my appreciation to my mother, wife, son and family for their love, dedication, support, patience and inspiration throughout my life.

This work was supported by the Web Handling Research Center at Oklahoma State University and National Science Foundation under Grant Nos. 0854612 and 1246854.

Acknowledgements reflect the views of the author and are not endorsed by committee members or Oklahoma State University.

Name: PRAMOD R RAUL

Date of Degree: MAY, 2015

Title of Study: DESIGN AND ANALYSIS OF FEEDBACK AND FEEDFORWARD CONTROL SYSTEMS FOR WEB TENSION IN ROLL-TO-ROLL MANUFACTURING

Major Field: MECHANICAL AND AEROSPACE ENGINEERING

Abstract: In Roll-to-Roll (R2R) manufacturing, efficient transport of flexible materials (webs) on rollers requires simultaneous control of web speed and tension. Webs experience disturbing forces during transport due to nonideal machine elements and processes such as printing, coating, lamination, etc. Since rotating machine elements are employed, these disturbances are in the form of periodic oscillations in web tension and speed. Design of efficient model-based web tension and speed control systems employing both feedback and feedforward actions that can adapt to changes in parameters and reject periodic disturbances were investigated in this research. Tools from adaptive and robust control theory and singular perturbation method are utilized for the design and analysis of these control systems.

Model reference and relay feedback based adaptive Proportional-Integral (PI) tension control schemes were developed to regulate web tension; these schemes overcome the tedious tuning procedures required for fixed gain PI schemes when process parameters and conditions change. To directly control the roll speed when belt-pulley and gear transmissions are employed, a control scheme that uses both motor and load speed feedback is developed. In the presence of a compliant transmission system, it is shown that using pure load speed feedback must be avoided as it results in an unstable system. In situations where linearization of the nonlinear web tension governing equation is not possible due to changes in operating conditions, a nonlinear tension regulator is designed via a solution method employed in the nonlinear servomechanism problem. The feedforward action is synthesized by considering a discretized form of the tension governing equation in conjunction with adaptive estimation of periodic disturbance parameters. It is also shown that interaction between different subsystems of the R2R system may be minimized by employing feedforward action. The strategy of utilizing the tension signal from the web tension zone downstream of the driven roller is shown to result in minimization of propagation of disturbances into further downstream tension zones. To evaluate and compare the performance of the developed designs, experiments conducted on a large R2R platform for different web materials and transport conditions are discussed. Implementation guidelines are provided for ease of applying the designs to other industrial R2R machines.

TABLE OF CONTENTS

LIST OF TABLES

Table Page

LIST OF FIGURES

CHAPTER 1

Introduction

Many types of materials and consumer products are manufactured and processed by transporting flexible materials on rollers. Any continuous, flexible strip material that is considerably long compared to its width and considerably wide compared to its thickness is referred to as a web. Web processing can be found in many industries today, and it facilitates manufacturing of a variety of products from continuous, flexible strip materials. Examples include paper, textiles, plastic films, thin metals, polymers, and composites. Emerging and new consumer products such as flexible printed electronics, solar films, etc., are being manufactured using Roll-to-Roll (R2R) methods to meet the growing market demand.

Web handling is the study of transport of webs on rollers through processing machinery. Many times web materials need to pass through many consecutive processing sections during manufacturing of a product, for example printing, coating, drying, laminating, slitting, cleaning, etc. Web handling issues related to transporting the web through processing machinery should be addressed for better quality and increased quantity of finished products.

Web handling deals with a variety of challenges in the following areas: longitudinal dynamics and tension control, lateral dynamics and control, guiding, mechanics of winding and unwinding, wrinkling, air-web interaction, etc. Lateral and longitudinal web dynamics play an important role in web tension control and ultimately the quality of the finished product. The web behavior in the lateral direction (cross machine

direction) and the longitudinal direction (transport or machine direction) is influenced by characteristics of various mechanical components, modulus of web material, web damping, web slippage, and web tension. Web guiding systems control the web at the desired lateral position on the roller. The longitudinal dynamics is primarily characterized by web tension and transport speed which play an important role in web transport. There is a need to maintain web tension within a specified tolerance band to ensure accurate and smooth operation. The growing market and cost competitive environment demands for higher production rate and it is challenging for web handling engineers to achieve highest possible line speed. At the same time, control of roller speed at a desired reference is also important, as speed variations create undesired strain in the web and disrupt process quality.

Any typical web transport line consists of mechanical and electrical components, such as idle and driven rollers, unwind and rewind rolls, accumulator, guides, master speed roller, motors, motor drives, tension sensing elements, such as load cells, dancers, etc. These components are arranged in a particular manner to ensure transport of the web through the processing machine. The unwind section contains the roll that releases the material to the machine. An accumulator is used to store the material during roll change without interrupting the process. A web guide controls the lateral position of the web on the roller. The master speed roller sets the speed for the entire web line. During processing, a driven roller is used to control web speed as well as tension. Idle rollers are used to support the web. Web tension is measured by load cells mounted on an idle roller or through a mechanism called a dancer. A dancer is a device consisting of a roller and a mechanical platform which facilitates motion of the axis of rotation of the roller. A dancer can be pendulum type or translational type depending on the motion of the axis of rotation of the roller, which is

restrained by a force applied either by a pneumatic or hydraulic cylinder. This force is typically twice the desired tension when the angle of web wrap on the dancer roller is 180°. Dancers can be used as a means to set tension or sense tension fluctuation in web with its roller displacement. Once passing through various processes, the finished web is rewound on a roll in the rewind section. Figure 1.1 shows a large experimental platform called the Euclid Web Line (EWL) which is located in the Web Handling Research Center (WHRC) at Oklahoma State University. The EWL mimics many typical features of an industrial process line and consists of four sections: unwind, master speed, process, and rewind.

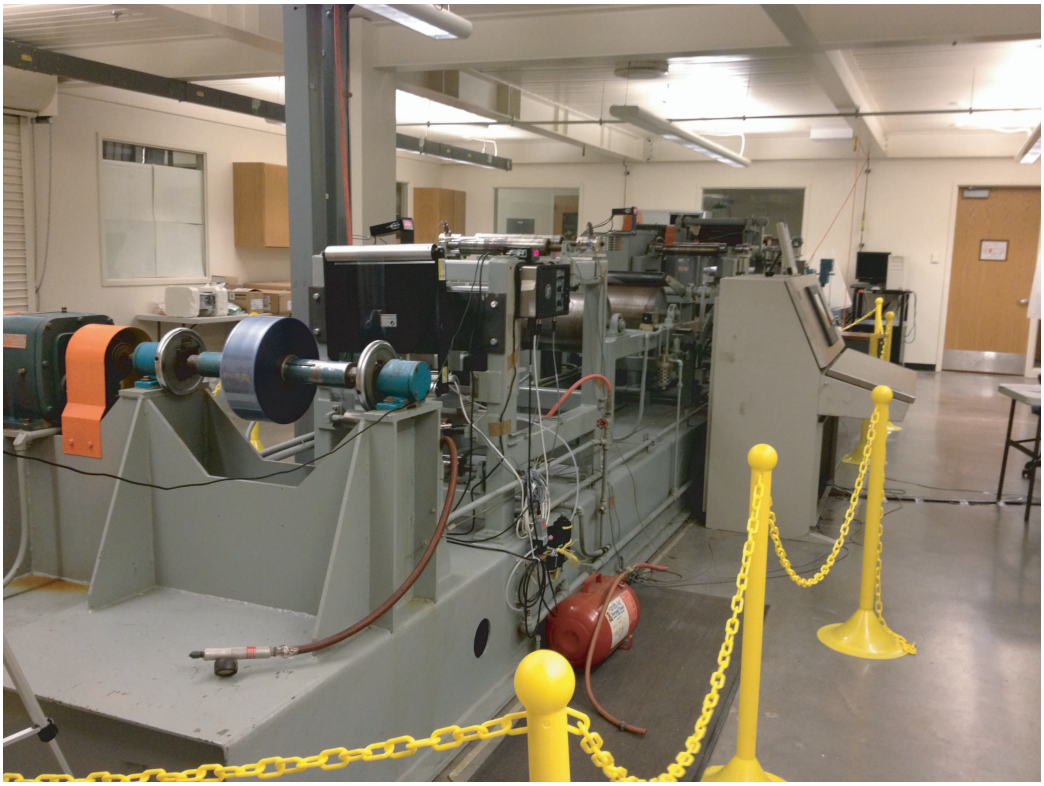

Figure 1.1: Euclid web processing line

Due to widespread use of roll-to-roll manufacturing in many sectors and the challenges in various fields that facilitate R2R manufacturing, there has been an increased

interest in studying web processing systems from various key aspects, such as process modeling, wrinkling, winding, control related issues, etc. Campbell [1], King [2], Brandenburg [3], and Shelton [4] laid fundamental background for the study of longitudinal dynamics of a moving web. The model that considers entering web span tension, was developed in King [2]. Brandenburg [3] and Shelton [4] assumed strain in the web to be very small and derived the governing equation for web tension in a span with the small strain assumption. An overview of the early research in longitudinal and lateral dynamic behavior and tension control can be found in Young and Reid [5]. Decentralized control and adaptive control design based on state space approach and its implementation for the web transport system is presented in Pagilla [6]. Tension control in multi span web system was described by Wolfermann [7] and Schroder [8]. Non-ideal effects such as moisture change and temperature variation on web tension were studied in Shin [9]. The focus of the current research is to develop accurate and effective feedback and feedforward tension control strategies for longitudinal web behavior to ensure efficient operation of web processing lines.

1.1 Motivation and Objectives

In R2R manufacturing of continuous materials, control of web tension is critical during transport of the materials through many processes such as printing, coating, lamination, etc. It plays an important role in ensuring the quality of the finished web products. During transport, many processes may require transport under different operating speeds and heating/cooling of the webs. Further, there are many process and machine induced disturbances which the tension control systems must compensate to achieve good tension regulation performance. Tension variations cause a variety of product defects. For example, high web tension may result in wrinkles and tears

while low tension may cause web slack, loss of traction on rollers during transport, and difficulty in guiding the webs on rollers. The consolidated effect of large web tension variations may result in disruption in production, diminishing product quality, and machine hardware damage. Accurate and effective tension control strategies for web handling systems are essential for efficient operation of web processing lines.

During transport, the web material undergoes a variety of dynamic conditions and changing surroundings. Different processing sections may require different levels of tension specifications. Hence, there is a need to develop adaptive and robust control techniques that provide desired performance under dynamic uncertainties during transport, such as changing web material, speed, and surrounding environment.

A control system can be designed to satisfy many performance indices, such as good transient responses, minimum steady state error, rejection of internal/external disturbances and measurement noises. Control systems can be made effective by designing both feedback and feedforward control actions as shown in Figure 1.2.

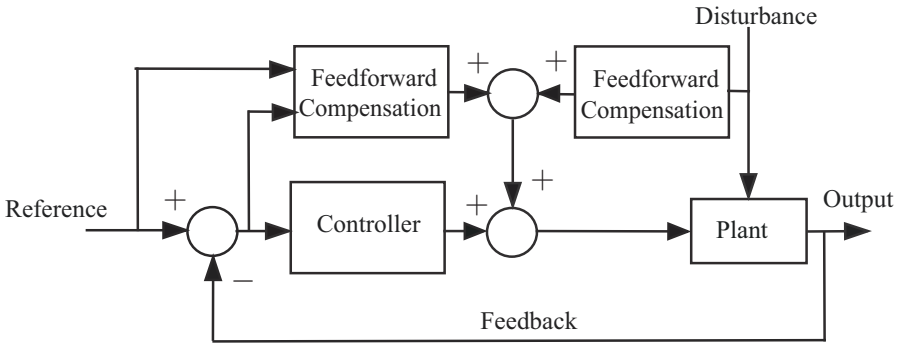

Figure 1.2: Control strategy employing both feedback and feedforward actions

Disturbances can be eliminated or attenuated by feedback. However, feedback control fails to take action until a deviation occurs in the controlled variable. Also, feedback control does not provide predictive action to compensate the effects of known or measurable disturbances. Further, the feedback action is less sensitive to variations

in the process model, whereas feedforward action can be dependent on the process model and hence more sensitive. In certain situations it may not be possible to measure the controlled variable, in these situations feedforward control may be employed. Feedforward action can be effectively used for disturbance rejection without knowing the plant model. It can be used for both linear and nonlinear systems. By using both feedback and feedforward actions one can improve the performance of a control system. In this research, the main objective is to investigate various feedback control schemes along with model based feedforward actions to regulate web tension as well as to reject disturbances generated by processes and process machines.

Industrial web tension control systems typically employ a fixed gain Proportional-Integral (PI) controller. The PI controller gains are tuned to give a stable response for a given operating condition and material. This is typically done empirically on the machine because analytical tuning of PI controllers is a challenging task due to changing operating conditions and uncertainty in the knowledge of web material parameters and machine parameters. In practice, the PI tension controllers are tuned on-site based on real-time observation of the tension response performance. When operating conditions or material properties change, the fixed gain PI tension controllers do not provide adequate performance or in some cases render the closed-loop tension control system unstable. The better approach is to use an adaptive control scheme that facilitates adjustment of controller parameters for such changing conditions. An adaptive controller can modify closed-loop system behavior by compensating for the changes in system parameters.

There are many approaches to design adaptive control schemes, such as gain scheduling, self-tuning regulators, and model reference adaptive control [10, 11]. The direct and indirect adaptive schemes are promising but the design and implementation of those controllers are cumbersome and provide many difficulties for practicing

engineers. For example, since many of these schemes are model based and the web system dynamic model is rather involved, the designs are complicated and result in a large number of estimated parameters. Simple adaptive control structures which mimic most of the features of the fixed gain PI schemes are desirable. These schemes can provide the automation to circumvent tuning under a wide variety of system parameter changes, and yet provide the ease of design and implementation.

Previously in [12], direct and indirect model reference adaptive control (MRAC) schemes for web tension control were considered. Although MRAC schemes are promising, the number of estimated parameters depends on the order of the process model. Control of web tension required estimation of six parameters, which could be cumbersome for practicing engineers in an industrial setting. There is a need for a simple adaptive scheme that resembles the implementation of an existing PI scheme. An adaptive PI scheme investigated in this research is discussed in Chapter 2.

The use of gear transmissions is essential in many applications due to the demand for speed reduction and variable torque transmission in many applications. For example, in automobiles, the need for a transmission is a result of the characteristics of the internal combustion engine. The transmission provides wide range of power and torque throughout the vehicle operation. Higher levels of torque are needed for starting of the engine or at low speed. On the other hand maximum power is needed at high speed. This varying need is satisfactorily performed by a speed reduction transmission system. In another application, in order to achieve high efficiency in ship transportation, the steam turbine should operate at a relatively higher range of its rotational speed. However, proper functioning of a propeller requires a relatively low speed range. For this reason, a reduction gear is used, which reduces the high speed motion of the steam turbine into low speed range required by the propeller. Hence, a transmission is necessary. In some applications belt-pulley transmissions are

employed in addition to a gear reduction system. Direct coupling for power transmission requires very accurate collinearity of the axes and takes considerable time and cost to assemble the unit. In such a scenario, a belt driven transmission provides great flexibility and small inaccuracies can be absorbed by the compliance in the belt. In R2R systems, typically a belt-pulley transmission coupled with a gear box is employed to transfer power from the motor shaft to the roll (load) shaft. The dynamics of the transmission system due to belt compliance and gear backlash introduce undesired web tension oscillations, especially during speed changes. The problem of load speed regulation and tension regulation when such transmissions are employed is discussed in Chapter 3.

In many situations of R2R manufacturing, the transient dynamic conditions due to web speed changes necessitate the consideration of nonlinear governing equations for the analysis and synthesis of control systems. Since many existing web tension control schemes rely on the linearization of the nonlinear equations which are used to either design linear or nonlinear adaptive controllers, tension transients due to speed changes and process variations are not controlled well. The nonlinear servomechanism web tension regulation problem is presented in Chapter 4. Existing work on the design of tension control systems used for the linearized R2R systems can be found in [13–16]. There is a need for a nonlinear tension control scheme that can simultaneously reject disturbances while providing improved tension regulation performance. Many web transport systems have non-ideal effects such as backlash in mechanical transmissions, out-of-round unwind/rewind rolls, eccentric rollers, and compliance in power transmitting shafts. These non-ideal effects together with rotating machinery generate periodic disturbances [17]. A nonlinear tension control scheme is expected to suppress these machine/process induced disturbances. It is also expected to achieve better steady state performance.

An R2R manufacturing system is a large scale interconnected system with subsystems such as unwind, rewind, and process sections. Disturbance propagation from upstream sections to downstream process sections may disrupt essential processes. There is a need to minimize the undesired interaction between subsystems and reduce propagation of disturbances. Control strategies to minimize interaction and disturbance propagation are discussed in Chapter 5.

The main goal of this research is to develop feedback and feedforward control strategies for web transport systems which are efficient and easy to implement. The following issues are addressed: develop efficient and easily implementable adaptive control schemes; propose control strategies to improve tension regulation and attenuate tension oscillations; develop control strategies to improve the performance of load speed regulation and apply it to improve web tension response. A research roadmap of this dissertation is provided in Figure 1.3.

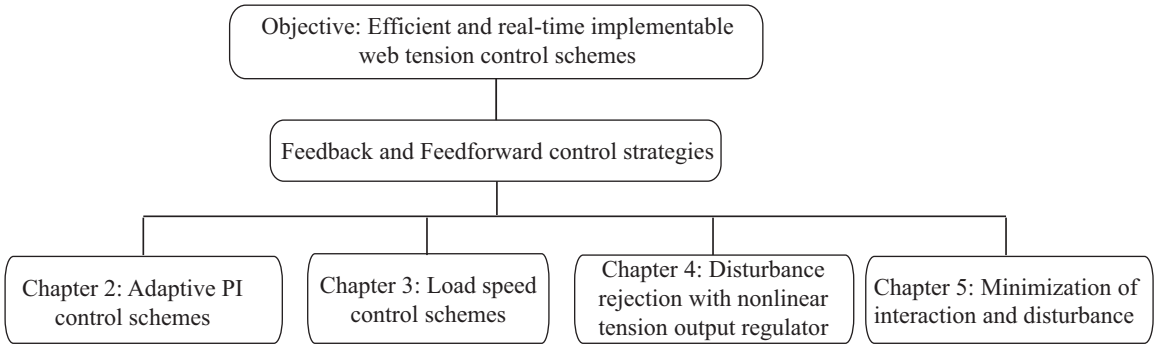

Figure 1.3: Research roadmap

1.2 Web Tension Control Schemes and Strategies

An R2R manufacturing system is a complex large-scale system which can be decomposed into a number of interconnected simpler subsystems. For large scale systems, two types of control strategies are used in general: centralized control and decen-

tralized control. Centralized control (shown in Figure 1.4) is complex in design and needs to handle large amounts of data from all the subsystems, though it may provide better performance. Also failure in any subsystem may disrupt the centralized system and make the overall system unstable or out of operation. In one form of decentralized control (shown in Figure 1.5), data related to neighboring subsystems is only required to generate control action and the implementation is relatively straightforward compared to centralized control. This study is focused on such decentralized control techniques. Different types of decentralized control schemes can be conceived for R2R manufacturing systems.

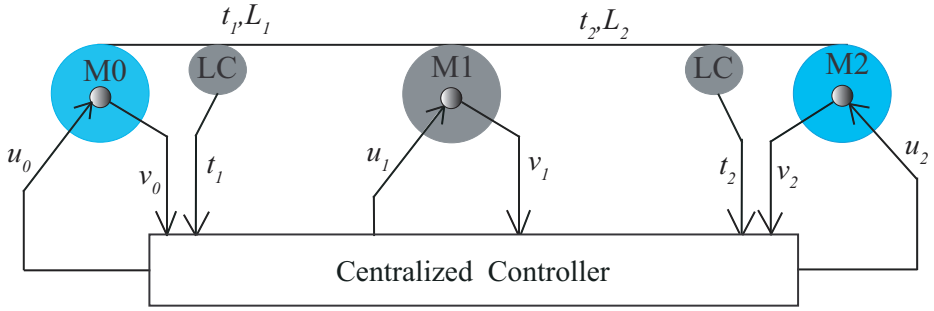

Figure 1.4: Centralized control scheme

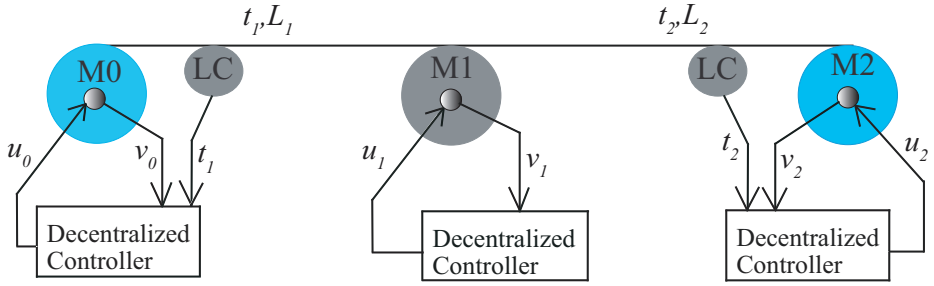

Figure 1.5: Decentralized control scheme

Two strategies are mainly used for web tension control: load-cell and dancer based feedback control systems. In a load-cell based tension control scheme, web tension measured by load cells mounted on idle rollers is used as feedback for the control

system. In the dancer based scheme, displacement of the dancer (either linear or rotational) due to web tension variations is sensed by a rotary variable differential transducer and used as feedback for the control system.

The commonly used control schemes in R2R systems are a two loop tension control scheme and a single loop pure speed control scheme. The two loop tension control scheme has speed control in the inner loop and tension control in the outer loop. In such a control system, there are two modes of control. One is the velocity mode, in which the inner-loop provides speed regulation and the outer-loop provides a correction to the reference speed based on either tension feedback from a load-cell or position feedback from a dancer. In the torque mode, the outer-loop provides a correction to the reference torque, based on tension feedback. The velocity mode and torque mode control strategies are shown in Figures 1.6 and 1.7. Second, in single

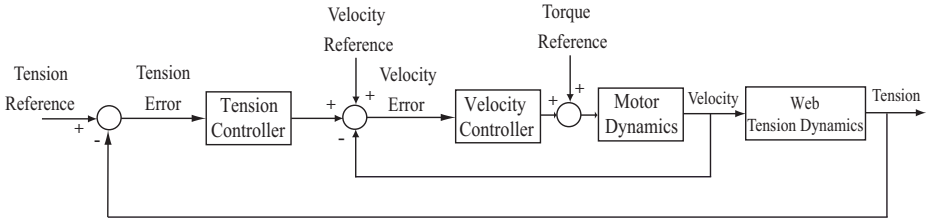

Figure 1.6: Cascaded loop control strategy: Velocity mode

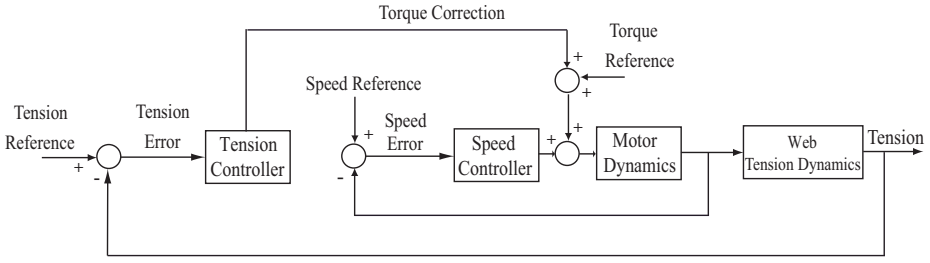

Figure 1.7: Cascaded loop control strategy: Torque mode

loop pure speed control, the roller speed is controlled with a single loop control strategy. Figure 1.8 represents the speed control scheme for a driven roller which is under

pure speed regulation.

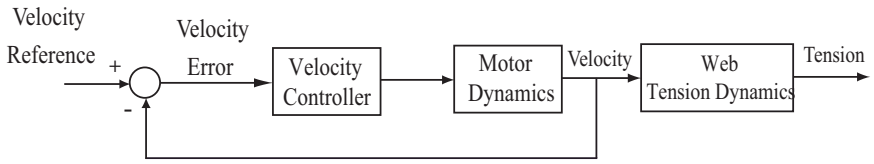

Figure 1.8: Single loop control strategy

Tension control is challenging at higher speeds and in the presence of web material properties variations, machine component non-idealities, and disturbances such as out of round roll, etc. The PI controller has been a mainstay in web control systems because of its simple structure. In recent years, there has been significant improvements in drive hardware and software. The advances in drive technology are making it possible to implement modern control algorithms that provides better performance over traditional PI controllers. Modern control algorithms can be designed to be robust and adaptable to changing scenarios of web transport systems, such as changing web material, transport speed, roll diameter, etc. Modern control algorithms also have the potential to provide better disturbance rejection as well as compensate for non-ideal effects.

1.3 Fixed Gain PI Control

A simple web transport system is considered in this section to discuss the web tension and speed control problem, shown in Figure 1.5. A fixed gain PI controller (feedback control scheme) is generally used to regulate tension and speed as shown in Figure 1.9. Although the PI control scheme has a simple structure, it requires extensive tuning to achieve the desired performance. Further, tuning must be performed every time there is a change in material properties or operating conditions.

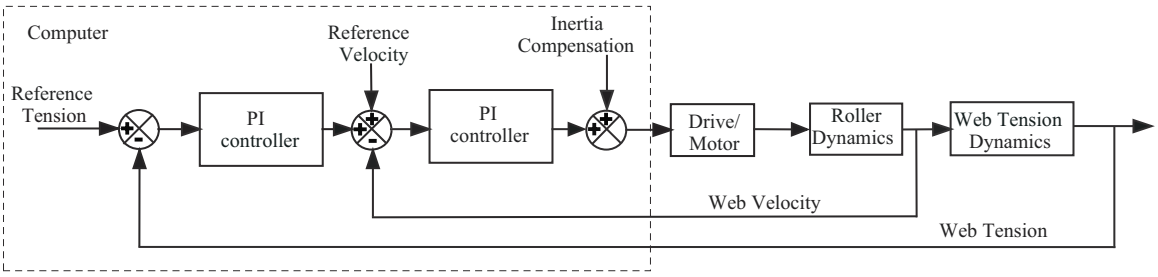

Figure 1.9: PI web tension control strategy

The following industrial speed PI controller is typically used

$$C_v(s) = \frac{k_{pv}(s + \omega_v)}{s} \tag{1.1}$$

where k_{pv} is the proportional gain and ω_v is the zero crossover frequency.

The web tension PI controller is given by

$$C_t(s) = \frac{k_{pt}(s + \omega_t)}{s} \tag{1.2}$$

where k_{pt} is the proportional gain and ω_t is the zero crossover frequency. The outer loop tension controller either gives a speed correction or a torque correction, based on the structure of the control mode described in the previous section. The proportional and integral gains are determined either by using tuning rules or empirical tuning.

1.4 Adaptive PI Control

An adaptive tension control scheme which is simple to design and easy to implement is presented in Chapter 2. A self tuning regulator for web tension regulation is given in [18]. A robust H_∞ controller is designed and implemented in [19]. Linearization of the web system dynamic model and development of a decentralized state feedback control scheme are given in [15]. A state space reference model based adaptive control technique is given in [16]; a special reference model is chosen based on the overall dynamics of the large-scale R2R system. Model reference direct and indirect adaptive

schemes for web tension control are investigated and implemented on an experimental platform in [12]; the motivation for the design and development of simple adaptive PI schemes came from this work. Application of fault tolerant control to a winding machine is given in [20]. Tension control in the web is also critical in the presence of key primitive elements used in R2R manufacturing such as accumulators [21, 22] and print cylinders.

An adaptive controller can modify closed loop system behavior by compensating for the changes in system parameters. An adaptive controller has adjustable parameters against the fixed gain parameters in traditional controllers and a mechanism for adjusting the system parameters.

In the current study, a simple direct model reference adaptive PI (MRA-PI) controller based on the gradient method is designed and implemented for the unwind section of an R2R system. Controller gains are estimated by matching the plant performance and desired characteristics provided by a reference model. The estimates of the controller parameters are initialized by considering the stability of the nominal closed-loop tension control system.

Another adaptive PI control scheme that could facilitate automatic initialization of estimated parameters is investigated. This adaptive PI control algorithm is simple and initialization of parameters does not require the knowledge of even nominal plant parameters. There are several ways to initialize the estimated parameters. Astrom and Hagglund [23] suggest the relay feedback technique to initialize the estimated parameters. This technique is an alternative to the conventional continuous cycling method used to generate sustained oscillations. The relay feedback method is known to be effective in determining the ultimate gain and ultimate frequency (frequency at which phase shift of plant is -180 degrees) of a system.

In the 1950's, relays were generally used in amplifiers. In the 1980's, there was

renewed interest on this topic after Astrom and others [24] showed its application in automatic tuning of a PID controller. Hagglund and Astrom [25] showed the application of the relay technique in industrial adaptive controllers. There have been many other efforts to extend the relay feedback technique to diverse applications. Lund and Astrom [26] describe automatic initialization of robust self-tuning regulators. Hagglund and Tengvall [27] applied the technique to develop a PID auto-tuning procedure to unsymmetrical processes with two different operating modes. Astrom and Hagglund [28] extended the relay auto-tuning method to general digital controllers. The relay feedback technique was used in the design of phase-lead and phase-lag filters for general frequency response compensation by Yang and Chen [29]. Li [30] and Chiang [31] describe an approach to derive low-order transfer function models using relay feedback. Palmor [32] developed auto tuners for advanced controllers like the Smith-predictor controller which can be implemented for complex systems. Relay feedback methods have been proposed for intelligent systems as integrated initialization and tuning modules by Astrom and Anton [33]. Balchen [34] proposed a method to estimate the ultimate frequency online by injecting a small sinusoidal disturbance.

As proposed in Astrom [23], the ultimate frequency is initially evaluated offline by injecting a relay oscillation in the system. The estimated offline ultimate frequency is used to update the proportional and integral gains. The transfer function is estimated by approximating the plant to the second order model. The proportional gain of the controller is updated with the magnitude of the estimated transfer function at the ultimate frequency. The online deviation to the initial value of the ultimate frequency is estimated by injecting a sinusoidal disturbance of small magnitude and sufficiently exciting signal in the reference tension. The integral gain is updated by estimated online ultimate frequency. The algorithm is robust and adaptable to changes in the

configuration of the web system with simplicity in design and implementation.

1.5 Load Speed Regulation

Mechanical transmissions are widely used in various industries where the mechanical power is typically transmitted from motor shafts to load shafts by utilizing transmission systems. Control of load speed is essential in many applications. When rigid transmissions are employed, there is no dynamics between the motor shaft and the load shaft, and typically the motor shaft speed is controlled to control the speed of the load shaft. However, due to the transmission dynamics, resulting from the compliance of belt as well as long shafts in the transmission, regulating load shaft speed is not the same as regulating motor shaft speed. In the presence of such a transmission, practicing engineers are often confronted with the question of whether to use (i) motor speed feedback to control load speed as is done in conventional practice, or (ii) use load speed feedback, or (iii) use a combination of motor and load speed feedback.

There is a large body of literature on the characteristics of belt drives and design of mechanisms using belt drives. The disturbances generated by belt compliance, gear backlash, shaft torsional compliance or external disturbances on load side must be compensated to achieve desired load speed regulation performance. The motion control system can be modeled as a multi-inertia system with springs and shaft elements [35]. The multi-inertia system can be simplified by considering a two-inertia system, in which the first inertia represents the motor and the second inertia represents the load connected through a transmission system. A linear model with backlash and belt compliance is presented in [36] and is considered in this work for further analysis. A common controller that is employed for regulation of load speed for a two-inertia elastic system is PI control [37]. PI control has the limitation on

performance, especially in the presence of disturbances. In order to overcome these limitations, a load torque observer is suggested in [38]. Though this technique is useful in preventing limit cycles, load speed remained uncontrolled in the presence of uncertainties. In [36], it is shown that only load speed feedback results in an unstable system which is also discussed in this work and further analyzed. The simultaneous feedback from motor and load speed feedback is first proposed in [39], which also suggested application of a preload to close the backlash gap. The simulation study showed that limit cycles are attenuated if the applied preload is smaller than backlash gap. In [40], a two degree freedom fuzzy controller, consisting of a feedback fuzzy controller and a feedforward acceleration compensator, is proposed to control a belt drive precision positioning table. In [41], a robust motion control scheme for belt-driven servomechanism is reported, but it fails to consider belt as interconnection between load and motor side. Similarly, [42] considers torsional oscillations of an induction machine in addition to saturation and hysteresis in the actuator, but compliance in drive train is ignored.

1.6 Output Regulator and Disturbance Rejection

The fundamental problem of controlling a dynamic system in order to have its output track a pre-specified signal or reject a disturbance is referred to in the control literature as the servomechanism problem. This problem has many engineering applications. For example, in robotics, the position of the robot end-effector is required to follow a specified trajectory. In R2R manufacturing, the tension in the material is regulated at a specified value while transporting the material on rollers through processing machinery. There is a need to develop intelligent control algorithms for R2R systems that can compensate for changes in process conditions as well as reject process and

machine induced disturbances.

The linear servomechanism problem has been studied in [43–46]. The solution to the servomechanism problem involves determination of two components of control - feedforward and feedback. In the linear case, the solution can be obtained by solving linear algebraic equations. In [47] the servomechanism problem for a class of nonlinear systems is approached along the same lines as [44] and a method is provided for computing the feedforward component of the control through the solution of a constrained partial differential equation. Essentially, the partial differential equation computes the center manifold of the equilibrium of an associated nonlinear system. It is known that this partial differential equation may not have a unique solution. An additional algebraic equation enforces the output to be zero when the state lies on this manifold. An approximate solution to the nonlinear servomechanism problem is provided in [48]. An inversion based approach via input-output linearization for exact output tracking is provided in [49]. The work in [50] involves modifying the output and making it track a modified trajectory, so that the original output tracks the original trajectory if the modified output tracks the modified trajectory. The approach adopted in this paper follows the work given in [51–53].

There are other available approximation methods in the literature, especially Taylor series expansion and the neural network approach [54]; it mimics the approach for the linear servomechanism problem and tries to approximate the partial differential-algebraic equation which was originally obtained in [47]. However, this approach has the following drawbacks: (1) one must solve a partial differential-algebraic equation in contrast to the ordinary algebraic differential equation, (2) the partial differential-algebraic equation is used to find the center manifold, which may not be unique [55], and (3) a neural network approach requires basis functions, the choice of their number as well as the functional forms is somewhat arbitrary. The presented work relies on

numerical algorithms for ordinary differential-algebraic equations, which is a much simpler proposition when compared to (1). The computation of center manifold is circumvented as we are only interested in finding the feedforward control input. Further, numerical analytical tools for ordinary differential-algebraic equations are better developed than those for partial differential-algebraic equations. There is also a fuzzy approach to output regulation problem which relies on approximating the drift vector using a set of linear approximations and resembles the gain scheduled approach as given in [56]; linear servomechanism tools are then used to get the feedforward control action. This provides an approximation for the feedforward control action.

In the current research, a novel solution is considered for the nonlinear servomechanism problem and applied to tension control in R2R manufacturing. The proposed scheme is capable of rejecting disturbance frequency components generated by non-ideal R2R machine elements and by converting processes, such as lamination, printing, coating, etc.

Implementation of the output regulator with only proportional feedback action may lead to a steady state error. It is necessary to incorporate integral feedback action to achieve zero steady-state error and improve desired steady-state performance. In [57], it is shown that the system with integral feedback can deliver stable performance in the presence of disturbances. An output regulator with integral action is designed to eliminate the steady-state error in the tension signal.

1.7 Feedforward Control Action for Interaction Minimization

Decentralized control schemes provide a practical and efficient option to regulate the system parameters that utilize only the state feedback of each subsystem without depending on the other subsystems [6]. In the past, efforts were made to minimize

interaction between subsystems of R2R system by designing filters along with existing PI control strategies [58]. The feedforward action can assist in decoupling of subsystems in R2R systems. In order to mitigate the propagation of disturbances into downstream subsections, use of downstream section web tension measurement as feedback is suggested and experimental results are provided to verify this strategy.

1.8 Contributions

The contributions of this research are summarized in the following:

- *Design and Implementation of a Model Reference Adaptive Proportional Integral (MRA-PI) Web Tension Control Scheme.* A MRA-PI control scheme for longitudinal web tension is designed by matching the system output with the desired characteristics generated by a reference model. The controller parameters are adapted based on the mismatch between the reference model output and the system output. To obtain initial estimates of the PI gains, the characteristic equation of the closed-loop system is evaluated by considering the nominal plant parameters. The initial PI gain estimates are obtained based on closed-loop system stability. The MRA-PI control scheme is implemented on the EWL for two different web materials, Tyvek and polyester. A comparison between fixed gain PI and MRA-PI on tension response is presented. Guidelines to implement the MRA-PI scheme for any R2R system are provided.

- *Design and Implementation of an Adaptive PI Web Tension Control Scheme Based on Automatic Controller Parameter Initialization.* An adaptive PI regulator is designed to regulate web tension (plant output) by automatically initializing controller parameters. The relay feedback technique is used to compute the plant ultimate frequency which is used to initialize controller parameters.

The plant model is assumed to be a second order model and the plant parameters are estimated online. Once evaluated by relay feedback technique, the ultimate frequency can be updated online if there are changes to the system. The adaptive PI controller gains are automatically obtained based on the estimated plant parameters and ultimate frequency. The designed adaptive PI controller is implemented on the EWL for two different web materials, Tyvek and polyester. Implementation guidelines for any general R2R manufacturing system are provided.

- *Design and Implementation of a Load Speed Regulation Scheme for a Two Inertia System Coupled with a Belt-pulley and Gear-pair Transmission System.* Based on the model of the two inertias (motor and load) connected by a belt-pulley and gear-pair transmission system, we have investigated the effect of using either motor or load feedback to control the load speed by utilizing the singular perturbation method. In each case, we consider a PI controller that is typical in the industry for the feedback controller. The small parameter in the singular perturbation method is proportional to the reciprocal of the square root of the belt compliance. The singular perturbation analysis revealed that the controller using pure load feedback results in an unstable system. Therefore, use of pure load feedback must be avoided. To directly control the load speed, we also proposed a control scheme that uses both the motor speed and load speed feedback and show that such scheme results in a stable closed-loop system. Since feedback action is not sufficient in rejecting periodic disturbances that commonly act on the load, we also consider an adaptive feedforward compensation action that is based on adaptive estimation of the coefficients of the periodic disturbance as suggested in [59]. This adaptive feedforward action is

suitable for this application because it preserves closed-loop stability achieved with the feedback controller. Experiments were conducted to evaluate the performance of the various control schemes on an industrial grade transmission system that is common in R2R manufacturing.

- *Design and Implementation of a Load Speed Regulation Scheme for Web Tension Control.* The two degree freedom load speed regulation scheme can be extended to web tension control in R2R manufacturing. The proposed scheme is simple and serves as an add-on feedforward control action to the existing web tension scheme. The proposed control scheme can provide an effective tool to reject periodic disturbances in the tension signal. The undesired frequencies generated due to eccentric rollers, out-of-round rolls, changing material diameters can be attenuated by a precise load speed regulation scheme on the driven material roll. The proposed scheme is implemented on the rewind roll of the Euclid web line and results show the rejection of the disturbance in tension signal.

- *Design and Implementation of a Nonlinear Tension Output Regulator to Reject Periodic Disturbances.* A nonlinear tension output regulator is designed for the web transport system in order to reject periodic disturbances generated by non-ideal machine elements. The disturbances are considered to be the output of a partially known exogenous system. The feedforward action is synthesized by considering the solution of the web tension governing algebraic-differential equations in conjunction with estimates of disturbance parameters (amplitude and phase). The output regulator design is validated through experiments conducted on the EWL by injecting a sinusoidal disturbance to the master speed roller. Experimental results show that the designed regulator has the ability to attenuate the disturbance. An output regulator with integral feedback action

is also considered to obtain zero steady state error in the tension signal. The output regulator is also capable of rejecting multiple frequency components. A web tension observer is designed and web tension estimation is incorporated into the output regulator design.

- *Implementation of a Feedforward Action to Minimize Interaction and Avoid Propagation of Disturbance between Subsystems in an R2R System.* The implementation of feedforward action with downstream tension feedback along with Perron root based interaction minimizing filters is investigated. The proposed implementation helps to minimize tension disturbance propagation to downstream sections and minimize interactions between subsystems. The proposed control strategy is validated through experiments on EWL in the rewind section.

CHAPTER 2

Design and Implementation of Adaptive PI Tension Control Schemes

In this chapter, two adaptive Proportional-Integral (PI) control schemes are designed and discussed for control of web tension. First, a direct model reference adaptive PI (MRA-PI) controller based on the gradient method is developed. Controller gains are estimated by matching the plant performance and desired characteristics provided by a reference model. The estimates of the controller parameters are initialized by considering the stability of the nominal closed-loop tension control system. The MRA-PI controller is simple in design compared to the controllers designed using standard MRAC methods since it has only two adjustable parameters compared to six.

Second, an indirect adaptive PI control scheme that would facilitate automatic initialization of estimated parameters based on relay feedback technique is investigated. The indirect adaptive PI control algorithm is simple and initialization of controller parameter estimates does not require the knowledge of nominal plant parameters. The relay feedback technique, which utilizes sustained oscillations in the system, is used to calculate the so called ultimate frequency of the system. The period of the oscillations can be determined by measuring the time between zero-crossings of amplitude by measuring peak-to-peak values of the system output oscillations. Once the process point corresponding to ultimate frequency is known, it is possible to design a variety of control schemes which can be based on the information obtained through that point.

In the current context, the proportional and integral gains of the adaptive PI

control are initialized based on the ultimate frequency. The adaptation of controller gains is facilitated by tracking the plant transfer function at ultimate frequency. An algorithm to compute the estimate of ultimate frequency in real-time is considered to account for its change due to plant parameter changes; the method given in [34] is employed where a small sinusoidal oscillation is introduced into the closed-loop tension control system. The phase shift and amplitude of the system are calculated based on the estimation of plant parameters and ultimate frequency. The amplitude magnitude determines the proportional gain, while integral gain is updated with the estimated ultimate frequency. The implementation of this type of adaptive PI algorithm is relatively easy since only three parameters are estimated. Note that in both the adaptive PI schemes, we are using some kind of a feedforward signal along with the feedback action. In the case of a fixed gain PI controller, gains are typically tuned by comparing the closed-loop speed transfer function characteristic equation with a standard second-order characteristic equation with design parameters as the damping ratio and natural frequency. These gains are further tuned in experimentation to obtain the best possible performance. The two adaptive PI schemes together with an industrial fixed gain PI tension control scheme are implemented on a large experimental R2R platform containing multiple driven rollers and tension zones. The implementation guidelines together with discussion of experimental results are provided.

The rest of the chapter is organized as follows. Governing equations for web tension and transport speed are discussed in Section 2.1. The design of the MRA-PI controller is presented in Section 2.2. In Section 2.3, design of an indirect adaptive PI scheme based on the relay feedback technique is presented; estimation of plant transfer function around the ultimate frequency is also discussed. The experimental setup and guidelines to implement the MRA-PI and adaptive PI controller to any general web line are provided in Section 2.4. The performance of the adaptive PI

control schemes is presented through experimental results in Section 2.5.

2.1 Governing Equations for Web Tension and Transport Speed

A roll-to-roll system consists of key primitive elements such as material rolls, driven and idle rolls, and web span (web between two adjacent rollers). A number of these primitive elements are employed sequentially to construct an R2R system. The governing equation for these primitive elements are derived and composed as per the configuration of the R2R system to develop a mathematical model that can describe the transport behavior of webs. For example, a line sketch of an experimental R2R platform is shown in Figure 2.1; the system consists of a number of driven and idle rollers and web spans between unwind and rewind rolls.

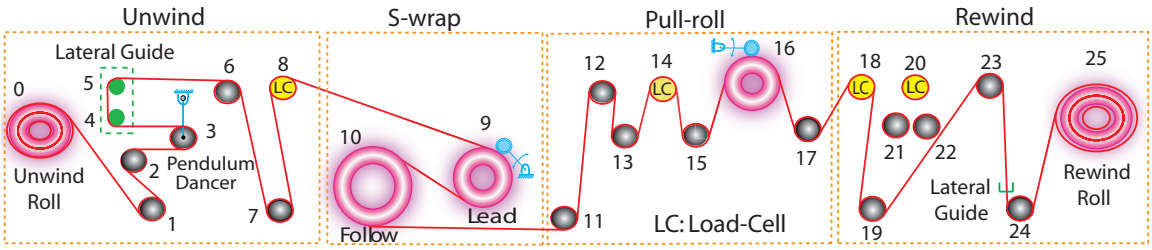

Figure 2.1: Line sketch of R2R experimental platform

The governing equation for web speed on a roller is obtained by considering the angular motion of the roller and web wrap on that roller. And the governing equation for web tension in a span is obtained by first applying conservation of mass to a control volume encompassing the web between two adjacent rollers to obtain a governing equation for web strain. Then, a constitutive law is used to relate web strain and web tension. In this chapter, the material is assumed to be linearly elastic and a linear relation is used via the modulus of elasticity of the material. The web material is transported at low strain and satisfies the small strain assumption. A simple two

roller setup with adjacent web spans is provided in Figure 2.2 to illustrate a portion of any R2R system and shows the nomenclature for presenting the governing equations below. It is assumed that web is not slipping on the roller during transport, that is, the peripheral velocity of the roller is assumed to be equal to the web velocity on the roller.

In this setup, t_i denotes web tension in the span between $(i-1)^{th}$ and i^{th} rollers, v_i is the web transport speed on the i^{th} roller, and ω_i is the angular velocity of the i^{th} roller. There has been significant reported work in the literature on modeling of web transport behavior and we will simply list the governing equations here and refer interested readers to the literature for more details.

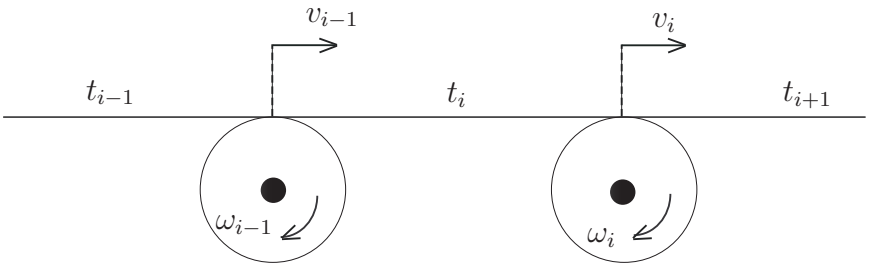

Figure 2.2: Two roller setup

The governing equation for web tension in the i^{th} span is given by

$$\dot{t}_i = \frac{EA_w}{L_i}(v_i - v_{i-1}) + \frac{1}{L_i}(t_{i-1}v_{i-1} - t_i v_i) \tag{2.1}$$

where E is the modulus of elasticity of the web material, A_w is the area of cross-section of the web material, and L_i is the span length. The governing equation for web transport speed on the i^{th} roller is given by

$$\dot{v}_i = \frac{R_i^2}{J_i}(t_{i+1} - t_i) + \frac{R_i}{J_i}n_i u_i - \frac{b_{fi}}{J_i}v_i \tag{2.2}$$

where R_i is the radius of the i^{th} roller, J_i is the inertia of the i^{th} roller, n_i is the gear ratio, and b_{fi} is the coefficient of viscous friction.

The above governing equations can be linearized around reference values. To do this, define the perturbations from references as $\triangle t_i = t_i - t_r$, $\triangle v_i = v_i - v_r$, and $\triangle u_i = u_i - u_{eq}$, where u_{eq} is the equilibrium control input. Therefore, the linearized governing equations in the frequency domain are given by

$$T_i(s) = \frac{EA_w/V_r}{\tau_{\omega i}s + 1}(V_i(s) - V_{i-1}(s)) + \frac{1}{\tau_{\omega i-1}s + 1}T_{i-1}(s), \tag{2.3}$$

$$V_i(s) = \frac{R_i^2}{J_i s + b_{fi}}(T_{i+1}(s) - T_i(s)) + \frac{R_i}{J_i s + b_{fi}}n_i U_i(s) \tag{2.4}$$

where $T_i(s)$ is the Laplace transform of $\triangle t_i(t)$, that is, $T_i(s) = \mathcal{L}\{\triangle t_i\}$, $V_i(s) = \mathcal{L}\{\triangle v_i\}$, $U_i(s) = \mathcal{L}\{\triangle u_i\}$, and $\tau_{\omega i} = L_i/v_r$ is the span time constant, that is, the time it takes for an element of material from entry to exit of that span. The term containing $T_{i-1}(s)$ in the tension governing equation appears due to transport of strain from upstream spans to downstream spans. From these two governing equations one can create a model for the entire R2R transport system by writing down web speed on each roller and web tension in each span. Many idle rollers (non-driven) are employed in addition to driven rollers to create web paths through processes and to provide support for the web during transport. In the presence of a large number of idle rollers the transport behavior model for the system is too cumbersome. Often the notion of tension zone is employed in practice to simplify the models as the idle rollers do not contribute much to the dynamics during steady state operation. The idea is to designate the web between any two driven rollers as a tension zone and consider each zone to be a web span. This simplifies the dynamic model significantly. A simplified line sketch showing the tension zones and driven rollers is provided in Figure 2.3; the rollers indicated as "LC" are mounted on load-cells to provide tension feedback for tension control systems. The two driven rollers in the S-wrap section are electronically slaved together and are under pure speed control; these are treated as one driven roller (M1) in the simplified sketch and are typically referred to as the

Master Speed Roller.

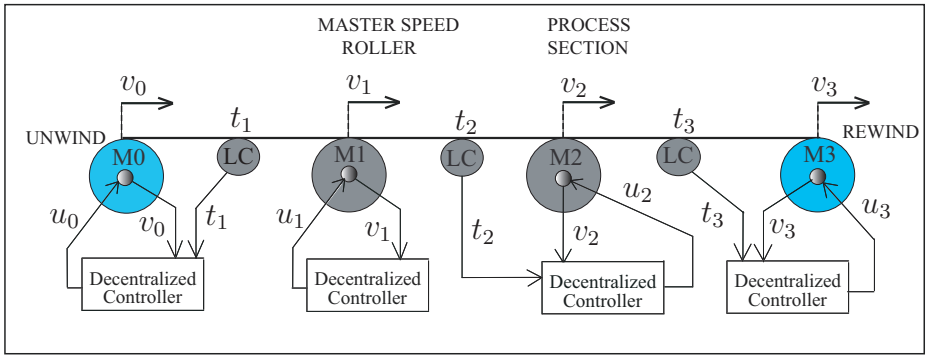

Figure 2.3: Simplified line sketch of R2R experimental platform

2.2 Control Scheme I: Model Reference Adaptive Proportional Integral (MRA-PI) Controller

In the MRA-PI control, the plant is parameterized in terms of the PI controller parameters and controller parameters are estimated online using parameter adaptation laws. The goal is to find a parameter adjustment mechanism to achieve zero error between the reference model output and the actual system output; tension is the output for this application. For the speed loop we use an industrial PI scheme that is implemented on the motor drive. The open loop transfer function for the speed loop is given by

$$G_v(s) = \frac{k_v(s+\omega_v)}{s} \frac{1}{n_{i-1}J_{i-1}s} \tag{2.5}$$

where k_v is the proportional gain and ω_v is the cutoff frequency. The closed-loop transfer function for the inner velocity loop takes the form of

$$G_{cv}(s) = \frac{(\beta_0 s + \beta_1)}{s^2 + \beta_0 s + \beta_1} \tag{2.6}$$

where $\beta_0 = k_v/(n_{i-1}J_{i-1})$, $\beta_1 = \beta_0\omega_v$, $\omega_v = \beta_0/(4\zeta^2)$, ζ is the damping ratio of the system.

The structure of the MRA-PI tension control scheme is shown in Figure 2.4. The outer loop fixed gain PI web tension controller is replaced by the MRA-PI controller as shown in Figure 2.4. The open loop transfer function from the velocity correction (output of the tension controller) to the tension variation (output of $G_p(s)$) is $G_{cv}G_p$. The closed-loop transfer function with the MRI-PI controller is given by

$$G_{ct}(s) = \frac{G_t G_{cv} G_p}{1 + G_t G_{cv} G_p} \tag{2.7}$$

where G_t is the MRA-PI transfer function.

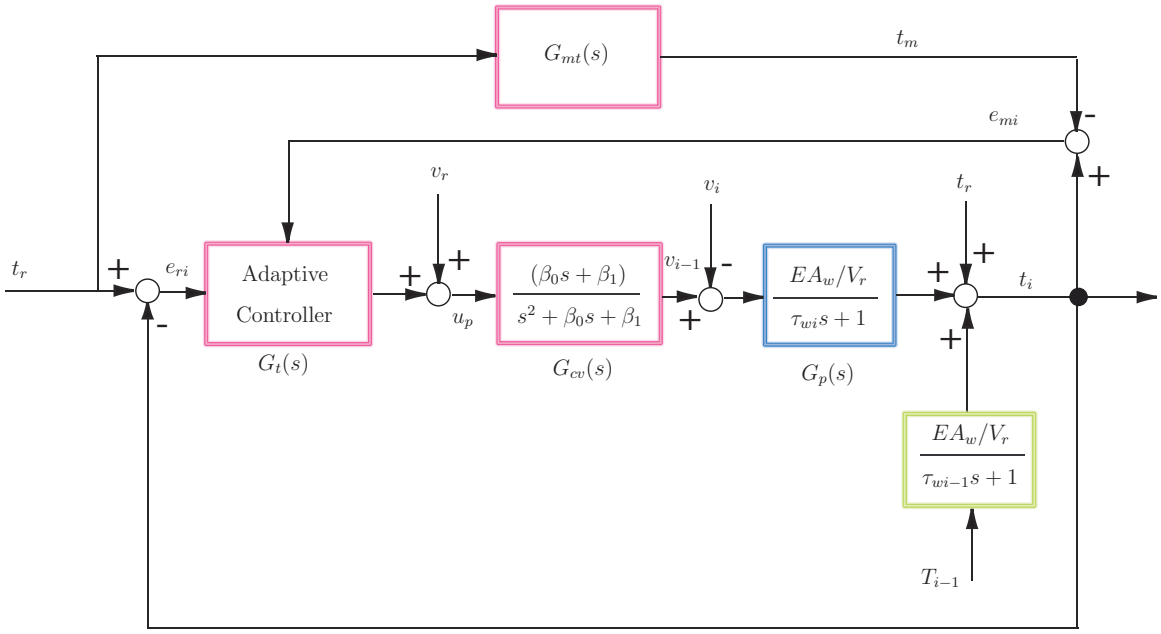

Figure 2.4: Model reference adaptive PI tension control strategy

The selection of the structure of the reference model is important. We choose a structure for the reference model that is similar to the closed-loop system obtained by using fixed gain PI controllers for the speed and tension loops. The relative degree of this closed loop transfer function is two. We select a reference model with relative degree two and having the same number of poles and zeros as the closed-loop transfer

function resulting from the MRA-PI controller. This is given by

$$G_{mt}(s) = \frac{k_m(as + z_1)(s + z_2)}{(s + p_1)(s + p_2)(s + p_3)(s + p_4)} \tag{2.8}$$

where the reference model parameters k_m, a, z_i and p_i are selected to provide the desired performance through model simulations of the MRA-PI tension control scheme. As it is typically done in model reference adaptive schemes, we develop parameter adaptation laws for the tension controller PI gains by minimizing the loss function corresponding to the model error $e_{mi} = t_i - t_m$. The MRA-PI controller has two adjustable parameters, proportional and integral gains. Define the parameter vector as $\theta = [k_p \;\; k_i]$. The parameter adaptation law by using the gradient method is given by

$$\frac{d\theta}{dt} = -\gamma e_{mi} \frac{\partial e_{mi}}{\partial \theta} \tag{2.9}$$

where $\partial e_{mi}/\partial\theta$ is the sensitivity of the model error to parameter θ. Since the reference model output does not depend on the controller parameters, the sensitivity is given by

$$\frac{\partial e_{mi}}{\partial \theta} = \frac{\partial(t_i - t_m)}{\partial \theta} = \frac{\partial t_i}{\partial \theta}. \tag{2.10}$$

Therefore, the resulting adaptation laws are

$$\frac{dk_p}{dt} = -\gamma_p e_{mi} \frac{s(EA_w/V_r)(\beta_0 s + \beta_1)}{s(s^2 + \beta_0 s + \beta_1)(\tau_{\omega i} s + 1) + (k_p s + k_i)(EA_w/V_r)(\beta_0 s + \beta_1)}, \tag{2.11}$$

$$\frac{dk_i}{dt} = -\gamma_i e_{mi} \frac{(EA_w/V_r)(\beta_0 s + \beta_1)}{s(s^2 + \beta_0 s + \beta_1)(\tau_{\omega i} s + 1) + (k_p s + k_i)(EA_w/V_r)(\beta_0 s + \beta_1)} \tag{2.12}$$

where γ_p and γ_i are adaptive gains. Since the system parameters are not known, the above adaptation laws cannot be used. The following adaptation laws that utilize the reference model structure and parameters are used instead:

$$\frac{dk_p}{dt} = -\gamma_p e_{mi} \frac{k_m s(s + z_2)}{(s + p_1)(s + p_2)(s + p_3)(s + p_4)}, \tag{2.13}$$

$$\frac{dk_i}{dt} = -\gamma_i e_{mi} \frac{k_m(s+z_2)}{(s+p_1)(s+p_2)(s+p_3)(s+p_4)}. \tag{2.14}$$

For online adaptation in real-time control, one requires good initialization for the controller parameter estimates. We consider the closed-loop characteristic equation with MRA-PI which is given by

$$s(s^2+\beta_0 s+\beta_1)(\tau_{\omega i}s+1)+(EA_w/V_r)(\beta_0 s+\beta_1)(k_p s+k_i)=0. \tag{2.15}$$

To obtain constraints on the gains k_p and k_i which provide an idea on how to initialize the estimated parameters, we consider the gains for which the roots of the characteristic equation are in the open left half of the complex plane, which gives the following constraints:

$$k_p > \frac{(1+\omega_v \tau_{\omega i})}{(EA_w/V_r)}, \tag{2.16}$$

$$k_i > -\frac{\omega_v}{(EA_w/V_r)} - k_p \omega_v. \tag{2.17}$$

Note that the right hand side of these constraints themselves require the system parameters. We use nominal system parameters to initialize the estimated PI controller parameters.

2.3 Control Scheme II: Indirect Adaptive PI Control Based on Relay Feedback Technique

An indirect adaptive PI control scheme is described in this section which does not require the knowledge of the nominal parameters of the model. The relay feedback technique is first employed to find the amplitude of the plant and the frequency at which the phase of the plant is -180 degrees. The parameters of the plant transfer function are estimated first and a controller is selected to provide the required gain and phase margins. The advantage of this indirect adaptive PI controller is that one

can automatically initialize the controller parameters. This is particularly useful for R2R manufacturing systems where it is sometimes difficult to determine the nominal values of the plant parameters. We describe the method in the following.

Let $P(s)$ be the transfer function of the plant to be controlled and $C(s)$ be the adaptive PI used to control the plant. The Nyquist plots of the plant and the open loop system along with the controller and the plant are shown in Figure 2.5.

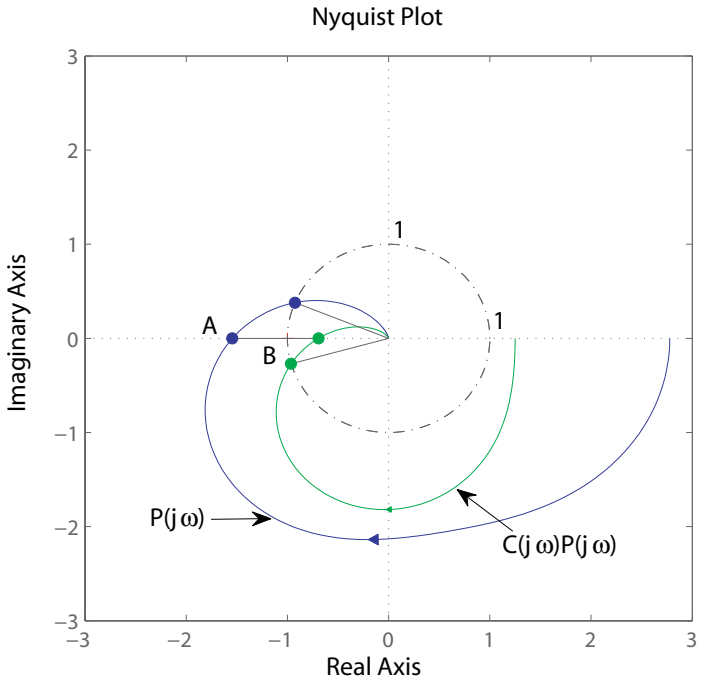

Figure 2.5: Example Nyquist plot for a plant with and without compensator

In traditional frequency response based controller design, if we have knowledge about the plant, one can obtain its frequency response and the controller can be designed by shaping the frequency response to the desired. If the frequency response of the plant is not known, one cannot use this approach. In such a scenario, if the magnitude and frequency corresponding to point A of the frequency response of $P(s)$ are available, then the plant transfer function can be estimated (from the

information of point A) which can be used to design the controller. Let $C(s)$ be the controller transfer function and B be the point on the Nyquist plot of the open loop system ($C(s)P(s)$) with the desired specifications (gain margin and phase margin) as indicated in Figure 2.5. The goal is to design the controller $C(s)$ such that point A corresponding to the plant transfer function can be moved to point B corresponding to the open loop transfer function. In order to determine point B, the magnitude of the plant transfer function and associated frequency at point A (ω_A) need to be identified. This frequency ω_A is typically referred to in the literature as the ultimate frequency.

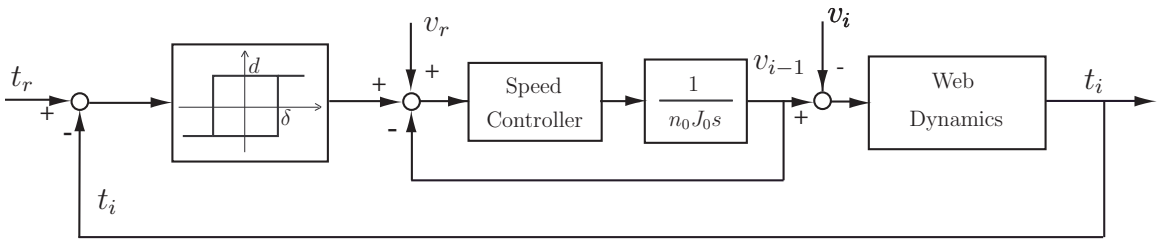

Figure 2.6: Relay feedback in tension outer loop

Relay feedback technique may be employed to obtain the ultimate frequency and the magnitude of the plant transfer function at point A. The relay feedback technique can be readily applied to an R2R system. Introduction of the relay into the outer tension loop is shown in Figure 2.6. A relay with hysteresis is employed to avoid high frequency switching of the standard relay. The relay logic is given by

If $e \geq \delta$, then $d = +\ 5\%$ of reference variable;

If $e \leq -\delta$, then $d = -\ 5\%$ of reference variable;

Else keep the previous output of relay;

where $e = t_i - t_r$ is the tension error, δ is the relay hysteresis, and d is the relay amplitude. The relay feedback method induces an oscillation in the controlled tension

output which is used to identify the ultimate frequency and the plant amplitude at that frequency.

The indirect adaptive PI control scheme is illustrated in Figure 2.7. The plant

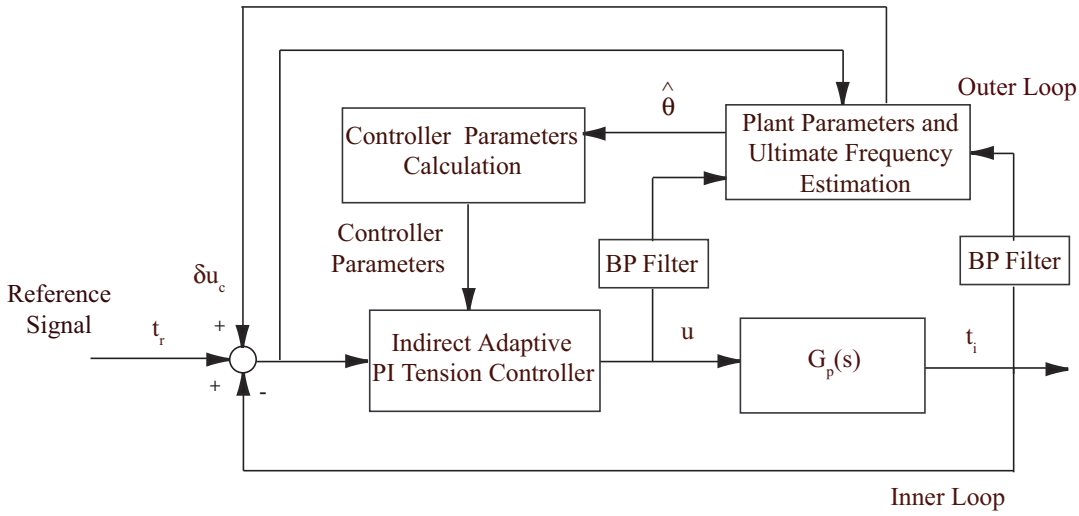

Figure 2.7: Indirect adaptive PI tension control strategy

$G_p(s)$ is a combined representation of the tension dynamics and inner velocity closed-loop transfer function whose frequency response can be represented as

$$G_p(j\omega) = \alpha e^{j\phi} \tag{2.18}$$

where α is the amplitude and ϕ is the phase shift of the plant. Since the relative degree of $G_p(s)$ is two, this can be approximated by a second-order discrete model as

$$\bar{t}_i(t) = b_1\bar{u}(t-T) + b_2\bar{u}(t-2T) \tag{2.19}$$

where $\bar{u}$ and $\bar{t}_i$ are the filtered control input and process tension output, respectively; b_1 and b_2 are the unknown parameters to be estimated; and T is the sampling period.

The parameters of $G_p(j\omega)$ are estimated in real-time by using the least squares method. In order to estimate the plant parameters, the control input and plant

output are filtered using the band-pass filter

$$G_f(s) = \frac{s}{s^2 + 2\zeta\omega_f s + \omega_f^2}, \tag{2.20}$$

where ω_f is the band pass filter frequency and can be chosen as the estimated ultimate frequency. The ratio of the filtered output amplitude to the filtered input amplitude is the plant magnitude α. The phase difference between the filtered output and input signals is the phase ϕ. Based on this estimate of the plant transfer function the indirect adaptive PI controller gains are given by

$$k_p = \frac{\beta_1}{\alpha} \tag{2.21a}$$

$$T_i = \frac{\beta_2}{\omega_A} \tag{2.21b}$$

where β_1 and β_2 are tunable gains. The indirect adaptive PI control law is given by

$$u = k_p \left(1 + \frac{1}{T_i s}\right) \tag{2.22}$$

The ultimate frequency is obtained by the relay feedback technique a priori and is fixed for real-time estimation of the plant transfer function. If there are changes in the plant such as changes in the material roll diameter, then the ultimate frequency found a priori is no longer relevant. In the following we describe a method to automatically estimate the ultimate frequency online using an algorithm provided in [34]. The method is illustrated in Figure 2.8. The ultimate frequency is estimated by injecting a small sinusoidal perturbation to the tension reference. The adaptation law for the ultimate frequency is

$$\dot{\omega} = \gamma \cos(\omega T)(u_0 - t_i) \tag{2.23}$$

where γ is the estimation gain and $u_0 = t_r + \delta u_c$ is the perturbed reference.

The phase shift of the plant is calculated based on the estimated parameters as

$$\phi = \tan^{-1}\left(\frac{\hat{b}_1 \sin(\hat{\omega}T)}{\hat{b}_1 \cos(\hat{\omega}T) + \hat{b}_2}\right) - 2\hat{\omega}T \tag{2.24}$$

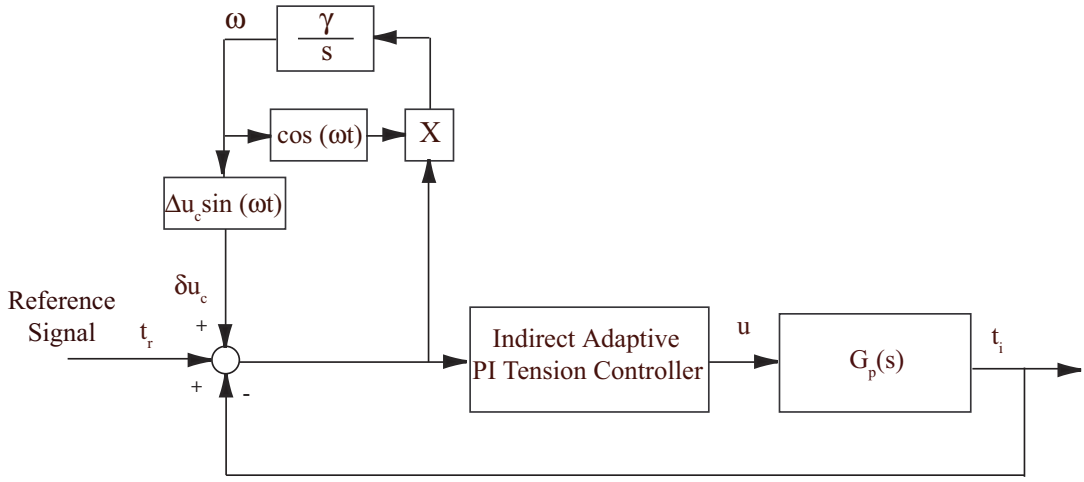

Figure 2.8: Online estimation of ultimate frequency

where $\hat{b}_1$ and $\hat{b}_2$ are estimated plant parameters and $\hat{\omega}$ is the estimated ultimate frequency. The amplitude of the plant is calculated based on the estimated plant parameters and the phase shift (2.24) as

$$\hat{\alpha} = \frac{\hat{b}_1 \sin(\hat{\omega}T)}{\sin(2\hat{\omega}T + \phi)}. \tag{2.25}$$

The controller gains given in (2.21) now use the estimates $\hat{\omega}$ and $\hat{\alpha}$.

2.4 Experimental Platform and Procedure

A schematic of the R2R experimental setup used for experimentation is shown in Figure 2.1. It is divided into four sections: unwind section, S-wrap section, pull-roll section, and rewind section. The five driven rollers in the machine are powered by AC motors, 15 HP (11.19 kW) for the unwind and rewind and 5 HP (3.76 kW) for the three intermediate driven rollers. The S-wrap section, acts as the master speed section, which sets the web speed in the machine. The two driven rollers in the S-wrap section are under pure speed control. The unwind, pull-roll and rewind are under a speed-based tension control scheme as shown in Figure 1.6. The cascaded control

approach is common in industrial practice where the outer tension loop provides correction to the inner loop speed reference. The outer tension loop is implemented in an external controller (for example, ControlLogix controller from Allen Bradley) and the inner speed loop is implemented in the motor drive (for example, Powerflex 755 AC drive from Allen Bradley). Encoders on motor shafts provide angular position feedback directly to the motor drives. The tension control algorithm is programmed in RSLogix 5000 software (Rockwell Automation PLC software). The real-time architecture used to run the R2R machine also includes analog/digital input/output modules and network boards. All the real-time hardware components of the machine are connected through a ControlNet communication network. The network is updated every 5 ms (Network Update Time) and data is communicated to the network every 10 ms (Request Package Interval). The lateral guides, which control the web lateral position, are controlled by dedicated controllers independent of the ControlLogix real-time architecture.

The two adaptive PI control schemes presented in the previous two sections are implemented for control of tension in the unwind section of the R2R experimental platform. The tension feedback is obtained using load cells mounted on roller R8 shown in Figure 2.1. The reference web tension is 20 lbf (89 N). In the first set of experiments, tension regulation experiments are carried out at the line speed of 100 FPM (0.51 m/s) for two web materials a polyester film and Tyvek (a polymer material manufactured by Dupont). In the second set of experiments, the web line is accelerated to 150 FPM (0.76 m/s) and 250 FPM (1.02 m/s), then decelerated to 100 FPM (0.51 m/s), to evaluate the performance of the designed algorithms for changing speeds. The nominal values of the key web material parameters are given in Table 2.1.

For the MRA-PI control scheme, the reference model for the web tension system

Parameter	Numerical Values	
	Tyvek	polyester
Modulus (E)	9.3×10^4 psi (641.2 N/mm^2)	4.6×10^5 psi (3171.6 N/mm^2)
Width (w)	6 in (152.4 mm)	4.25 in (107.95 mm)
Thickness (h_w)	0.005 in (0.127 mm)	0.0038 in (0.097 mm)

Table 2.1: Web material parameters

is selected based on model simulations (offline using MATLAB):

$$G_{mt}(s) = \frac{15(1/1.2s+1)(1/50s+1)}{(1/12s+1)(1/5s+1)(s+5)(s+3)}. \tag{2.26}$$

The implementation of MRA-PI controller scheme is shown in Figure 2.9. In Figure 2.9, $F_p(s)$ and $F_i(s)$ are filters given by equations (2.13) and (2.14), respectively.

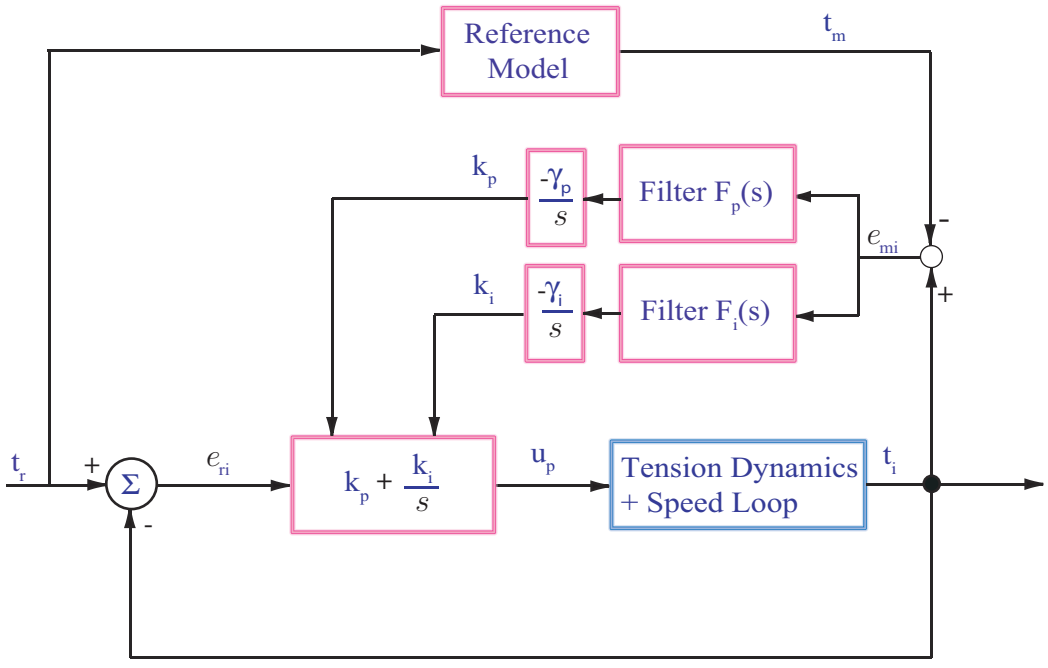

Figure 2.9: Implementation of MRA-PI control

For the indirect adaptive PI scheme based on automatic initialization, the initial plant parameter values are chosen as $b_1 = 0.5$ and $b_2 = 0.5$. The proportional and integral gain values are initialized with ultimate frequency obtained by relay feedback experiment for Tyvek and polyester web materials. The adjustable parameters of the controller are selected empirically based on the performance of the system as $\beta_1 = 0.5$ and $\beta_2 = 0.2$. In the following we provide step-by-step guidelines for the implementation of the two adaptive schemes.

Implementation Guidelines for MRA-PI Controller

Step 1: Select reference model parameters given in equation (2.8) based on the desired tension loop performance.

Step 2: Choose initial controller parameter estimates that satisfy the stability constraint criteria. The lower limit on the controller parameters can be imposed based on the constraint criteria.

Step 3: Estimate the controller gains online and generate controller output.

Step 4: The initial value of the proportional and integral gains may be increased in steps until the desired response is achieved.

Step 5: If the estimated controller parameters drift, an upper limit can be imposed on the estimates with suitable value that can be evaluated empirically or a method to project the parameters into a bounded set can be employed.

Implementation Guidelines for Indirect Adaptive PI Controller

Step 1: Evaluate the plant ultimate frequency offline by injecting relay oscillations in the system under tension but at zero speed.

Step 2: Initialize the integral gain with the ultimate frequency evaluated offline.

Step 3: Initialize the second order plant parameters. Then initialize proportional gain based on the ultimate frequency and plant parameters initial values.

Step 4: Filter the plant output and control input using the band pass filter at the estimated ultimate frequency.

Step 5: Estimate the ultimate frequency and plant parameters online to account for dynamic changes in the plant.

Step 6: Evaluate the phase shift and amplitude ratio of the plant based on the estimated plant parameters and ultimate frequency.

Step 7: Select the adjustable controller parameters β_1 and β_2, and update the proportional and integral gains based on the estimated amplitude and ultimate frequency.

2.5 Experimental Results

The tension response with a well-tuned fixed gain PI controller at 100 FPM (0.51 m/s) for Tyvek and polyester web materials are shown in Figure 2.10. The standard deviation is calculated for tension data in the steady-state and used as a performance metric. The standard deviation values indicate that at steady-state the web tension varies between ± 0.51 lbf for Tyvek web and ± 0.71 lbf for the polyester web. The fixed speed PI controller gains are tuned based on a desired second-order characteristic equation that has the damping ratio $\xi = 1.1$ and the natural frequency $\omega = 4$ Hz. The outer tension loop fixed PI gains are tuned based on the second-order closed-loop speed dynamics and first-order tension transfer function. The tuning was further fine-tuned empirically during experimentation. The following are tuned values for the fixed gains of the tension PI controller: the proportional and integral gain values are

25 and 0.5 for Tyvek and 39 and 0.75 for polyester material. Since the elastic modulus of polyester material is larger than Tyvek material, larger proportional and integral gains are needed for the polyester material for a similar performance as that of Tyvek.

The tension response with the MRA PI control scheme at 100 FPM (0.51 m/s) for Tyvek and polyester web materials are shown in Figure 2.11. The same initial values of the controller parameter estimates and design parameters are used for both web materials. The standard deviation values for the web tension in the unwind section at steady state vary between ± 0.53 lbf for Tyvek web and ± 0.66 lbf for polyester web; these values are comparable or better than what is observed with a well-tuned fixed gain PI controller. Further, the MRA-PI scheme does not require tuning if different web materials are transported in the same R2R process line. This provides significant benefits to many R2R industries as tedious tuning is not required when processing different materials. The evolution of the estimates of controller parameters are shown in Figures 2.12 through 2.13. Figure 2.14 shows the performance of the MRA-PI algorithm to acceleration and deceleration of the web line at different speeds (AB: 100 FPM, BC: 150 FPM, CD: 250 FPM, and DE: 100 FPM) for the Tyvek web. The controller gain estimates adapt to compensate for the speed changes.

In the implementation of the indirect adaptive PI controller, first the relay feedback is introduced at zero web speed and when the tension is at its reference value. The relay amplitude is selected as 0.9, which is about 5% of the reference web tension of 20 lbf (89 N); this selection follows the guidance given on the selection of relay amplitude in the literature. The hysteresis is selected to be 0.006, based on the observation of the tension error fluctuation range. The relay feedback is given for short period of time to obtain sustained oscillations. The tension response data with oscillations is shown in Figure 2.15. A close-up view of the relay output and the tension response for the Tyvek web is shown in Figure 2.16. The amplitude of

tension oscillations measured is 0.9. The period of tension oscillations is 2.6 sec. So, the frequency of tension oscillations (ultimate frequency) for Tyvek web is 2.42 rad/s. A similar experiment is performed for the polyester web, which gave the frequency of tension oscillations (ultimate frequency) to be 2.07 rad/s. Adaptive gains are initialized with the ultimate frequency obtained by relay feedback technique as formulated in equations (2.24), (2.25) and (2.21). Once the controller estimates are initialized, non-zero speed experiments are performed to regulate tension.

The tension response with the indirect adaptive PI control scheme at 100 FPM (0.51 m/s) for Tyvek and polyester web materials are shown in Figure 2.17. The standard deviation values are ± 0.54 lbf for Tyvek web and ± 0.75 lbf for polyester web. The evolution of the estimates of the controller parameters are shown in Figures 2.18 through 2.19. Figure 2.20 shows the performance of indirect adaptive PI algorithm to the acceleration and deceleration of the line (AB: 100 FPM, BC: 150 FPM, CD: 250 FPM, and DE: 100 FPM) for Tyvek web. The controller gains adapt to compensate for the changing speed.

Both the MRA-PI and indirect adaptive PI controllers provide similar or better performance when compared to a well-tuned fixed gain PI controller. This performance is achieved without the need for any changes in controller gain initial estimates or design parameters when transporting different materials and during speed changes. A fixed gain PI requires tuning of controller gains for each material as well as for different speeds. Among the two adaptive PI schemes, the implementation of the indirect adaptive PI scheme has several advantages over the MRA-PI scheme: (1) there is no need for nominal plant parameters; (2) reference model is not required; (3) the controller parameter estimates in indirect adaptive PI controller are automatically initialized based on ultimate frequency which can be estimated online. For the indirect adaptive PI scheme implementation, one has to implement the relay feedback to

obtain the initial estimate of the ultimate frequency. This does not pose a problem in R2R systems because in practice web tension of desired value is generated at zero speed (typically called as tension-on) and then line speed is increased to the desired value along a given acceleration profile. The relay feedback technique to obtain initial value of the ultimate frequency can be implemented in a straightforward fashion during the tension-on phase of the system operation. Further, all steps of the indirect adaptive PI scheme can be automated without the need for operator intervention.

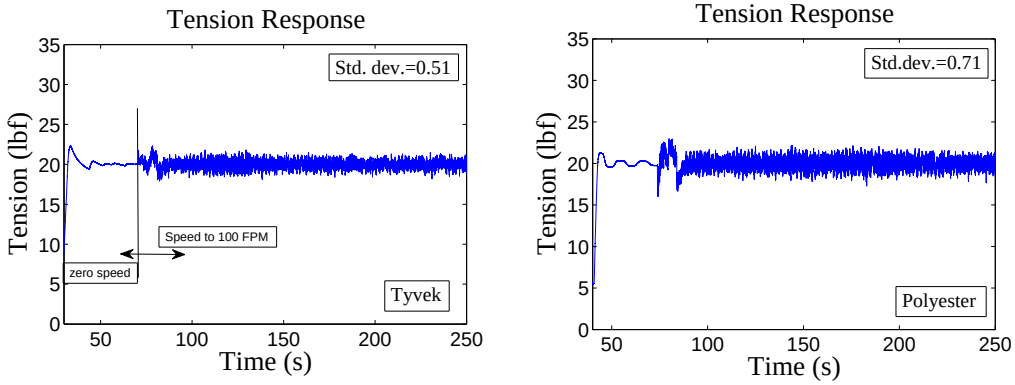

Figure 2.10: Tension response at 100 FPM with a well-tuned industrial PI controller; Left: Tyvek; Right: polyester

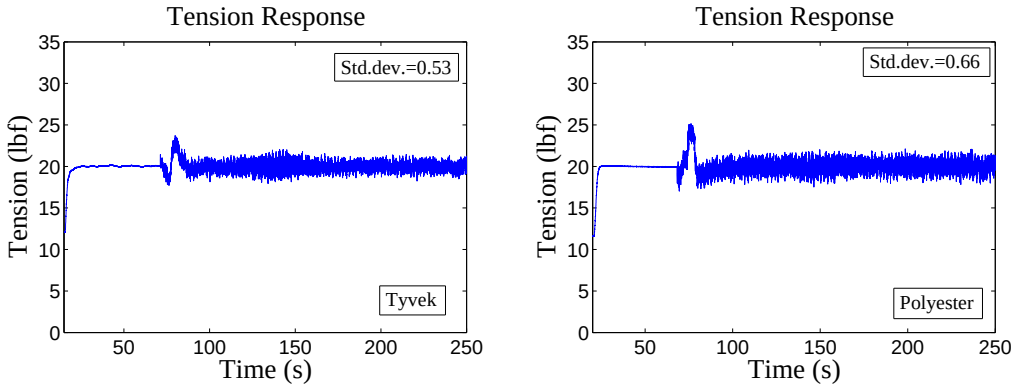

Figure 2.11: Tension response at 100 FPM with MRA-PI controller; Left: Tyvek; Right: polyester

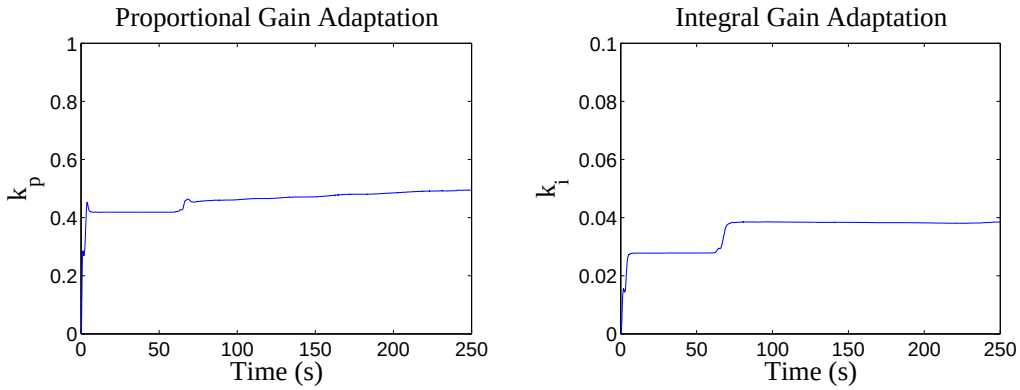

Figure 2.12: Proportional and Integral gain adaptation with MRA-PI controller for Tyvek web

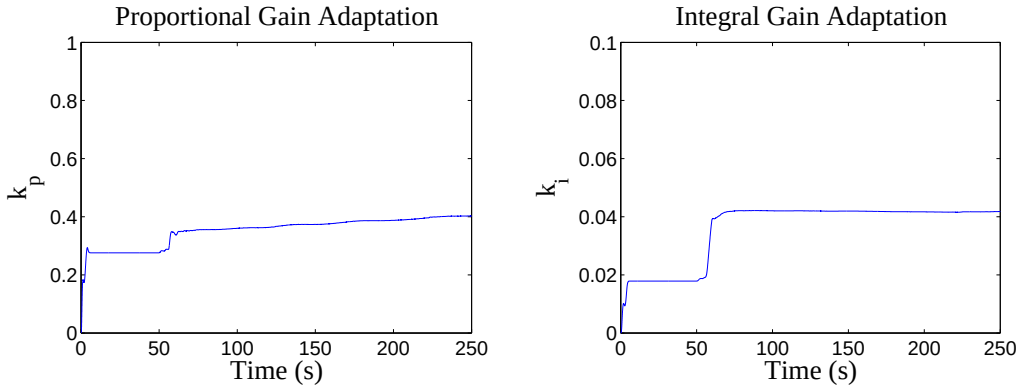

Figure 2.13: Proportional and Integral gain adaptation with MRA-PI controller for polyester web

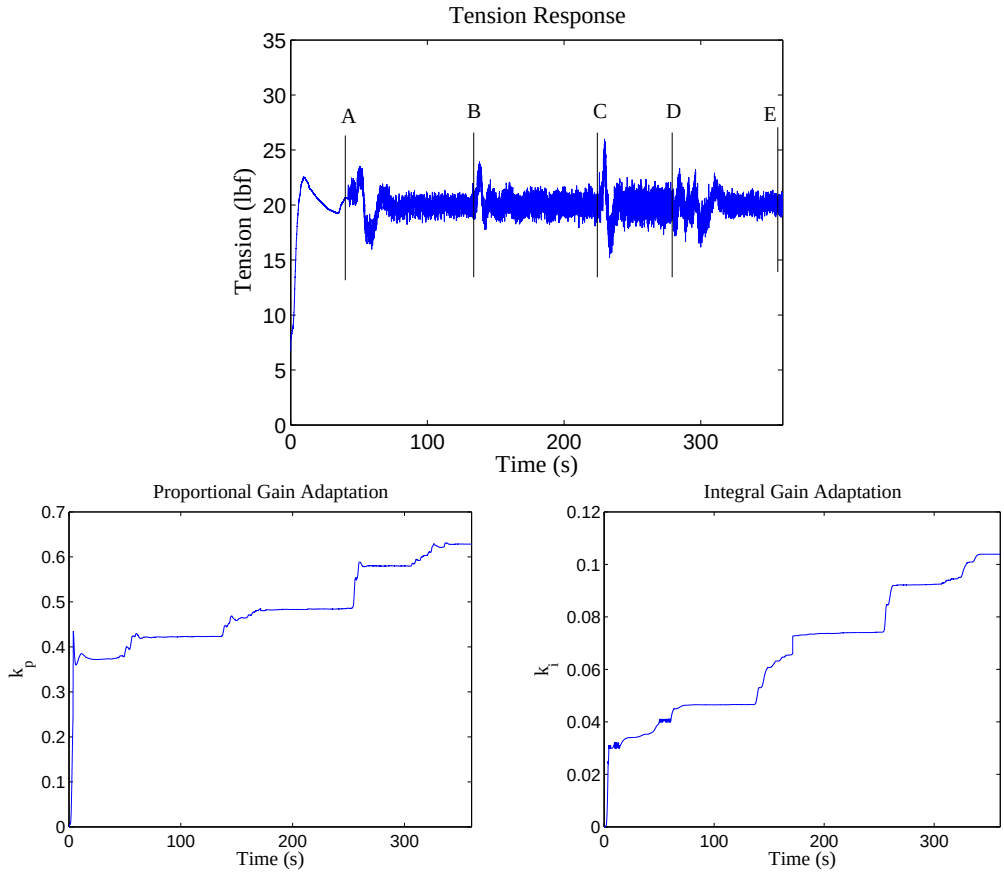

Figure 2.14: Tension response and gain adaptation with MRA-PI Controller for line speed changes

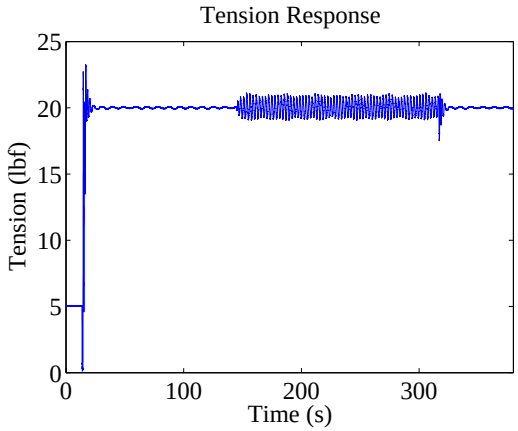

Figure 2.15: Tension response to relay feedback for Tyvek web

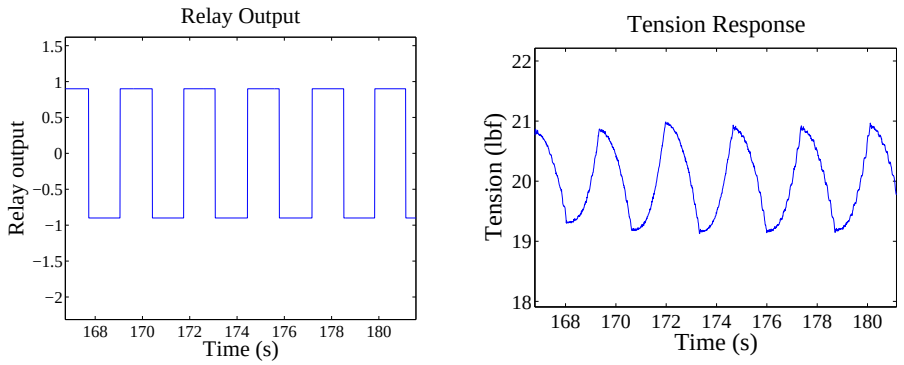

Figure 2.16: Relay output and oscillating tension response for Tyvek web

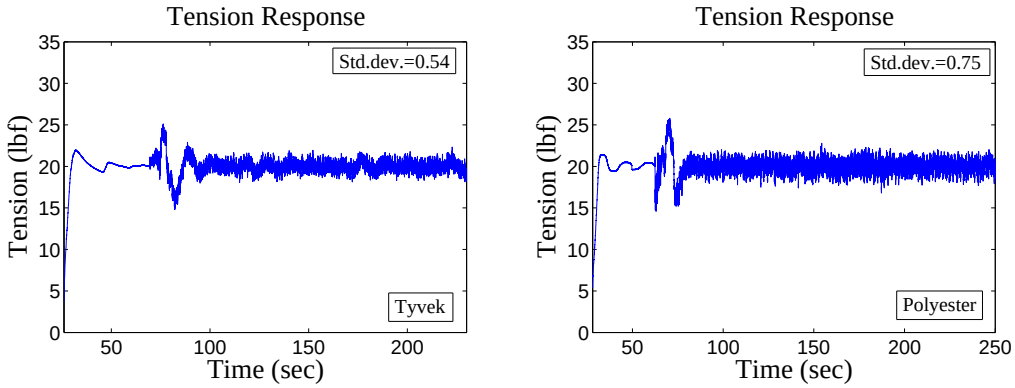

Figure 2.17: Tension response at 100 FPM with indirect adaptive PI controller

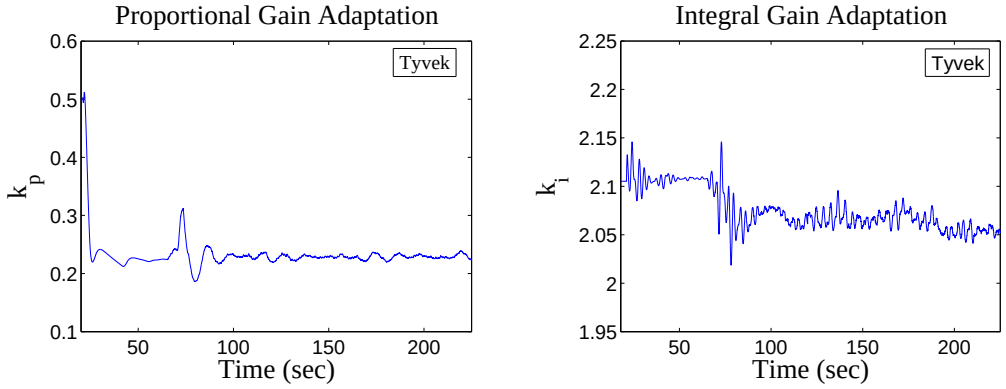

Figure 2.18: Proportional and Integral Gain adaptation with indirect adaptive PI controller for Tyvek web

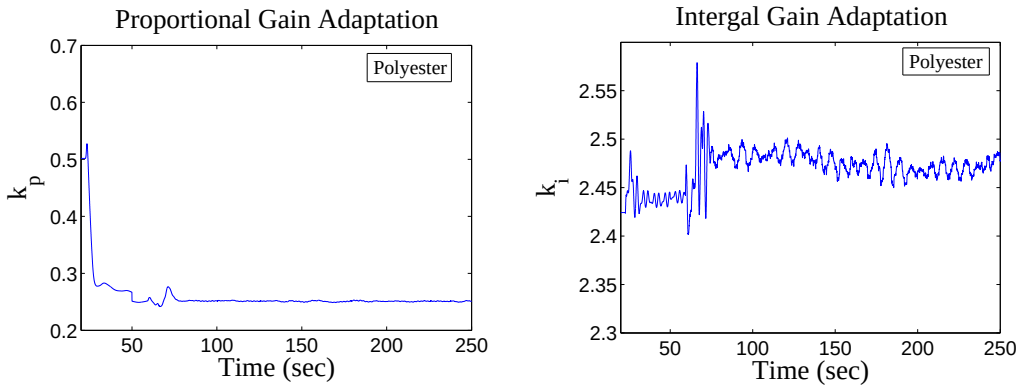

Figure 2.19: Proportional and Integral gain adaptation with indirect adaptive PI controller for polyester web

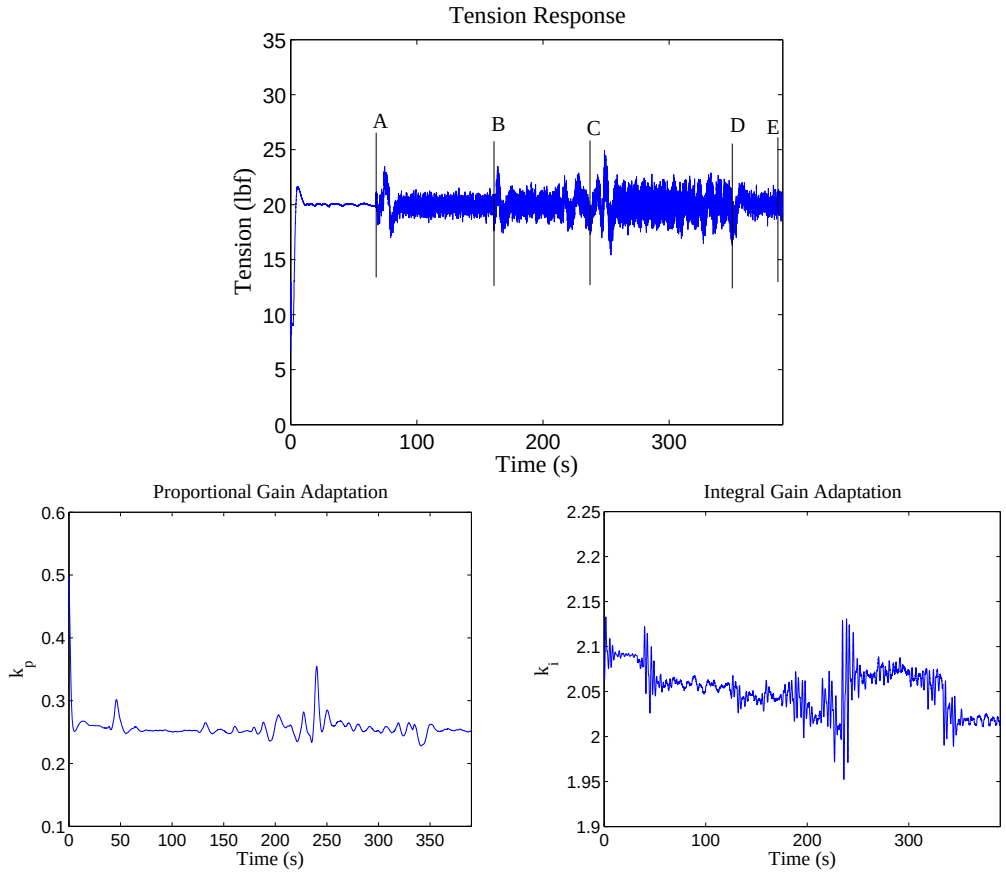

Figure 2.20: Tension response and gain adaptation with indirect adaptive PI controller for line speed changes

CHAPTER 3

Load Speed Regulation in Compliant Mechanical Transmission Systems with Application to Web Tension Control

A load and motor speed model which consider belt-pulley and gear pair power transmission is considered in this chapter. In the given model, motor torque is considered as input while speed of the driven roller (load speed) as the output of the system. A simultaneous load and motor speed feedback control scheme is considered for obtaining better load speed regulation by attenuating disturbances. Further, in order to reject periodic disturbance, an add-on adaptive feedforward (AFF) control action along with motor and load speed feedback (two degree freedom control) is considered.

The proposed two degree freedom load speed regulation scheme is extended to web tension control. It is expected to control the web tension to desired value by regulating the load speed in the presence of disturbances. The proposed control scheme is implemented to regulate the load speed in the presence of periodic disturbances. The two-inertia system includes belt-pulley and gear pair transmission elements which mimics most of power/torque transmission applications. This system utilizes an AC motor, drive and control hardware used in industrial practice. Comparative experimental results with an existing industrial control scheme and proposed control scheme are presented in frequency and time domain, and further discussions are provided. The proposed load speed regulation scheme is further implemented in the rewind section in order to investigate web tension control in the presence of disturbances. Comparative experiments are performed with an existing control scheme

and proposed control scheme and results are presented and discussed.

The remainder of the chapter is organized as follows. The model of the system is described in Section 3.1. Sections 3.2 and 3.3 describe the motor speed feedback only and load speed feedback only cases, respectively. A control scheme that utilizes both motor and load speed feedback is discussed in Section 3.4. An add-on adaptive feedforward compensation to reject load speed disturbances is discussed in Section 3.5. The proposed load speed regulation scheme is extended to web tension control in Section 3.6. Section 3.7 provides a description of the experimental platform and a comparison of the results with the various control schemes.

3.1 Model of the System

A schematic of the belt-pulley and gear transmission system connecting the motor with the load is shown in Figure 3.1. In the schematic, J_i denotes the i^{th} roll inertia, b_i denotes the viscous friction coefficient, R_i denotes the radii of the pulleys and gears of the i^{th} transmission, θ_i denotes the angular displacements of the inertias, τ_m denotes the motor torque, τ_L denotes the torque disturbance on the load, and K_b denotes the stiffness of the belt.

To derive the governing equations for this system we consider the action of the belt in transmitting power. For a given direction of rotation of the pulley, the belt has a *tight side* and a *slack side* as shown in Figure 3.1. It is assumed that the transmission of power is taking place on the tight side and the transport of the belt is taking place on the slack side. Under this assumption, the net change in tension on the slack side will be much smaller than that in the tight side and thus may be ignored. The tight side of the belt can then be modeled as a spring with spring constant of K_b. For given angular displacements θ_m and θ_L, the net elongation of the tight side of the belt can

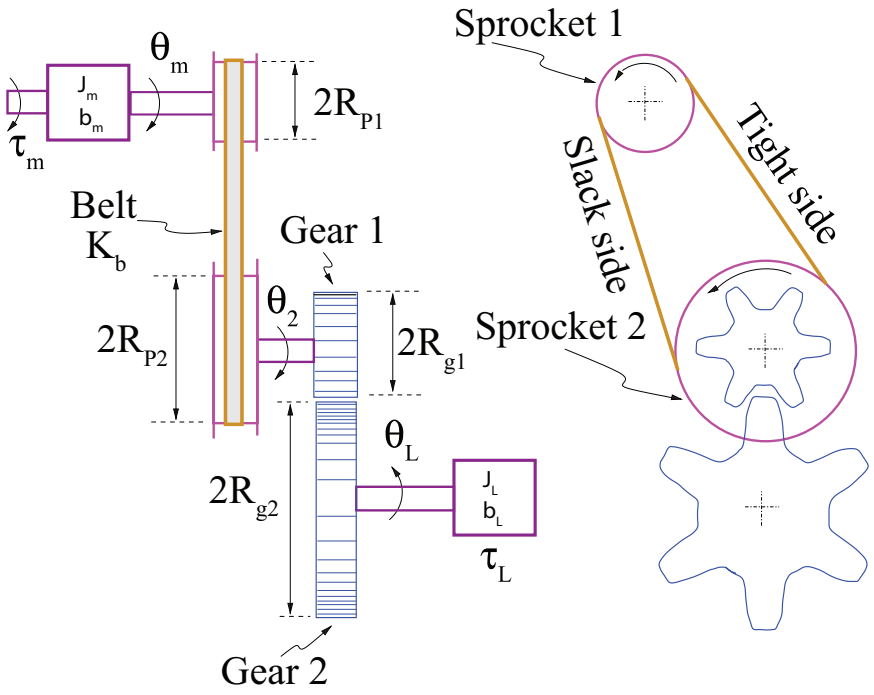

Figure 3.1: Schematic of a belt-pulley and gear-pair transmission system

be written as $(R_{P1}\theta_m - G_R R_{P2}\theta_L)$. Because of this elongation, the driving pulley experiences a torque of $(R_{P1}\theta_m - G_R R_{P2}\theta_L)K_b R_{P1}$ and the driven pulley experiences a torque of $(R_{P1}\theta_m - G_R R_{P2}\theta_L)G_R R_{P2} K_b$. Under the assumption that the inertias of the pulleys and gears are much smaller than the motor and the load, the governing equations of motion for the motor-side inertia and the load-side inertia are given by [36]

$$J_m\ddot{\theta}_m + b_m\dot{\theta}_m + R_{P1}K_b(R_{P1}\theta_m - G_R R_{P2}\theta_L) = \tau_m, \tag{3.1a}$$

$$J_L\ddot{\theta}_L + b_L\dot{\theta}_L - G_R R_{P2}K_b(R_{P1}\theta_m - G_R R_{P2}\theta_L) = \tau_L. \tag{3.1b}$$

A block diagram representation of the system given by (3.1) is provided in Figure 3.2; note that this block diagram represents the open-loop system and the two "loops" appearing in the block diagram represent the interconnections in (3.1). The open-

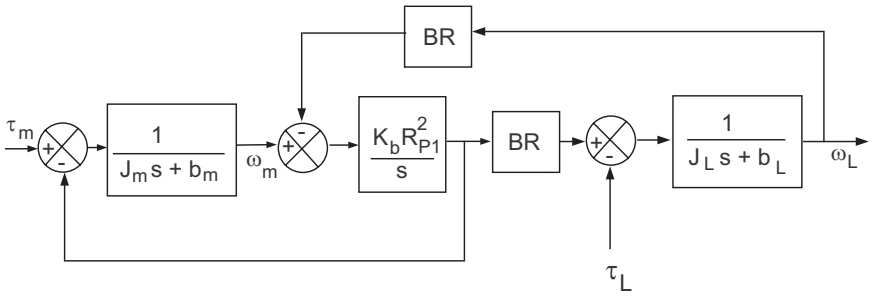

Figure 3.2: Block diagram of the belt-pulley and gear transmission system; BR denotes the overall speed ratio, $BR = (R_{P2}/R_{P1})G_R$.

loop transfer functions from the motor torque signal τ_m to the motor speed ω_m and load speed ω_L are given by

$$G_{\tau_m\omega_m}(s) \triangleq \frac{\omega_m(s)}{\tau_m(s)} = \frac{J_L s^2 + b_L s + G_R^2 R_{P2}^2 K_b}{D(s)}, \tag{3.2a}$$

$$G_{\tau_m\omega_L}(s) \triangleq \frac{\omega_L(s)}{\tau_m(s)} = \frac{G_R R_{P1} R_{P2} K_b}{D(s)}, \tag{3.2b}$$

where

$$D(s) = J_m J_L s^3 + (b_L J_m + J_L b_m)s^2 + (K_b J_{eq} + b_m b_L)s + K_b b_{eq}, \tag{3.3a}$$

$$J_{eq} = G_R^2 R_{P2}^2 J_m + R_{P1}^2 J_L, \tag{3.3b}$$

$$b_{eq} = G_R^2 R_{P2}^2 b_m + R_{P1}^2 b_L. \tag{3.3c}$$

The goal is to control the load speed ω_i. In the following we will discuss the closed-loop control systems that consider three scenarios: (i) pure motor speed feedback, (ii) pure load speed feedback, (iii) a combination of motor and load speed feedback.

3.2 Motor Speed Feedback Control Scheme

It is common to control load speed by using the measurement of motor speed ω_m as feedback. This control scheme is shown in Figure 3.3. The control structure is

designed to regulate motor speed ω_m to the reference ω_{rm}, and thereby indirectly regulate load speed ω_L.

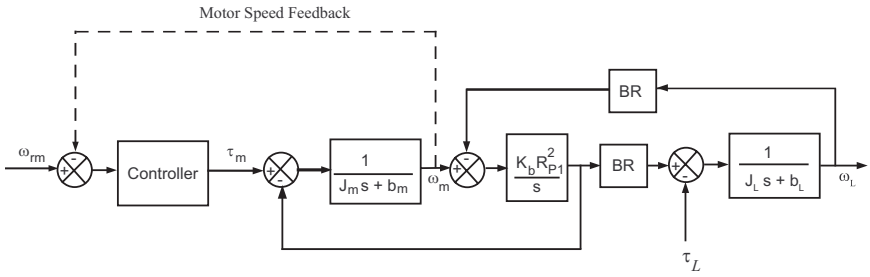

Figure 3.3: Motor speed feedback control scheme

We consider the often used Proportional-Integral (PI) control action which is given by

$$\tau_m = K_{pm}(\omega_{rm} - \omega_m) + K_{im}\int(\omega_{rm} - \omega_m)d\tau. \tag{3.4}$$

With this control law, the closed-loop transfer function from ω_{rm} to ω_L is obtained as

$$\frac{\omega_L(s)}{\omega_{rm}(s)} = \frac{(G_R R_{P1} R_{P2} K_b / J_m J_L)(sK_{pm} + K_{im})}{\psi_m(s)}, \tag{3.5}$$

where

$$\begin{aligned}
\psi_m(s) &= s^4 + c_3 s^3 + c_2 s^2 + c_1 s + c_0, \\
c_3 &= \frac{(b_m J_L + J_m b_L + K_{pm} J_L)}{J_m J_L}, \\
c_2 &= \frac{(K_b J_{eq} + b_m b_L + K_{pm} b_L + K_{im} J_L)}{J_m J_L}, \\
c_1 &= \frac{(K_b b_{eq} + G_R^2 R_{P2}^2 K_b K_{pm} + K_{im} b_L)}{J_m J_L}, \\
c_0 &= \frac{G_R^2 R_{P2}^2 K_b K_{im}}{J_m J_L}.
\end{aligned} \tag{3.6}$$

Note the the coefficients c_0 to c_3 depend on the controller gains. We consider the singular perturbation method for analyzing such a system with the small parameter

equal to the reciprocal of the square root of the belt stiffness K_b. For conducting singular perturbation analysis, we express the equations in the form

$$\dot{x} = A_{11}x + A_{12}z,\ x(t_0) = x^0 \tag{3.7a}$$

$$\varepsilon\dot{z} = A_{21}x + A_{22}z,\ z(t_0) = z^0 \tag{3.7b}$$

where x and z are the states of the slow and the fast subsystems, respectively, and ε is the small parameter; for our system we will consider $\varepsilon^2 = 1/K_b$. The elements of the matrices A_{ij} may depend on ε. However, to use the singular perturbation method, the matrix A_{22} needs to be nonsingular [60] at $\varepsilon = 0$. A natural choice of the state variables for the singular perturbation analysis is θ_m, $\dot{\theta}_m$, θ_L and $\dot{\theta}_L$. However, with this choice of the state variables, the matrix A_{22} becomes singular at $\varepsilon = 0$. To obtain a state-space representation in the form that would enable the use of the singular perturbation method, we consider the following transformation of variables [36] :

$$\theta_c \triangleq \frac{J_m\theta_m + J_L G_R(R_{P2}/R_{P1})\theta_L}{J_m + J_L}, \tag{3.8a}$$

$$\theta_s \triangleq \theta_m - G_R(R_{P2}/R_{P1})\theta_L. \tag{3.8b}$$

The variable θ_c is a weighted average of angular displacements (θ_m and θ_L) referred to the motor side and the variable θ_s is difference between the angular displacements (θ_m and θ_L) referred to the motor side; transformations similar to these have been used in prior studies of two inertia systems, see for example [61]. The idea of the weighted average of the displacements arises naturally in the case of a translational system wherein θ_c represents the position of the centroid of the masses. Now, choosing the state variables as $x = [\theta_c,\ \dot{\theta}_c]^\top$ and $z = [\theta_s/\varepsilon^2,\ \dot{\theta}_s/\varepsilon]^\top$, the state space representation

of the system is obtained in the form given by (3.7) where

$$A_{11} = \begin{bmatrix} 0 & 1 \\ f_1 & f_3 \end{bmatrix},\ A_{12} = \begin{bmatrix} 0 & 0 \\ \varepsilon^2 f_{21} + f_{22} & \varepsilon f_4 \end{bmatrix},$$

$$A_{21} = \begin{bmatrix} 0 & 0 \\ g_1 & g_3 \end{bmatrix},\ A_{22} = \begin{bmatrix} 0 & 1 \\ \varepsilon^2 g_{21} + g_{22} & \varepsilon g_4 \end{bmatrix}, \tag{3.9}$$

$$f_1 = -K_{im}/J_0,\ f_{21} = -K_{im}J_L/J_0^2,$$
$$f_{22} = (G_R^2 R_{P2}^2 - R_{P1}^2)/J_0,\ f_3 = -(K_{pm} + b_m + b_L)/J_0,$$
$$f_4 = (b_L J_m - b_m J_L - K_{pm} J_L)/J_0^2,$$

$$g_1 = -K_{im}/J_m,\ g_{21} = -K_{im}J_L^2/(J_m J_L J_0),$$
$$g_{22} = -(R_{P1}^2 J_L + G_R^2 R_{P2}^2 J_m)/(J_m J_L),$$
$$g_3 = (b_L J_m - b_m J_L - K_{pm} J_L)/(J_m J_L),$$
$$g_4 = -(K_{pm} J_L^2 + b_m J_L^2 + b_L J_m^2)/(J_m J_L J_0),$$

where $J_0 = J_m + J_L$, and $1/\varepsilon^2 = K_b$. Notice that $det(\,A_{22}(\varepsilon)|_{\varepsilon=0}) = -g_{22} \neq 0$, thus satisfying the requirement of non-singularity of the matrix A_{22} at $\varepsilon = 0$. The characteristic equation for the system given by (3.9) can be factored as [60]

$$\psi_m(s,\varepsilon) \approx \frac{1}{\varepsilon^2}\psi_{ms}(s,\varepsilon)\psi_{mf}(p,\varepsilon) = 0 \tag{3.10}$$

with

$$\psi_{ms}(s,\varepsilon) \triangleq \det[sI_2 - (A_{11} - A_{12}L(\varepsilon))] \tag{3.11a}$$

$$\psi_{mf}(p,\varepsilon) \triangleq \det[pI_2 - (A_{22} + \varepsilon L(\varepsilon)A_{12})] \tag{3.11b}$$

where $\psi_{ms}(s,\varepsilon)$ is the characteristic polynomial for the slow subsystem and $\psi_{mf}(p,\varepsilon)$ is the characteristic polynomial of the fast subsystem exhibited in the high-frequency scale $p = \varepsilon s$. The matrix $L(\varepsilon)$ is obtained using the iterative scheme given in [60].

Using the matrices given by equations (3.9), the slow and the fast characteristic polynomials are obtained as

$$\psi_{ms}(s,\varepsilon) \approx s^2 + \alpha_1 s + \alpha_0, \tag{3.12a}$$

$$\psi_{mf}(p,\varepsilon) \approx p^2 + \alpha_1' p + \alpha_0' \tag{3.12b}$$

where

$$\begin{aligned}
\alpha_1 &= \frac{G_R^2 R_{P2}^2 b_m + R_{P1}^2 b_L + G_R^2 R_{P2}^2 K_{pm}}{G_R^2 R_{P2}^2 J_m + R_{P1}^2 J_L}, \\
\alpha_0 &= \frac{G_R^2 R_{P2}^2 K_{im}}{G_R^2 R_{P2}^2 J_m + R_{P1}^2 J_L}, \\
\alpha_1' &= \frac{G_R^2 R_{P2}^2 K_{pm} J_L}{J_m (G_R^2 R_{P2}^2 J_m + R_{P1}^2 J_L)} \varepsilon, \\
\alpha_0' &= \frac{G_R^2 R_{P2}^2 J_L + R_{P1}^2 J_m}{J_m J_L}.
\end{aligned} \tag{3.13}$$

Equation (3.12) indicates that both the fast and the slow subsystems are stable for all $K_{pm},\ K_{im} > 0$. The result is true even without the approximation introduced by $L(\varepsilon)$ as shown in [36].

3.3 Load Speed Feedback Control Scheme

One can employ the load speed feedback scheme shown in 3.4, where the measured variable is ω_L. This seems to have the advantage of directly controlling load speed and attenuating the effect of the disturbance τ_L. The feedback law is given by

$$\tau_m = K_{pL}(\omega_{rL} - \omega_L) + K_{iL} \int (\omega_{rL} - \omega_L) d\tau, \tag{3.14}$$

and the closed-loop transfer function from ω_{rL} to ω_L is obtained as

$$\frac{\omega_L(s)}{\omega_{rL}(s)} = \frac{(G_R R_{P1} R_{P2} K_b / J_m J_L)(sK_{pL} + K_{iL})}{\psi_L(s)} \tag{3.15}$$

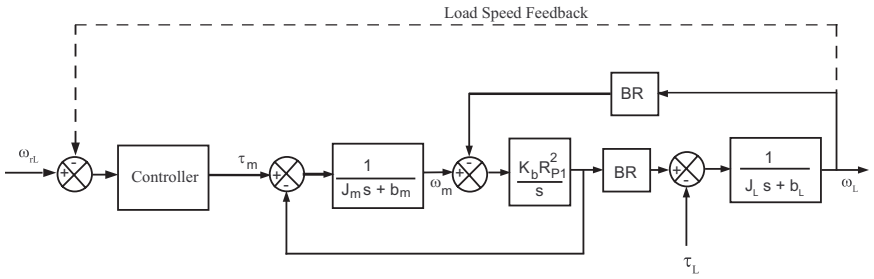

Figure 3.4: Load speed feedback control scheme

where

$$\begin{aligned}
\psi_L(s) &= s^4 + d_3 s^3 + d_2 s^2 + d_1 s + d_0, \\
d_3 &= \frac{(b_m J_L + J_m b_L)}{J_m J_L}, \\
d_2 &= \frac{(K_b J_{eq} + b_m b_L)}{J_m J_L}, \\
d_1 &= \frac{(K_b b_{eq} + G_R R_{P1} R_{P2} K_b K_{pL})}{J_m J_L}, \\
d_0 &= \frac{G_R R_{P1} R_{P2} K_b K_{iL}}{J_m J_L}.
\end{aligned} \tag{3.16}$$

Singular perturbation analysis pertaining to this control scheme results in the following slow and fast characteristic polynomials:

$$\psi_{ls}(s, \varepsilon) \approx s^2 + \beta_1 s + \beta_0 \tag{3.17a}$$

$$\psi_{lf}(p, \varepsilon) \approx p^2 - \beta_1' p + \beta_0' \tag{3.17b}$$

where

$$\begin{aligned}
\beta_1 &= \frac{G_R^2 R_{P2}^2 b_m + R_{P1}^2 b_L + G_R R_{P2} R_{P1} K_{pL}}{G_R^2 R_{P2}^2 J_m + R_{P1}^2 J_L}, \\
\beta_0 &= \frac{G_R R_{P2} R_{P1} K_{iL}}{G_R^2 R_{P2}^2 J_m + R_{P1}^2 J_L}, \\
\beta_1' &= \frac{G_R^2 R_{P2}^2 b_m + R_{P1}^2 b_L + G_R^2 R_{P2}^2 K_{pL}}{G_R^2 R_{P2}^2 J_m + R_{P1}^2 J_L} \varepsilon, \\
\beta_0' &= \frac{G_R^2 R_{P2}^2 J_L + R_{P1}^2 J_m}{J_m J_L}.
\end{aligned} \tag{3.18}$$

Note that the slow subsystems are stable for all K_{pL}, $K_{iL} > 0$. However, the fast subsystem is unstable for all $K_{pL} > 0$ and $K_{iL} > 0$. Also, note that the characteristic polynomials given by equations (3.12b) and (3.17b) are identical when $\varepsilon = 0$. Thus, analyzing the limiting case of an infinitely stiff belt, that is, $\varepsilon = 0$ will not reveal the instability exhibited by (3.17b).

The load speed ω_L can attain steady-state only when motor speed ω_m attains steady-state first. This is shown by the following differential equation,

$$J_L\ddot{\omega}_L + b_L\dot{\omega}_L + R_{P2}^2 K_b\omega_L = R_{P1}R_{P2}K_b\omega_m, \tag{3.19}$$

which is obtained by differentiating (3.1b). Even when the motor speed ω_m attains steady-state, ω_L continues to exhibit damped oscillations. Thus, by measuring only ω_L and using the control law given by (3.14), the damped oscillations of the load speed cannot be distinguished from oscillations due to the motor speed fluctuations. Therefore, the controller reacts also to the damped oscillations of the load speed, hence avoiding ω_m (and as a consequences also ω_l) to settle to its steady-state value. Thus, the control law given by (3.14) does not present a desirable situation.

3.4 Simultaneous Motor and Load Speed Feedback Control Scheme

In this scheme, the load speed control corrects directly the torque input to the system as shown in Figure 3.5. The closed-loop transfer function from ω_{rL} to ω_L is given by

$$\frac{\omega_L(s)}{\omega_{rL}(s)} = \frac{\alpha_{mLt}}{\psi_{mLt}(s)} \tag{3.20}$$

where

$$\begin{aligned} \alpha_{mLt}(s) &= a_1 s + a_0, \\ a_1 &= \frac{(G_R R_{P1} R_{P2} K_b K_{pL} + G_R R_{P2} K_{pm}/R_{P1})}{J_m J_L}, \\ a_0 &= \frac{(G_R R_{P1} R_{P2} K_b K_{iL} + G_R R_{P2} K_{im}/R_{P1})}{J_m J_L}. \end{aligned} \tag{3.21}$$

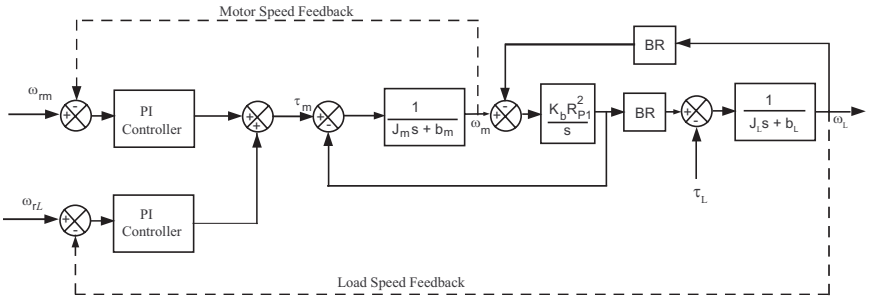

Figure 3.5: Simultaneous motor and load speed feedback scheme: Torque mode

$$\begin{aligned}
\psi_{mLt}(s) &= s^4 + f_3 s^3 + f_2 s^2 + f_1 s + f_0, \\
f_3 &= \frac{(b_m J_L + J_m b_L + J_L K_{pm})}{J_m J_L}, \\
f_2 &= \frac{(K_b J_{eq} + b_m b_L + K_{pm} b_L + J_L K_{im})}{J_m J_L}, \\
f_1 &= \frac{(K_b b_{eq} + G_R^2 K_b K_{pm} + K_{im} b_L + G_R R_{P1} R_{P2} K_b K_{pL})}{J_m J_L}, \\
f_0 &= \frac{K_{im} G_R^2 R_{P2}^2 K_b + G_R R_{P1} R_{P2} K_b K_{iL}}{J_m J_L}.
\end{aligned} \tag{3.22}$$

Note that the coefficients f_0 to f_3 depend on the gains of the control law. Singular perturbation analysis for this case results in the slow and fast characteristic polynomials as

$$\psi_{mls}(s, \varepsilon) \approx s^2 + \gamma_1 s + \gamma_0 \tag{3.23a}$$

$$\psi_{mlf}(p, \varepsilon) \approx p^2 + \gamma_1' p + \gamma_0' \tag{3.23b}$$

where

$$\begin{aligned}
\gamma_1 &= \frac{G_R^2 R_{P2}^2 b_m + R_{P1}^2 b_L + G_R R_{P2} R_{P1} K_{pL} + G_R^2 R_{P2}^2 K_{pm}}{G_R^2 R_{P2}^2 J_m + R_{P1}^2 J_L}, \\
\gamma_0 &= \frac{G_R^2 R_{P2}^2 K_{im} + G_R R_{P2} R_{P1} K_{iL}}{G_R^2 R_{P2}^2 J_m + R_{P1}^2 J_L}, \\
\gamma_1' &= \frac{G_R^2 R_{P2}^2 b_m + R_{P1}^2 b_L + G_R^2 R_{P2}^2 K_{pL} + G_R^2 R_{P2}^2 K_{pm} (J_L / J_m)}{G_R^2 R_{P2}^2 J_m + R_{P1}^2 J_L} \varepsilon, \\
\gamma_0' &= \frac{G_R^2 R_{P2}^2 J_L + R_{P1}^2 J_m}{J_m J_L}.
\end{aligned} \tag{3.24}$$

Therefore, the slow and fast subsystems are stable for all positive controller gains. Note that the outputs of both load speed and motor speed controller combine to form a torque input to the motor; this is typically referred to as the torque mode in practice when multiple loops such as this are employed. Another strategy is to use the output of the load speed controller as the motor speed reference correction; a block diagram of such a scheme is provided in Fig. A.1 in Appendix A. This strategy results in an unstable system which is shown in Appendix A.

3.5 Adaptive Feedforward (AFF) Compensation to Reject Load Disturbances

The use of feedforward compensation to reject known disturbances by direct cancelation or unknown disturbances by their estimation has been known to be effective in attenuating disturbances. We consider the rejection of periodic disturbances on the load by using an adaptive feedforward action based on load speed error. The control scheme that utilizes the feedforward action is shown in Figure 3.6. We use an adaptive

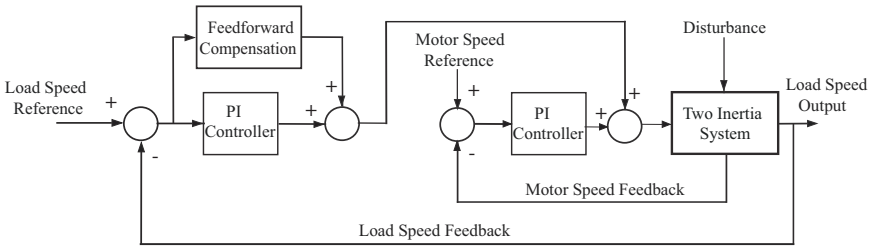

Figure 3.6: Control scheme with feedback and feedforward compensation

feedforward algorithm given in [59] that is particularly applicable in this situation as the feedforward action preserves the stability of the overall system with the feedback controller with simultaneous motor and load speed feedback. The approach is briefly discussed as applicable to this problem; the details are given in [59]. The idea is to

estimate the amplitude and phase of the disturbance for a known frequency of the disturbance. The disturbance can be expressed in the form

$$\begin{aligned} d &= \theta_1^* \cos(\omega t) + \theta_2^* \sin(\omega t) \\ &:= \phi(t) w_0^* \end{aligned} \tag{3.25}$$

where ω is a known frequency, θ_1^* and θ_2^* are unknown parameters. The adaptation laws for the unknown parameters θ_1^* and θ_2^* are given by the following simple pseudo-gradient algorithm:

$$\dot{\theta}_1 = \gamma e(t) \cos(\omega t), \tag{3.26a}$$

$$\dot{\theta}_2 = \gamma e(t) \sin(\omega t), \tag{3.26b}$$

where θ_1 and θ_1 are the parameter estimates, $e(t) = \omega_{rL} - \omega_L$ is the load speed error, and γ is the adaptation gain. Using the estimated parameters, the feedforward control action is given by

$$u_f = -\theta_1 \cos(\omega t) - \theta_2 \sin(\omega t). \tag{3.27}$$

The estimation of the disturbance and its cancelation when the load speed error contains a sinusoidal component with frequency ω may be intuitively explained as follows. If the load speed error is $e(t) = \bar{e}(t) + e_{\theta_1} \sin(\omega t)$, in the adaptive algorithm the product $e(t) \sin(\omega t)$ will generate a positive $e_{\theta_1} \sin^2(\omega t)$ term. This will result in a parameter drift which results in the attenuation of disturbance until it reaches its nominal value. At this point the load speed error is free of the sinusoidal component as the disturbance is compensated by feedforward control u_f. With the compensation, the product term $e(t) \sin(\omega t)$ in the parameter adaptive law becomes zero and the parameter estimates converge. Since the regressor vector $\phi(t)$ is persistently exciting, the parameter vectors converge to zero. In fact, this adaptive feedforward action with

estimation of disturbance parameters using the pseudo-gradient algorithm has been shown to be equivalent to the use of the internal model of the disturbance in [59].

3.6 Web Tension Control

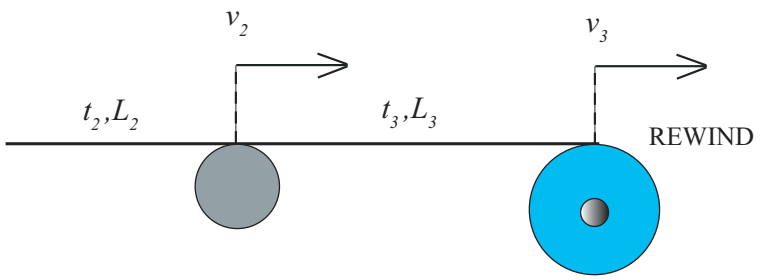

Figure 3.7: Rewind section

Consider a rewind section as shown in Figure 3.7. This section is a part of R2R system shown in Figure 2.3. The web span tension dynamics in the rewind section is given by

$$\dot{t}_3 = \frac{EA_w}{L_3}(v_3 - v_2) + \frac{1}{L_3}(t_2 v_2 - t_3 v_3). \tag{3.28}$$

The periodic torque disturbance is injected on the load side of the rewind roll by employing a brake. The disturbance is expressed in the form of equation (4.63). The injected disturbance affects the velocity v_3 and as a consequences to web tension t_3. The relation between the web velocity v_3 and web tension t_3 can be seen through equation (3.28). It is assumed that the velocity v_2 is well regulated. The proposed load speed regulation scheme is applied to rewind roll to regulate velocity v_3 in the presence of disturbance on load side and this control scheme is expected to regulate web tension due to dynamics between velocity and tension.

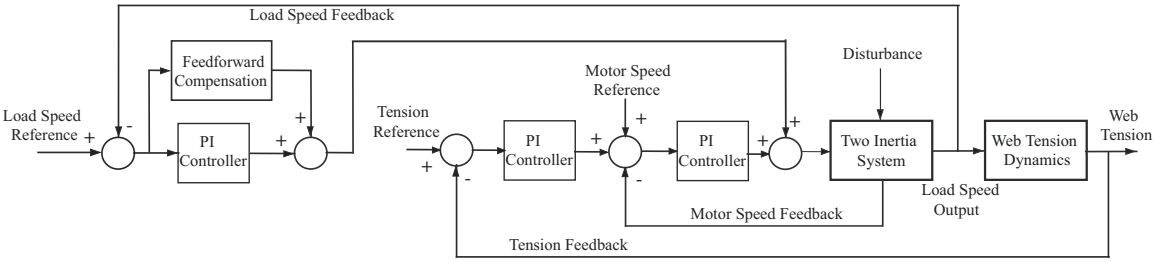

Figure 3.8: Load speed control scheme for web tension control

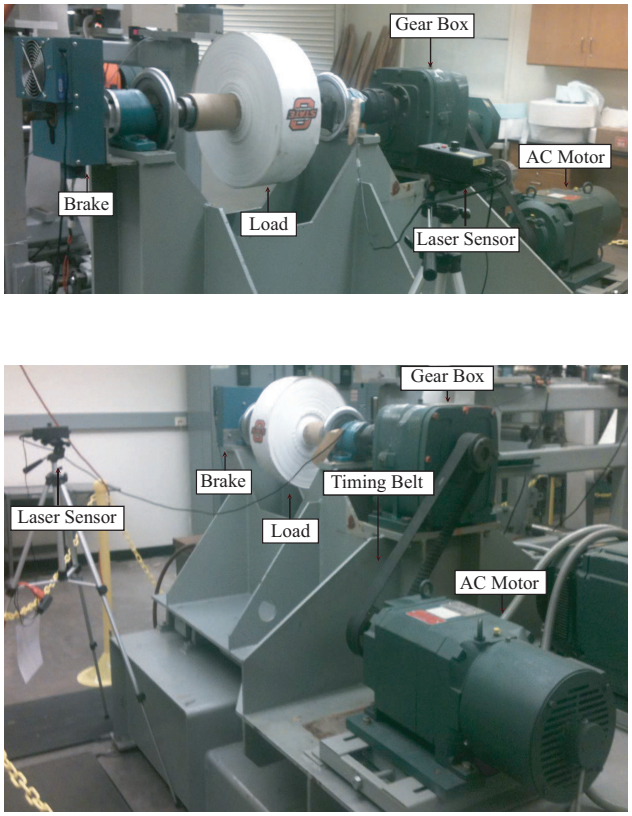

Figure 3.9: Picture of the experimental platform. Top view: Load side. Bottom view: Motor side.

3.7 Experiments

A picture of experimental setup is shown in Figure 3.9. It consists of an AC motor shaft connected to the load shaft (roll) via a belt-pulley and gear-pair transmission. A 15 HP (11.19 KW) AC motor with a rated speed of 1750 RPM is employed.

The belt ratio ($BR = (R_{P2}/R_{P1})G_R$) for the transmission is 3.825. An encoder on the motor shaft is employed to measure the motor shaft speed and a laser sensor is used to measure the load shaft speed. The real-time hardware, including the drives, controller, and communication network, was provided by Rockwell Automation (Allen-Bradley). All the real-time hardware components of the machine are connected through a ControlNet communication network. The network is updated every 5 ms (Network Update Time) and data is communicated to the network every 10 ms (Request Package Interval). A brake is attached on the other side of the load shaft to inject periodic torque disturbances; a magnetic clutch brake (Magpower GBC 90) that can apply 26 lb-ft torque is used.

The PI controller gains for the motor speed loop were chosen to be $K_{pm} = 15$ and $K_{im} = 3.09$ and for the load speed loop to be $K_{pL} = 0.07$ and $K_{iL} = 0.001$. A number of experiments were conducted at different reference speeds to evaluate the performance of proposed control scheme. In each experiment, the brake provides an external periodic disturbance torque of the form $A + B\sin(\omega_d t)$ $(A = 2, B = 1.5)$. The following disturbance frequencies were injected to evaluate the control schemes: $\omega_d = 0.05, 0.15, 0.25$ Hz. These disturbances are typical of the disturbances that are observed in roll-to-roll manufacturing machines where such transmission systems are typically employed. The adaptation gain $\gamma = 1$ is chosen and the initial values of the estimates are set to zero.

The proposed control scheme is extended to an R2R system and implemented in the rewind section of experimental platform shown in Figure 2.1. The experiments are performed at web speed reference of 150 FPM and 200 FPM, and web tension reference of 20 lbf. A disturbance torque of the form $A + B\sin(\omega_d t)$ $(A = 1.3, B = 1)$ is applied using a brake attached on the load side. Disturbances of frequencies 0.25 Hz

and 0.3 Hz are injected at 150 FPM and 200 FPM, respectively. The upstream pull roll to the rewind section is under pure speed control. The proposed motor and load speed feedback control scheme with adaptive feedforward is applied to the rewind roll and compared with a commonly used motor speed feedback scheme. The tension and velocity response real-time data are collected for each scenario.

Figure 3.10 shows the evolution of the load speed (reflected to the motor side) in the presence of disturbance with frequency 0.25 Hz when the reference speed is 719 RPM with and without the use of the adaptive feedforward action. Figure 3.11 shows the Fast Fourier Transform (FFT) of the load speed for the two cases. It is evident that the control scheme with the AFF action (shown in Figure 3.6) can provide significantly improved load speed regulation. Figure 3.12 control torque input corresponding to the two cases, without and with adaptive feedforward compensation. It is evident that the torque input is larger when the adaptive feedforward is employed. Table 3.1 shows the standard deviation of the load speed signal from its reference for the various schemes. It is clear that the employing load speed feedback in addition to motor speed feedback can improve performance. Further, use of the adaptive feedforward action based on load speed feedback can significantly improve the regulation performance.

Table 3.1: Comparison of different control schemes

Disturbance Frequency	Standard Deviation		
	Only Motor Feedback	Motor + Load Feedback	Motor + Load Feedback + AFF
0.25 Hz	2.09	1.35	0.34
0.15 Hz	4.71	3.53	0.87
0.05 Hz	3.89	2.47	0.68

Figure 3.13 shows web tension response in the presence of disturbance with fre-

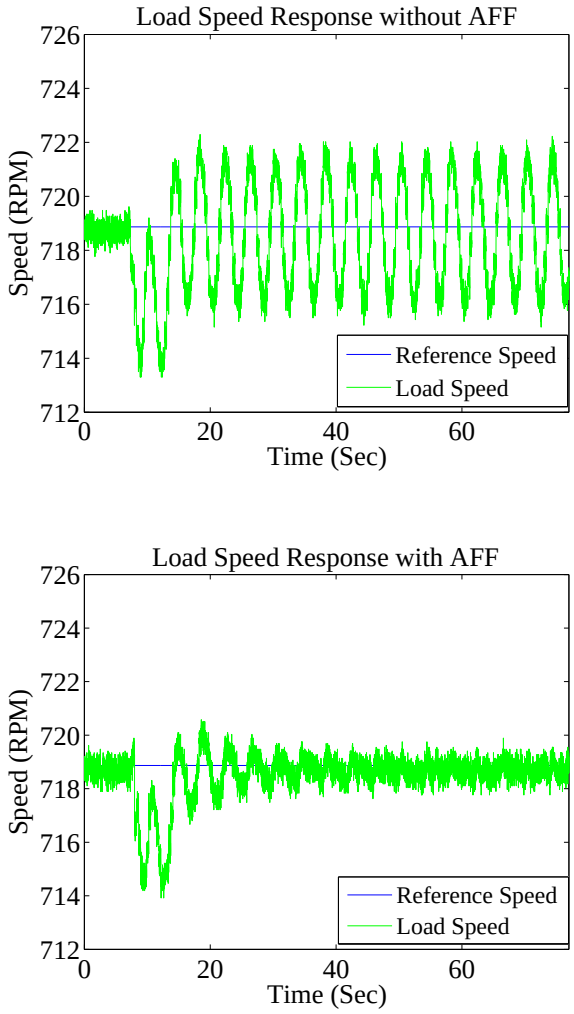

Figure 3.10: Load speed response with 0.25 Hz torque disturbance. Top: Without AFF. Bottom: With AFF

quency 0.25 Hz at 150 FPM. The control strategy that uses only motor speed was unable to attenuate the disturbance which is reflected in the tension response (shown in Figure 3.13(a)). The motor and load speed feedback control scheme attenuates disturbance in tension response; however the attenuation is not significant (shown in Figure 3.13(b)). The proposed control scheme with feedforward action rejects the disturbance and regulates the tension to its desired value (shown in Figure 3.13(c)).

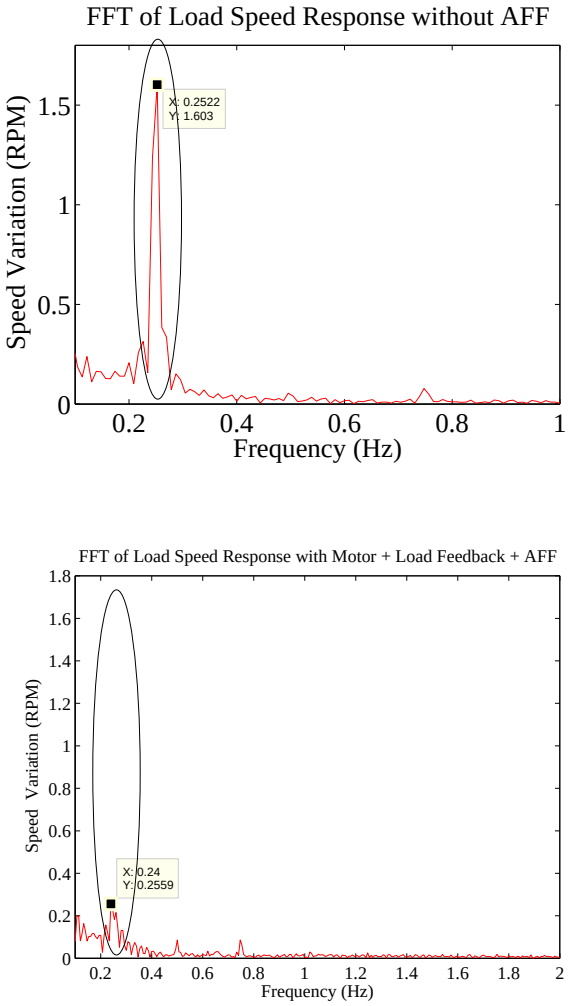

Figure 3.11: FFT of load speed response with and without AFF

Figure 3.14 shows the FFT of the tension response with three separate control schemes. The proposed control scheme attenuates the disturbance amplitude at 0.25 Hz significantly. Figure 3.15 shows corresponding load and motor speed response in the presence of disturbance at 150 FPM. Similar results can be seen at 200 FPM which are provided in Figures 3.16 to 3.18.

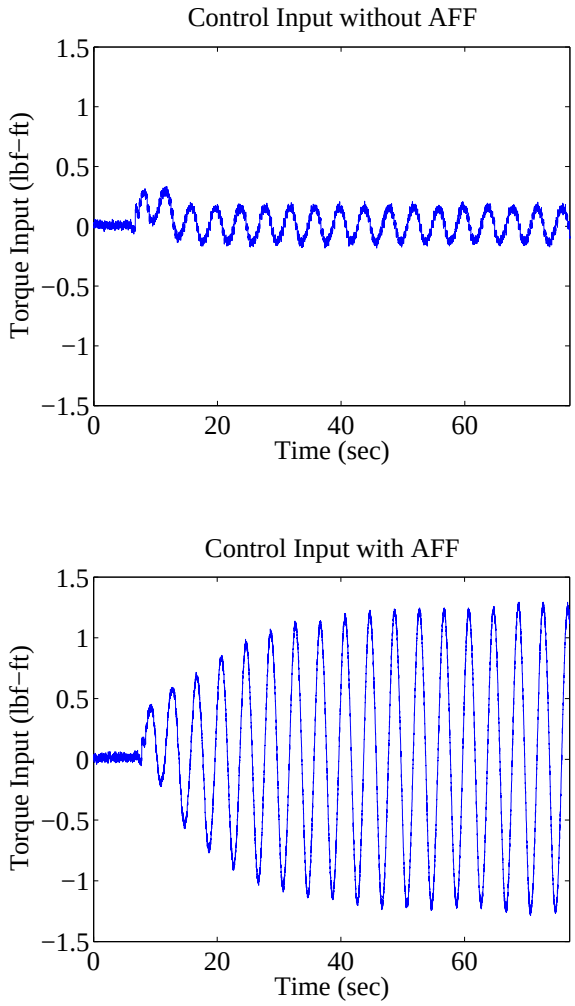

Figure 3.12: Control input with 0.25 Hz torque disturbance. Top: Without AFF. Bottom: With AFF

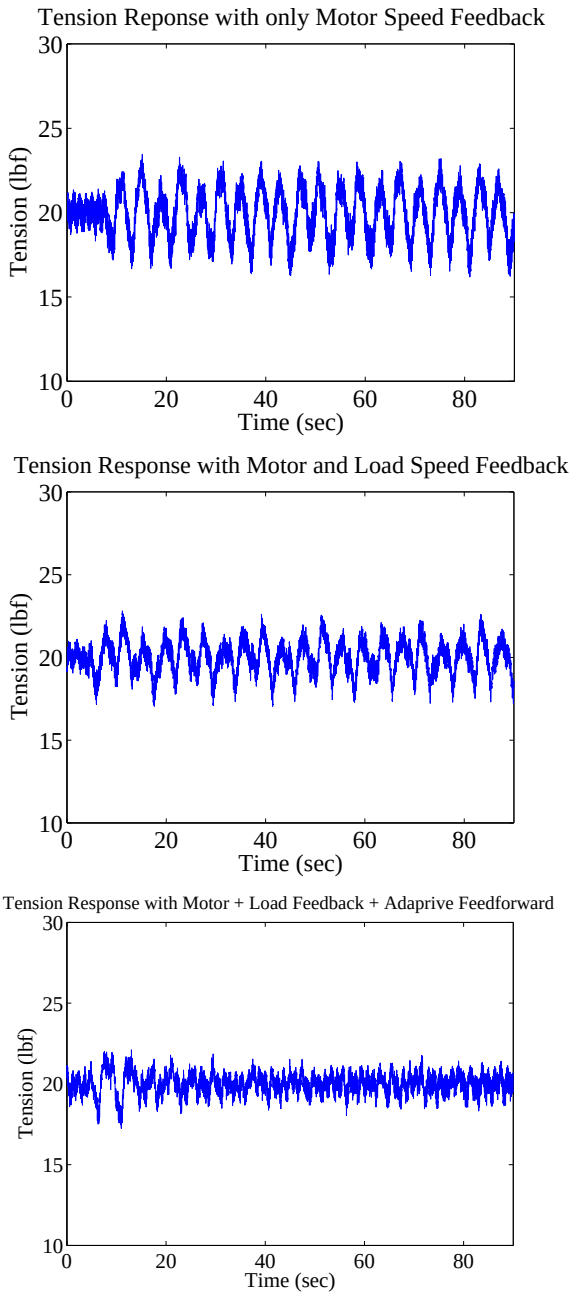

Figure 3.13: Tension response at 150 FPM with 0.25 Hz disturbance; Top: only motor feedback, Middle: motor + load feedback, Bottom: motor + load feedback + AFF

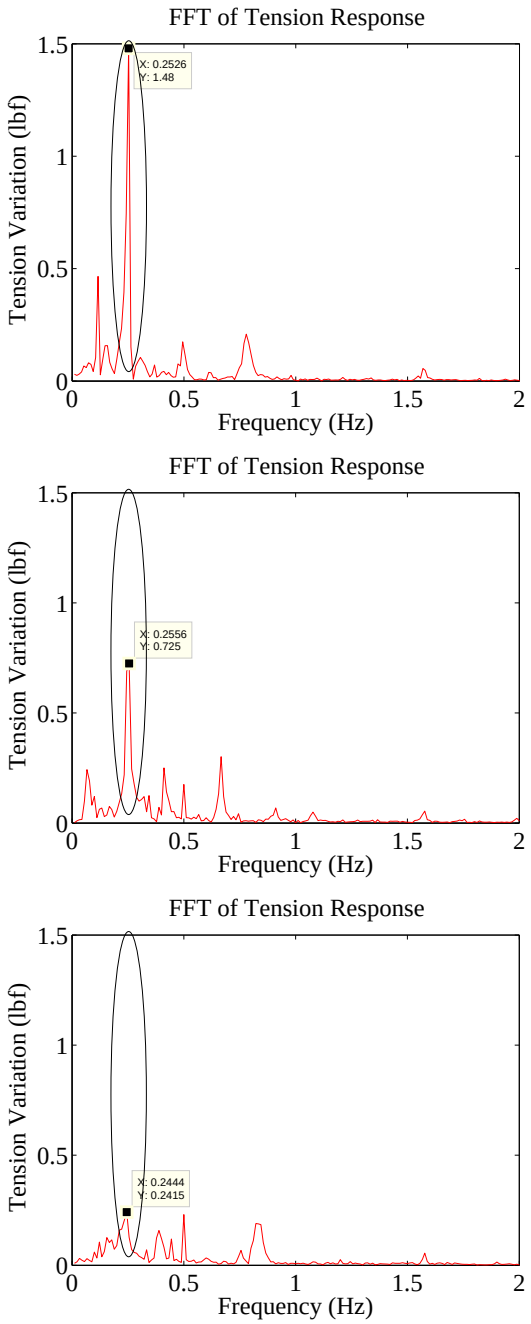

Figure 3.14: FFT of tension response at 150 FPM with 0.25 Hz disturbance; Top: only motor feedback, Middle: motor + load feedback, Bottom: motor + load feedback + AFF

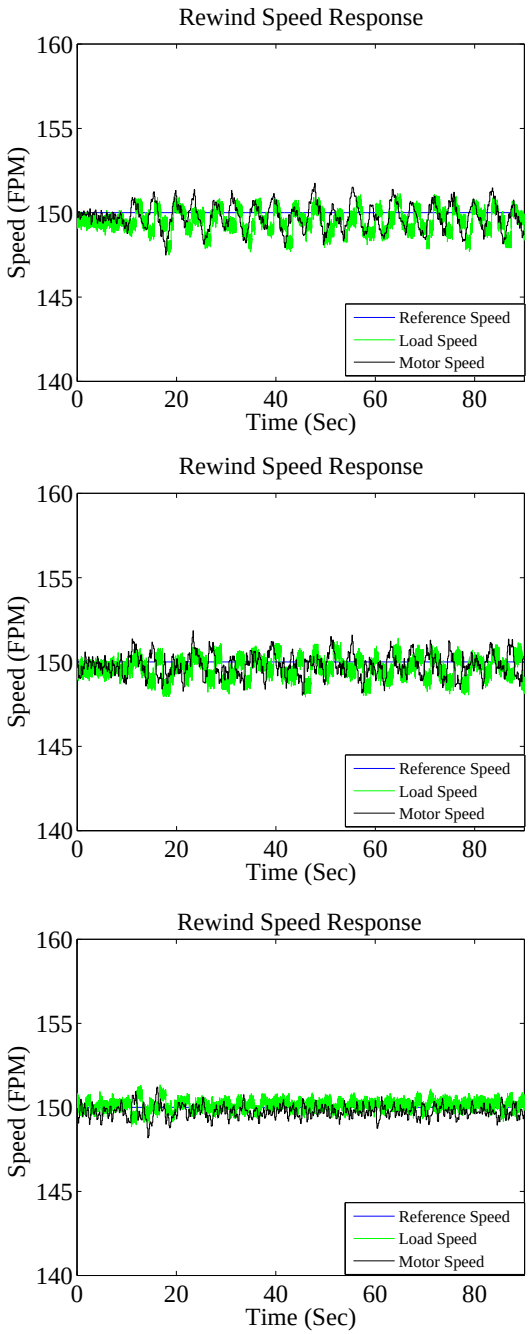

Figure 3.15: Load speed and motor speed response at 150 FPM with 0.25 Hz disturbance; Top: only motor feedback, Middle: motor + load feedback, Bottom: motor + load feedback + AFF

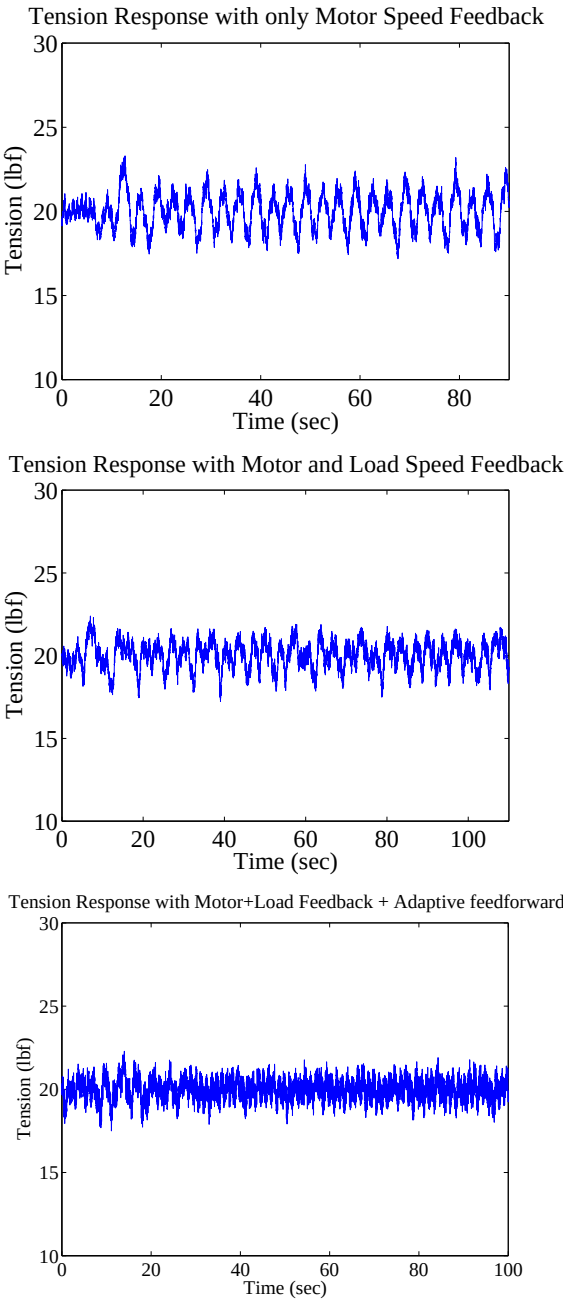

Figure 3.16: Tension response at 200 FPM with 0.3 Hz disturbance; Top: only motor feedback, Middle: motor + load feedback, Bottom: motor + load feedback + AFF

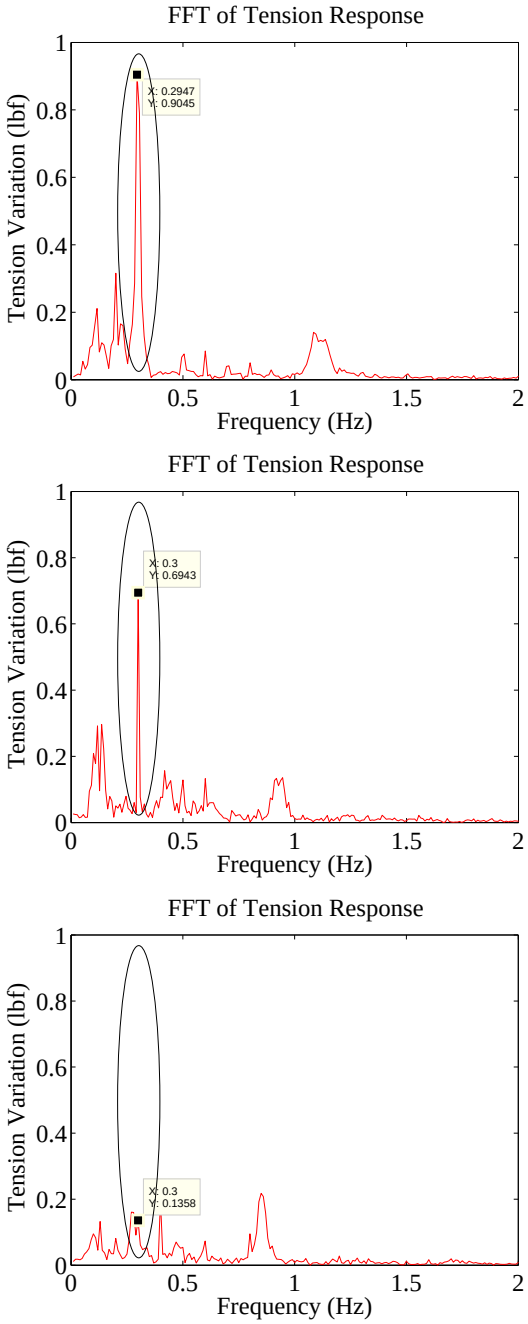

Figure 3.17: FFT of tension response at 200 FPM with 0.3 Hz disturbance; Top: only motor feedback, Middle: motor + load feedback, Bottom: motor + load feedback + AFF

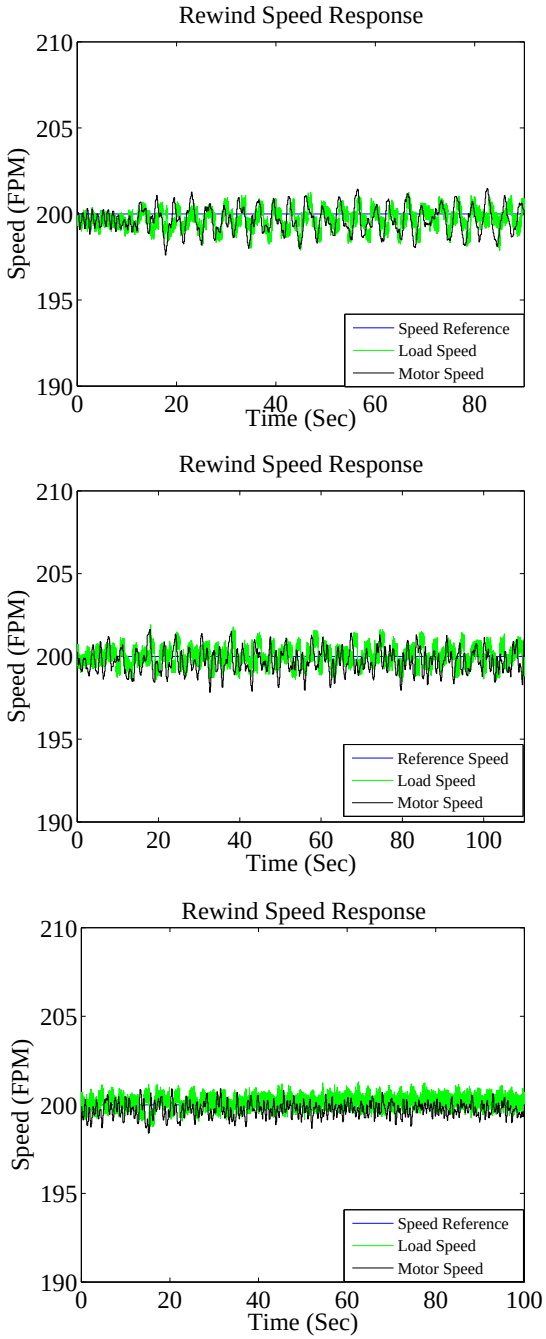

Figure 3.18: Load speed and motor speed response at 200 FPM with 0.3 Hz disturbance; Top: only motor feedback, Middle: motor + load feedback, Bottom: motor + load feedback + AFF

CHAPTER 4

Output Regulation of Nonlinear Systems with Application to Roll-to-Roll Manufacturing Systems

In this chapter, we consider the problem of regulating the output of the nonlinear system to a specified reference in the presence of disturbances with application to R2R manufacturing systems. We assume that the disturbances are sinusoidal functions of known frequency, but their phase and amplitude are unknown. This is a reasonable approximation in R2R manufacturing systems because the frequency of the disturbing force due to out-of-round or eccentric rollers is known but the amplitude and phase may not be known. The initial conditions for the exogenous system associated with the disturbance are assumed to be unknown parameters and the amplitude and phase of the disturbance are estimated. We use a gradient-based parameter estimation technique provided in [62], and the parameter estimates in conjunction with the solution of the differential-algebraic equation help to determine the feedforward control component. If the differential algebraic system of equations can be solved exactly and if the initial conditions of the system are close to the "ideal" feedforward trajectory of the system at the beginning, then the regulation error decays asymptotically. An output regulator with integral feedback action is effective in eliminating steady state error and is also developed in this work. The output regulator also has the ability to reject multiple frequency components.

We design and implement the proposed scheme for control of web tension in a large experimental R2R platform which can transport a variety of web materials. First the

tension output regulator is applied in the unwind section. A velocity disturbance is injected in the master speed roller and the output regulator is tested for disturbance rejection. Second the output regulator is applied in the pull roll and rewind sections and investigated for disturbance rejection with integral action. The ability of the output regulator to reject multiple frequency components is also investigated in this chapter. Comparative experimental results with the nonlinear output regulation scheme and an industrial PI scheme are presented and discussed. Experimental results of the nonlinear output regulation scheme with integral feedback control and its application to R2R manufacturing system are also presented and discussed.

The remainder of the chapter is organized as follows. The nonlinear system under consideration, governing equations for web speed and web tension for a typical R2R system, and the control objective are given in Section 4.1. The proposed solution to the output regulation problem in the presence of periodic disturbances is given in Section 4.2. The tension output regulator with integral feedback control action is presented in Section 4.3. The ability of the tension output regulator to reject multiple harmonics is discussed in Section 4.4. The effect of backlash in mechanical transmissions on web tension is discussed in Section 4.5. Web tension observer design is discussed in Section 4.6. Experimental setup, application of the output regulation scheme to the R2R system, and experimental procedure are discussed in Section 4.7. Comparative experimental results are presented and discussed in Section 4.8.

4.1 Problem Statement

We consider nonlinear systems of the form:

$$\dot{\mathbf{x}} = \mathbf{f}(\mathbf{x}) + \mathbf{g_1}(\mathbf{x})d(t) + \mathbf{g_2}(\mathbf{x})\mathbf{u}, \tag{4.1a}$$

$$y = h(\mathbf{x}). \tag{4.1b}$$

Equation (4.1a) describes the evolution of a nonlinear system with state $\mathbf{x}$, defined on a neighborhood $\mathbf{X}$ of the origin of $\mathbb{R}^n$, and input to the system $\mathbf{u}(t) \in \mathbb{R}^r \; \forall t \geq 0$. The term $d(t)$ represents a disturbing input to the system. The second equation (4.1b) defines the output of the system $y(t) \in \mathbb{R}^m$. Without loss of generality, we will assume that $\mathbf{f}(0) = 0$ and $h(0) = 0$, thus the system (4.1) has an equilibrium state $\mathbf{x} = 0$ when $\mathbf{u}(t) = 0,\ d(t) = 0$. We will also assume that the functions $\mathbf{f}(\mathbf{x})$, $\mathbf{g_1}(\mathbf{x})$ and $\mathbf{g_2}(\mathbf{x})$ are sufficiently smooth. Governing equations for many engineering and manufacturing applications may be cast into the form given by (4.1). In the following we discuss and present the governing equations for R2R manufacturing systems.

The governing equations for web speed on the roller and web tension for each section of the R2R system shown in Figure 2.3 are given below [15]:

Unwind section:

$$\dot{v}_0 = \frac{R_0^2}{J_0} t_1 - \frac{b_{f0}}{J_0} v_0 + \frac{R_0}{J_0} n_0 u_0 - \frac{1}{2\pi} \left(\frac{h_w}{R_0^2} - \frac{2\pi\rho A_w R_0^2}{J_0} \right) v_0^2 \tag{4.2}$$

$$\dot{t}_1 = \frac{EA_w}{L_1}(v_1 - v_0) + \frac{1}{L_1}(t_0 v_0 - t_1 v_1) \tag{4.3}$$

Master speed roller:

$$\dot{v}_1 = \frac{R_1^2}{J_1}(t_2 - t_1) - \frac{b_{f1}}{J_1} v_1 + \frac{R_1}{J_1} n_1 u_1. \tag{4.4}$$

Process section:

$$\dot{v}_2 = \frac{R_2^2}{J_2}(t_3 - t_2) - \frac{b_{f2}}{J_2} v_2 + \frac{R_2}{J_2} n_2 u_2 \tag{4.5}$$

$$\dot{t}_2 = \frac{EA_w}{L_2}(v_2 - v_1) + \frac{1}{L_2}(t_1 v_1 - t_2 v_2) \tag{4.6}$$

Rewind section:

$$\dot{v}_3 = -\frac{R_3^2}{J_3} t_3 - \frac{b_{f3}}{J_3} v_3 + \frac{R_3}{J_3} n_3 u_3 - \frac{1}{2\pi}\left(\frac{h_w}{R_3^2} + \frac{2\pi\rho A_w R_3^2}{J_3}\right) v_3^2 \tag{4.7}$$

$$\dot{t}_3 = \frac{EA_w}{L_3}(v_3 - v_2) + \frac{1}{L_3}(t_2 v_2 - t_3 v_3) \tag{4.8}$$

where h_w is the web thickness, ρ is the density of the web material and rest of nomenclature are similar to given in equations (2.1) and (2.2). The governing equations (4.2) to (4.8) can be extended to industrial R2R process machines which typically contain many process sections between the master speed roll and the rewind roll. There are many disturbing forces acting on the web which may be either due to machine imperfections or process induced. Since rotating machinery is employed, these disturbing forces are periodic and appear as periodic oscillations in both measured tension and speed signals. For example, machine and roller imperfections that cause periodic disturbances include backlash and compliance in mechanical transmissions, out-of-round material rolls, and eccentric driven and idle rollers. Process induced disturbances include heating/cooling of the web required for processing the web and air flow around the web. The fundamental frequency and its harmonics are known for the R2R system since the rotating angular speed of the rollers are known. But the magnitude and phase of these periodic disturbances are not known and must be estimated online.

The control objective is to design controllers for each section to regulate web tension in the presence of these partially known periodic disturbances while transporting the web at the desired speed. Each section of the R2R system can be cast into the form of equations given by (4.1). The output is web tension and the input is the motor torque.

4.2 Output Regulation and Disturbance Rejection

A state feedback and feedforward control is considered for the output regulation and disturbance rejection problem,

$$\mathbf{u} = \mathbf{u}_f - \mathbf{K}_x(\mathbf{x} - \mathbf{x}_f), \tag{4.9}$$

where $\mathbf{K}_x \in R^{r\times n}$. Here $\mathbf{u}_f$ and $\mathbf{x}_f$ are feedforward control and the associated state when the feedforward control input alone is applied. In other words, $\mathbf{u}_f$ and $\mathbf{x}_f$ satisfy the differential algebraic constraints (4.10a) and (4.10b). The problem now reduces to the problem of finding $\mathbf{u}_f$ and $\mathbf{x}_f$ satisfying the following differential algebraic equations.

$$\dot{\mathbf{x}}_f = \mathbf{f}(\mathbf{x}_f) + \mathbf{g}_1(\mathbf{x}_f)\hat{d} + \mathbf{g}_2(\mathbf{x}_f)\mathbf{u}_f, \tag{4.10a}$$

$$0 = h(\mathbf{x}_f). \tag{4.10b}$$

where $\hat{d}$ is the estimate of partially unknown disturbances. We first discuss a solution procedure for solving these differential-algebraic system of equations (4.10) followed by a method to attenuate the disturbances [53], [63].

4.2.1 Solution procedure for differential-algebraic system of equations

The function $\mathbf{f}(\mathbf{x}_f)$ is approximated with the first two terms in the Taylor series expansion of $\mathbf{f}(\mathbf{x}_f)$. The time variable is discretized into $N+1$ time instants as t_n $(n = 0, 1, ..., N)$. The time steps are assumed to be uniform and each time step is $\Delta t := t_n - t_{n-1}$. The state vector $\mathbf{x}_f(t)$ at the time instant t_n is denoted as

$$\mathbf{x}_f(t = t_n) = \mathbf{x}_f^{(n)}, \quad n = 0, 1, ..., N. \tag{4.11}$$

Using the backward difference formula $\dot{\mathbf{x}}_f(t_{n+1})$ may be discretized as

$$\dot{\mathbf{x}}_f(t_{n+1}) = \frac{\mathbf{x}_f^{(n+1)} - \mathbf{x}_f^{(n)}}{\Delta t}, \tag{4.12}$$

and the equations (4.10a) and (4.10b) at time instant t_{n+1} can be written as

$$\frac{\mathbf{x}_f^{(n+1)} - \mathbf{x}_f^{(n)}}{\Delta t} = \mathbf{f}(\mathbf{x}_f^{(n+1)}) + \mathbf{g_1}(\mathbf{x}_f^{(n+1)})\hat{d} + \mathbf{g_2}(\mathbf{x}_f^{(n+1)})\mathbf{u}_f^{(n+1)}, \tag{4.13}$$

$$0 = h(\mathbf{x}_f^{(n+1)}). \tag{4.14}$$

Define variables $z^{(n)}$ and $v^{(n)}$ as:

$$z^{(n)} := \mathbf{x}_f^{(n+1)} - \mathbf{x}_f^{(n)}, \tag{4.15}$$

$$v^{(n)} := \mathbf{u}_f^{(n+1)} - \mathbf{u}_f^{(n)}. \tag{4.16}$$

If the time step Δt were sufficiently small, the variables $z^{(n)}$ and $v^{(n)}$ may be assumed to be $<< 1$. The functions $\mathbf{f}(\mathbf{x}_f^{(n+1)})$, $\mathbf{g}_1(\mathbf{x}_f^{(n+1)})$, and $\mathbf{g}_2(\mathbf{x}_f^{(n+1)})$ may be expanded using the Taylor series as:

$$\begin{aligned}
\mathbf{f}(\mathbf{x}_f^{(n+1)}) &= \mathbf{f}(\mathbf{x}_f^{(n)} + z^{(n)}), \\
&= \mathbf{f}(\mathbf{x}_f^{(n)}) + \frac{\partial \mathbf{f}}{\partial \mathbf{x}_f}(\mathbf{x}_f^{(n)})\, z^{(n)} + O(|z^{(n)}|^2), \\
\mathbf{g}_1(\mathbf{x}_f^{(n+1)}) &= \mathbf{g}_1(\mathbf{x}_f^{(n)} + z^{(n)}), \\
&= \mathbf{g}_1(\mathbf{x}_f^{(n)}) + \frac{\partial \mathbf{g}_1}{\partial \mathbf{x}_f}(\mathbf{x}_f^{(n)})\, z^{(n)} + O(|z^{(n)}|^2), \\
\mathbf{g}_2(\mathbf{x}_f^{(n+1)}) &= \mathbf{g}_2(\mathbf{x}_f^{(n)} + z^{(n)}), \\
&= \mathbf{g}_2(\mathbf{x}_f^{(n)}) + \frac{\partial \mathbf{g}_2}{\partial \mathbf{x}_f}(\mathbf{x}_f^{(n)})\, z^{(n)} + O(|z^{(n)}|^2).
\end{aligned}$$

Since $z^{(n)} << 1$, the higher order terms in the Taylor series expansion $O(|z^{(n)}|^2)$ may be neglected. Then the function $\mathbf{f}(\mathbf{x}_f^{(n+1)}) + \mathbf{g_1}(\mathbf{x}_f^{(n+1)})\hat{d} + \mathbf{g}_2(\mathbf{x}_f^{(n+1)})\mathbf{u}_f^{(n+1)}$ may be approximated as

$$\begin{aligned}
\mathbf{f}(\mathbf{x}_f^{(n+1)}) + \mathbf{g_1}(\mathbf{x}_f^{(n+1)})\hat{d} + \mathbf{g}_2(\mathbf{x}_f^{(n+1)})\mathbf{u}_f^{(n+1)} &\approx \mathbf{f}(\mathbf{x}_f^{(n)}) + \mathbf{g_1}(\mathbf{x}_f^{(n)})\hat{d} + \mathbf{g}_2(\mathbf{x}_f^{(n)})\mathbf{u}_f^{(n)} \\
&+ \mathbf{g}_2(\mathbf{x}_f^{n})v^{(n)} + \left[\frac{\partial \mathbf{f}}{\partial \mathbf{x}_f}(\mathbf{x}_f^{(n)}) + \frac{\partial \mathbf{g}_1}{\partial \mathbf{x}_f}(\mathbf{x}_f^{(n)})\hat{d} + \frac{\partial \mathbf{g}_2}{\partial \mathbf{x}_f}(\mathbf{x}_f^{(n)})\mathbf{u}_f^{n}\right] z^{(n)}.
\end{aligned} \tag{4.17}$$

Similarly the function $h(\mathbf{x}_f^{(n+1)})$ may be approximated as

$$h(\mathbf{x}_f^{(n+1)}) \approx h(\mathbf{x}_f^{(n)}) + \frac{\partial h}{\partial \mathbf{x}_f}(\mathbf{x}_f^{(n)})\, z^{(n)}. \tag{4.18}$$

The equations (4.13), (4.14), (4.17) and (4.18) may be arranged as a system of linear equations in terms of $z^{(n)}$ and $v^{(n)}$ as:

$$z^{(n)} = \Delta t \left[\mathbf{f}(\mathbf{x}_f^{(n)}) + \mathbf{g_1}(\mathbf{x}_f^{(n)})\hat{d} + \mathbf{g}_2(\mathbf{x}_f^{(n)})\mathbf{u}_f^{(n)}\right] + \Delta t \left[\mathbf{g}_2(\mathbf{x}_f^n)v^{(n)}\right] + \Delta t \left[\frac{\partial \mathbf{f}}{\partial \mathbf{x}_f}(\mathbf{x}_f^{(n)}) + \frac{\partial \mathbf{g}_1}{\partial \mathbf{x}_f}(\mathbf{x}_f^{(n)})\hat{d} + \frac{\partial \mathbf{g}_2}{\partial \mathbf{x}_f}(\mathbf{x}_f^{(n)})\mathbf{u}_f^n\right] z^{(n)}, \tag{4.19}$$

$$0 = h(\mathbf{x}_f^{(n)}) + \frac{\partial h}{\partial \mathbf{x}_f}(\mathbf{x}_f^{(n)})z^{(n)}. \tag{4.20}$$

Given $\mathbf{x}_f^{(n)}$, $\hat{d}$ and $\mathbf{u}_f^{(n)}$, the system of linear equations (4.19) and (4.20) can be solved for $z^{(n)}$ and $v^{(n)}$. Then, $\mathbf{x}_f(t_{n+1})$ and $\mathbf{u}_f(t_{n+1})$ are given by

$$\mathbf{x}_f^{(n+1)} = \mathbf{x}_f^{(n)} + z^{(n)}, \tag{4.21}$$

$$\mathbf{u}_f^{(n+1)} = \mathbf{u}_f^{(n)} + v^{(n)}. \tag{4.22}$$

Thus, given $\mathbf{x}_f(t_0)$, $\hat{d}(t_0)$, and $\mathbf{u}_f(t_0)$, we can compute $\mathbf{x}_f(t_n)$, $\mathbf{u}_f(t_n)$ for $n = 1, ...N$. Note that this solution procedure is perfectly suitable for digital implementation of controllers in industrial practice. The control input $\mathbf{u}(t)$ may then be obtained by using (4.9) once $\mathbf{u_f}(t)$ and $\mathbf{x_f}(t)$ are computed as outlined above.

4.2.2 Attenuation of the effect of disturbances

The disturbance $d(t)$ is considered to be the output of an exogenous linear system:

$$\dot{w} = Sw,\ d = Fw,\ w(0) = w_0^*. \tag{4.23}$$

The state of the exogenous system w is defined on a neighborhood $\mathbf{W}$ of the origin of $\mathbb{R}^s$, $S \in \mathbb{R}^{s\times s}$ and $F \in \mathbb{R}^{1\times s}$. In this case, one may not know w_0^*. The evolution equation (4.1a) can be written as

$$\dot{\mathbf{x}} = \mathbf{f}(\mathbf{x}) + \mathbf{g}_1(\mathbf{x})\phi(t)w_0^* + \mathbf{g}_2(\mathbf{x})\mathbf{u}, \tag{4.24}$$

where $\phi(t) = Fe^{St}$ is a function of sinusoids. Assuming we have the measurements of all the states, we can develop an estimate $\hat{w}_0$ to estimate w_0^* and thus obtain the estimate of the disturbance signal.

Let $\lambda > 0$ be the bandwidth of the filter to be used in the identification scheme. Let $\overline{\mathbf{x}}$ represent the filtered values of the state $\mathbf{x}(t)$, i.e.,

$$\dot{\overline{\mathbf{x}}} + \lambda \overline{\mathbf{x}} = \mathbf{x}. \tag{4.25}$$

Similarly, let ${\mathbf{W}_f}^T$ represent the filtered value of $\mathbf{g}_1(x)\phi(t)$ and $\mathbf{W_g}$ represent the filtered value of $\mathbf{g}_2(x)u(t)$ as shown below:

$$\dot{\mathbf{W}}_f^T + \lambda {\mathbf{W}_f}^T = \mathbf{g}_1(\mathbf{x})\phi(t), \tag{4.26}$$

$$\dot{\mathbf{W}}_\mathbf{g} + \lambda \mathbf{W_g} = \mathbf{g}_2(\mathbf{x})\mathbf{u}. \tag{4.27}$$

Similarly, let $\bar{\mathbf{f}}$ represent the filtered value of $\mathbf{f}(\mathbf{x})$, i.e.,

$$\dot{\bar{\mathbf{f}}} + \lambda \bar{\mathbf{f}} = \mathbf{f}(\mathbf{x}). \tag{4.28}$$

The identifier is developed as shown below:

$$\dot{\mathbf{x}} + \lambda \mathbf{x} = \mathbf{f}(\mathbf{x}) + \mathbf{g}_1(\mathbf{x})\phi(t)w_0^* + \mathbf{g}_2(\mathbf{x})\mathbf{u} + \lambda \mathbf{x}, \tag{4.29}$$

$$\mathbf{x} = \bar{\mathbf{f}} + \lambda \overline{\mathbf{x}} + {\mathbf{W}_f}^T w_0^* + \mathbf{W_g}. \tag{4.30}$$

Define output estimation error e_o as

$$e_o := \mathbf{x} - \lambda \overline{\mathbf{x}} - \overline{\mathbf{f}} - \mathbf{W_g} - {\mathbf{W}_f}^T \hat{w}_0, \tag{4.31}$$

$$= {\mathbf{W}_f}^T (w_0^* - \hat{w}_0). \tag{4.32}$$

Then consider the following gradient adaptation law

$$\dot{\hat{w}}_0 = \gamma \mathbf{W}_f e_o,\ \gamma > 0. \tag{4.33}$$

From the properties of a gradient parameter estimation scheme [62], one can conclude that $e_o(t) \to 0$ asymptotically. However, it is not guaranteed that $w_0^* - \hat{w}_0 \to 0$ asymptotically. We observed that it does converge for this problem because the condition of persistence of excitation in terms of the number of frequency components seems to be met [62]. The amplitude and phase information of a sinusoidal signal, say $\theta_1 \cos(\omega t) + \theta_2 \sin(\omega t)$ can be inferred by the two constants θ_1 and θ_2. Hence, for each sinusoidal component, one can at most have two constants and this is the condition for persistence of excitation for identifying linear systems [62]. If the solution of equation (4.33) eventually converges to w_0^*, the estimate of the disturbance can be accurately obtained. Once an estimate of $d(t)$ is known (via the estimate $\hat{w}_0$), one can compute the feedforward control ($\mathbf{u}_f$) by solving the differential algebraic system as discussed in subsection 4.2.1. Then the control as in equation (4.9) drives the states of the system to an output zeroing manifold.

Let us express the functions $\mathbf{f}$, and $\mathbf{g_2}$ as follows:

$$\mathbf{f}(\mathbf{x}) = A\mathbf{x} + \mathbf{A}_2(\mathbf{x}), \quad \mathbf{g_2}(\mathbf{x}) = B + \mathbf{B}_1(\mathbf{x}), \tag{4.34}$$

where $\mathbf{Ax}$ is the linear part of $\mathbf{f}(\mathbf{x})$, $\mathbf{A_2}(\mathbf{x})$ contains second and higher order terms of $\mathbf{f}(\mathbf{x})$, $B = \mathbf{g_2}(0)$, $\mathbf{B_1}(\mathbf{x})$ contains linear and higher order terms of $\mathbf{g}_2(\mathbf{x})$.

Theorem 4.2.1 *Suppose the following assumptions hold:*

A1: *The matrix $A - B\mathbf{K}_x$ is Hurwitz.*

A2: *All of the eigenvalues of the matrix S in equation (4.23) lie on the imaginary axis, i.e., the disturbance ($d(t)$) is purely sinusoidal and $w(t) \in \mathbf{W}$ a neighborhood of the origin of $\mathbb{R}^s$.*

A3: *The estimate ($\hat{w}_0$) converge to w_0^* or we have the complete knowledge of the disturbance.*

Then with the control $\mathbf{u}$, the output of the system (4.1) converges to zero, i.e., $y \to 0$

as $t \to \infty$, if u_f satisfies equation (4.10).

Proof: *With the control (4.9), the nonlinear system (4.1) yields the closed loop system*

$$\dot{\mathbf{x}} = \mathbf{f}(\mathbf{x}) + \mathbf{g_1}(\mathbf{x})Fw + \mathbf{g_2}(\mathbf{x})(\mathbf{u}_f - \mathbf{K}_x(\mathbf{x} - \mathbf{x}_f)). \tag{4.35}$$

Linearizing the system around the origin $\mathbf{x} = 0$, we get

$$\dot{\mathbf{x}} = A\mathbf{x} + B(\mathbf{u}_f - \mathbf{K}_x(\mathbf{x} - \mathbf{x}_f)) + Cw, \tag{4.36}$$

where A and B are as given in equation (4.34) and C is given by

$$C = \left[\frac{\partial(g_1 F)}{\partial \mathbf{x}}\right]_{\mathbf{x}=0}. \tag{4.37}$$

Similarly linearizing the equation (4.10a) and using assumption A3, we can write:

$$\dot{\mathbf{x}}_\mathbf{f} = A\mathbf{x}_f + B\mathbf{u}_f + Cw. \tag{4.38}$$

Let $\xi = \mathbf{x} - \mathbf{x}_f$. Then,

$$\begin{aligned} \dot{\xi} &= \dot{\mathbf{x}} - \dot{\mathbf{x}}_f \\ &= (A - B\mathbf{K}_\mathbf{x})\xi, \end{aligned} \tag{4.39}$$

where $\mathbf{K}_\mathbf{x}$ is selected such that $(A - B\mathbf{K}_\mathbf{x})$ is Hurwitz and therefore the origin is locally attractive equilibrium point, i.e., for $\mathbf{x}(0)$ and $\mathbf{x}_f(0)$ sufficiently close to the origin,

$$(\mathbf{x}(t) - \mathbf{x}_f(t)) \to 0 \quad as \quad t \to \infty. \tag{4.40}$$

By the continuity of $h(\mathbf{x})$ and equation (4.53), for all $\mathbf{x}(0)$ and $\mathbf{x}_f(0)$ sufficiently close to 0,

$$h(\mathbf{x}) \to h(\mathbf{x}_f) = 0 \quad as \quad t \to \infty. \tag{4.41}$$

Q.E.D.

Thus with an identifier as developed above and the control of the form (4.9), the output of the system (4.1) can be zeroed or regulated at reference value.

4.3 Output Regulator with Integral Feedback

In the preceding section, we considered only proportional action. In this section we consider both proportional and integral actions for the output regulation and disturbance regulation problems given by

$$\mathbf{u} = \mathbf{u}_f - \mathbf{K}_{xp}(\mathbf{x} - \mathbf{x}_f) - \mathbf{K}_{xi} \int (\mathbf{x} - \mathbf{x}_f) d\tau, \tag{4.42}$$

where $\mathbf{K}_{xp} \in R^{r \times n}$ and $\mathbf{K}_{xi} \in R^{r \times n}$. Let $K = [K_{xp}\ K_{xi}]$. Here $\mathbf{u}_f$ and $\mathbf{x}_f$ are feedforward control and the associated state when the feedforward control input alone is applied. In other words, $\mathbf{u}_f$ and $\mathbf{x}_f$ satisfy the differential algebraic equations (4.10a) and (4.10b). The disturbance $d(t)$ is considered to be the output of an exogenous linear system as in (4.23).

In addition to $\mathbf{f}$ and $\mathbf{g_2}$ expressed in equation (4.34), $\mathbf{h}(\mathbf{x})$ is expressed as follows:

$$\mathbf{h}(\mathbf{x}) = C\mathbf{x} + \mathbf{C}_1(\mathbf{x}) \tag{4.43}$$

where $\mathbf{Cx}$ is the linear part of $\mathbf{h}(\mathbf{x})$ and $\mathbf{C_1}(\mathbf{x})$ contains the higher order terms of $\mathbf{h}(\mathbf{x})$.

Theorem 4.3.1 *Suppose the following assumptions hold:*

A1: *The matrix* $(\mathbf{A}, \mathbf{B})$ *is stabilizable.*

A2: *The matrix* $\begin{bmatrix} A & B \\ C & 0 \end{bmatrix}$ *is of full row rank* $n + m$.

A3: *All of the eigenvalues of the matrix* S *in equation (4.23) lie on the imaginary axis, i.e., the disturbance* $d(t)$ *is purely sinusoidal and* $w(t) \in \mathbf{W}$, *a neighborhood of the origin of* $\mathbb{R}^s$.

A4: *The estimate* $\hat{w}_0$ *converge to* w_0^* *or we have the complete knowledge of the disturbance.*

Then with the control $\mathbf{u}$ *as given by* (4.42) , *the output of the system (4.1) converges*

to zero, i.e., $y \to 0$ as $t \to \infty$, if u_f satisfies equation (4.10).

Proof: *With the control (4.42), the nonlinear system (4.1) yields the closed loop system*

$$\dot{\mathbf{x}} = \mathbf{f}(\mathbf{x}) + \mathbf{g_1}(\mathbf{x})Fw + \mathbf{g_2}(\mathbf{x})(\mathbf{u}_f - \mathbf{K}_{xp}(\mathbf{x} - \mathbf{x}_f) - \mathbf{K}_{xi}\int(\mathbf{x} - \mathbf{x}_f)d\tau). \tag{4.44}$$

Linearizing the system around the origin $\mathbf{x} = 0$, we get

$$\dot{\mathbf{x}} = A\mathbf{x} + B\mathbf{u} + Ew, \tag{4.45a}$$

$$y = C\mathbf{x}. \tag{4.45b}$$

where A, B, and C are as given in equation (4.43) and E is given by

$$E = \left[\frac{\partial(g_1 F)}{\partial \mathbf{x}}\right]_{\mathbf{x}=0}. \tag{4.46}$$

Similarly linearizing the equation (4.10a) and using assumption A4, we can write:

$$\dot{\mathbf{x}}_\mathbf{f} = A\mathbf{x}_f + B\mathbf{u}_f + Ew. \tag{4.47}$$

Let $\xi = \mathbf{x} - \mathbf{x}_f$. Then,

$$\dot{\xi} = A\xi + Bu_{PI} \tag{4.48a}$$

$$y = C\xi. \tag{4.48b}$$

where u_{PI} is control input with proportional and integral actions.

Define $z = [\dot{\xi} \;\; y]^T$, and $v = \dot{u}_{PI}$, Then

$$\dot{z} = \hat{A}z + \hat{B}v. \tag{4.49}$$

where $\hat{A} = \begin{bmatrix} A & 0 \\ C & 0 \end{bmatrix}$, $\hat{B} = \begin{bmatrix} B \\ 0 \end{bmatrix}$. Rank of matrix z lie in the space $m + n$.

The combined requirements $\xi \to 0$ *and* $y \to 0$ *as* $t \to \infty$ *can be stated as: the origin of the* z *space must be accessible from the entire space. A necessary and sufficient condition for this to be possible is that the pair* $(\hat{A}, \hat{B})$ *is stabilizable. It is shown in [57] that this is equivalent to:*

- *The matrix* $(\mathbf{A}, \mathbf{B})$ *is stabilizable.*
- *The matrix* $\begin{bmatrix} A & B \\ C & 0 \end{bmatrix}$ *is full row rank,* $n + m$.

A stable linear feedback control can be designed for the transformed system given in equation (4.49) *by various methods available for linear control systems design, such as pole placement, optimal control, etc. The control law is of the form*

$$v = Kz. \tag{4.50}$$

where $K = [K_{xp}\ K_{xi}^{'}]$ *is gain matrix. Now after transformation to the original system the control input is*

$$u_{PI} = K_{xp}\xi + K_{xi}^{'} \int y d\tau + c. \tag{4.51}$$

where c *is the initial condition and* $y = C\xi$. *The control law can be expressed as*

$$u_{PI} = K_{xp}(x - x_f) + K_{xi} \int (x - x_f) d\tau. \tag{4.52}$$

This control law ensures that the output of the system converges to zero, i.e., $y \to 0$ *as* $t \to \infty$. *For* $\mathbf{x}(0)$ *and* $\mathbf{x}_f(0)$ *sufficiently close to the origin, we have*

$$(\mathbf{x}(t) - \mathbf{x}_f(t)) \to 0 \quad as \quad t \to \infty. \tag{4.53}$$

By the continuity of $h(\mathbf{x})$ *and equation (4.53), for all* $\mathbf{x}(0)$ *and* $\mathbf{x}_f(0)$ *sufficiently close to the origin, we have*

$$h(\mathbf{x}) \to h(\mathbf{x}_f) = 0 \quad as \quad t \to \infty. \tag{4.54}$$

Q.E.D.

Thus with a disturbance identifier and the control of the form (4.42), the output of the system (4.1) can be zeroed or regulated at a given reference value.

4.4 Disturbances with Multiple Frequency Components

In the preceding analysis we considered rejection of disturbance with only one frequency component. The output regulator design is capable of rejecting multiple frequency components. The disturbance identifier must be designed to estimate all the parameters involved in disturbance signal that can be expressed as

$$\begin{aligned} d(t) &= A_1 \sin(\omega_1 t + \phi_1) + \ldots + A_n \sin(n\omega_1 t + \phi_n) \\ &= A_1 \cos(\phi_1) \sin(\omega_1 t) + A_1 \sin(\phi_1) \cos(\omega_1 t) + \ldots \\ &+ A_n \cos(\phi_n) \sin(n\omega_1 t) + A_n \sin(\phi_n) \cos(n\omega_1 t) \end{aligned} \tag{4.55}$$

where A_1,.....,A_n, and ϕ_1,.....,ϕ_n are parameters to be estimated, and ω_1 is the known frequency of disturbance. The stability properties are not affected by the number of frequency components if the persistent of excitation condition is satisfied and assumption A4 is true.

4.5 Compensation of Transmission Backlash Effect on Web Tension

In any R2R machine, the process section typically contains many driven rollers in addition to the unwind, the rewind, and the master speed roller. The imperfections in the machine due to out-of-round material rolls, eccentric driven and idle rollers, and backlash and compliance in mechanical transmissions may cause periodic tension oscillations. Also processes such as heating or cooling of web and air flow around the web induce disturbances. Due to the presence of rotating components, these disturbing forces are periodic and appear as periodic oscillations in the measured

tension and speed signals. In this section, rejection of disturbances due to backlash on web tension is discussed using the output regulator.

The rewind section of the R2R process line shown in Figure 2.3 is considered. Figure 4.1 shows a schematic of the rewind section including the transmission mechanism and the pull roll. In the rewind schematic shown in Figure 4.1, ω_m is the

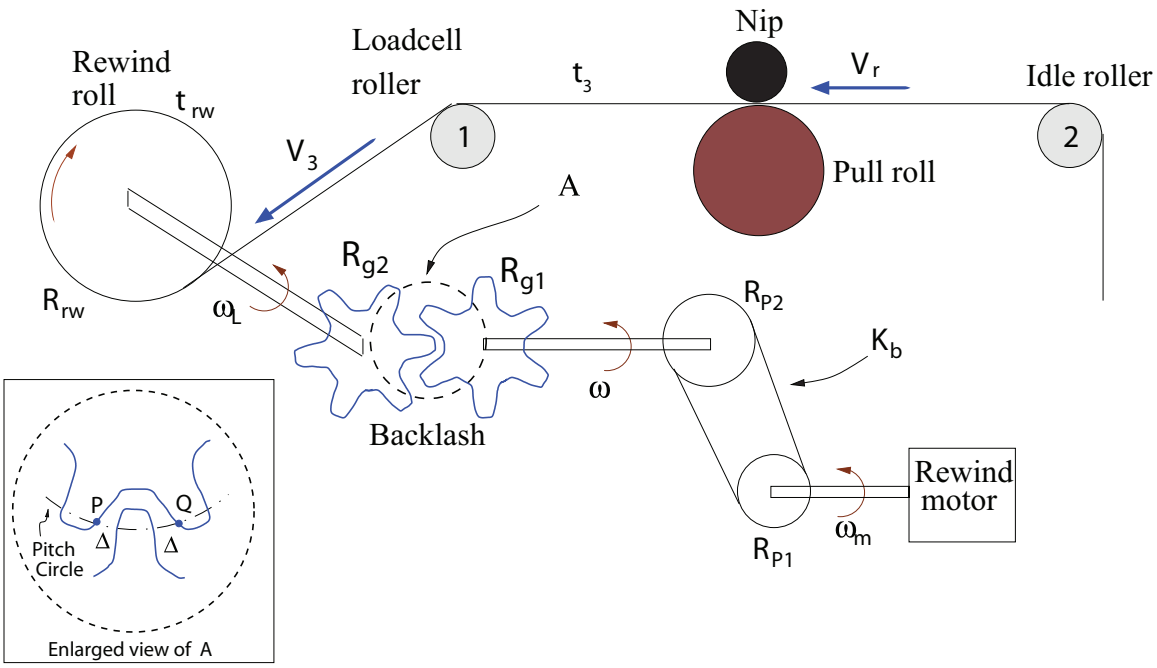

Figure 4.1: Schematic of the rewind section

angular velocity of the motor shaft, ω_L is the angular velocity of the load shaft, K_b is the stiffness of the belt, R_{P1} and R_{P2} are the radii of the two pulleys, R_{g1} and R_{g2} are the radii of the two gears, ω is the angular velocity of the shaft connecting the pulley to the gear, Δ is half of the backlash width in mating gears, R_{rw} is the radius of the rewind roll. J_m is the motor inertia, J_L is the load inertia, θ_m is the motor angular position, θ_L is the load angular position, and τ_m is the motor input torque. The dynamic model that includes the backlash and compliance effect on the motor speed and load speed of the rewind roll were studied in [36] and given in equations

(4.56a) to (4.56d):

$$\dot{\theta}_m = \omega_m, \tag{4.56a}$$

$$\dot{\omega}_m = -\frac{K_b R_{P1}^2}{J_m}\theta_m - \frac{b_m}{J_m}\omega_m + \frac{K_b R_{P1}\alpha_1}{J_m}\theta_L + \frac{\tau_m}{J_m} - \frac{R_{P1}}{J_m}\phi(\theta_m,\ \theta_L), \tag{4.56b}$$

$$\dot{\theta}_L = \omega_L, \tag{4.56c}$$

$$\dot{\omega}_L = \frac{K_b R_{P1}\alpha_1}{J_L}\theta_m - \frac{K_b \alpha_1^2}{J_L}\theta_L - \frac{b_L}{J_L}\omega_L + \frac{\tau_L}{J_L} + \frac{\alpha_1}{J_L}\phi(\theta_m,\ \theta_L). \tag{4.56d}$$

where $\alpha_1 = R_{P2}(R_{g2}/R_{g1})$, $\phi(\theta_m,\ \theta_L)$ is the term due to backlash effect, and the load torque τ_L in these equations is due to web tension t_3. The backlash and compliance models are considered for the rewind section and incorporated into the tension and web velocity dynamics given by equations (4.2) to (4.8).

4.6 Web Tension Estimation

In certain situations, such as in an oven where tension measurements from a roller mounted on load cells are unreliable, it is beneficial to have a tension observer that is capable of estimating tension and using it for feedback. In this section, the system shown in Figure 2.3 is considered for the design of a tension observer. The particular tension observer to estimate tension in a span requires downstream and upstream roller velocities and tension measurements from the neighboring web spans. As an example, tension observer for estimating tension in the pull roll tension zone, i.e., estimate of t_2, is considered. The governing equations for web tension and roller velocities for the pull roll section are given by equations (4.4) to (4.6). The state

vector, input vector, and measurement vector is

$$\mathbb{X}^T = [t_2 \ v_1 \ v_2], \tag{4.57a}$$

$$\mathbb{U}^T = [u_1 \ u_2], \tag{4.57b}$$

$$\mathbb{Y}^T = [v_1 \ v_2]. \tag{4.57c}$$

Let z_e denote the estimate of web tension, i.e., $z_e = \hat{t}_2$. Define an auxiliary variable ζ given by

$$\zeta = z_e - L\mathbb{Y}. \tag{4.58}$$

where $L = [L_1 \ L_2]$ is the observer gain. Differentiating ζ we get

$$\begin{aligned} \dot{\zeta} &= \dot{z}_e - L\dot{\mathbb{Y}} \\ &= F_1(\mathbb{Y}, \zeta + L\mathbb{Y}) - LF_2(\mathbb{Y}, \zeta + L\mathbb{Y}). \end{aligned} \tag{4.59}$$

where

$$\begin{aligned} F_1(\mathbb{Y}, \zeta + L\mathbb{Y}) &= \frac{EA}{L_2}(v_2 - v_1) + \frac{t_1 v_1}{L_2} - \frac{(\mathbb{Y}, \zeta + L\mathbb{Y})v_2}{L_2} \\ F_2(\mathbb{Y}, \zeta + L\mathbb{Y}) &= \begin{bmatrix} \frac{R_1^2}{J_1}(\zeta + L\mathbb{Y} - t_1) + \frac{R_1}{J_1} n_1 u_1 \\ \frac{R_2^2}{J_2}(t_3 - \zeta - L\mathbb{Y}) + \frac{R_2}{J_2} n_2 u_2 \end{bmatrix} \end{aligned} \tag{4.60}$$

The value of ζ is obtained using the equation (4.59). The tension estimation can be obtained from

$$\hat{t}_2 = \zeta + L\mathbb{Y} \tag{4.61}$$

The estimated web tension $\hat{t}_2$ can be employed in the output regulator. The web tension observer design is illustrated in Figure 4.2.

4.7 Experimental Setup and Procedure

The same R2R experimental setup that is used in Chapter 2 is considered. The proposed output regulation scheme is implemented in the unwind section of the R2R

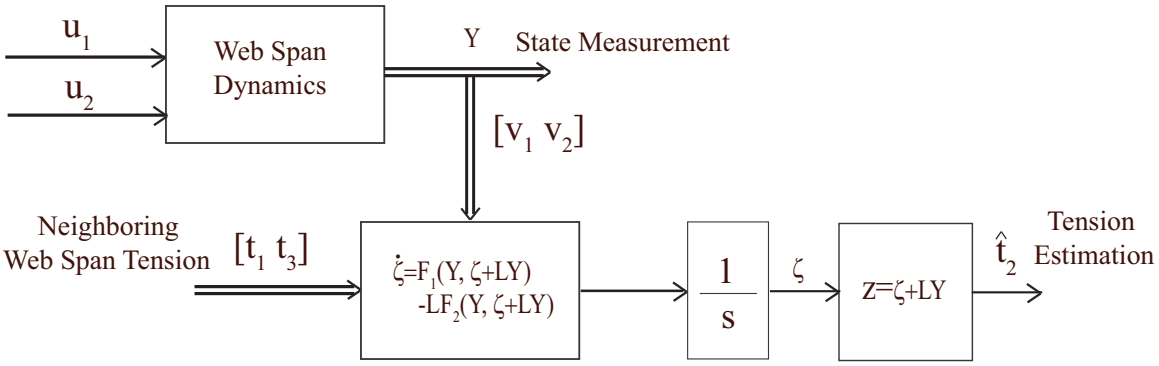

Figure 4.2: Web tension observer design

machine. The tension control law for the unwind roll is given by:

$$u = u_f - K_{t_1}(t_1 - t_f) \tag{4.62}$$

where K_{t_1} is the gain matrix, t_1 is the web tension in the unwind section, and t_f is the web tension when only feedforward control u_f is applied. A schematic of the output regulation tension control system is provided in Figure 4.3.

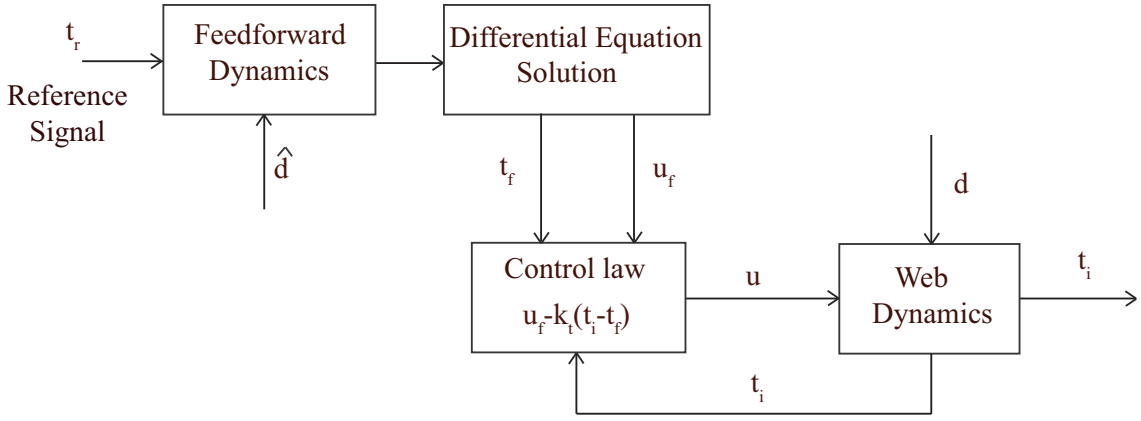

Figure 4.3: Tension output regulator design

The first driven S-wrap roller (R9) is used to generate a sinusoidal disturbance in

web speed of the form

$$\begin{aligned} d &= \theta_1 \cos(\omega t) + \theta_2 \sin(\omega t) \\ &:= \phi(t) w_0^* \end{aligned} \tag{4.63}$$

where ω is a known frequency, θ_1 and θ_2 are unknown parameters that represent the initial conditions of the exogenous system given in equation (4.23); $w_0^* = [\theta_1 \ \theta_2]^T$, and $\phi(t) = [\cos(\omega t) \ \ \sin(\omega t)]$. The disturbance parameters are estimated as discussed in subsection 4.2.2 and are used to compute the feedforward control input u_f.

A number of experiments are conducted at different web speeds to evaluate the proposed output regulation scheme and the PI scheme used in industrial practice. Two types of web materials are considered: a polymer material called Tyvek that is used in building insulation, medical and commercial packaging and a generic polyester material used in manufacturing of consumer products. The modulus, web width and thickness for these materials are given in Table 2.1. The reference tension is 89 N (20 lbf).

A speed disturbance of frequency 0.25 Hz is injected using the driven roller R9 whose diameter is 305 mm (12 inches). There are also periodic disturbances in web tension due to the eccentricity or out-of-roundness of the rollers in the experimental machine; the effect of nonideal rollers is discussed in detail in [17] which used the same experimental platform. Note that disturbance frequency is a function of the line speed; once the line speed is known, one can compute the disturbance frequency. Although we have shown results for 0.25 Hz, the proposed method also works for other frequencies. The speed controller is a PI controller and it is implemented in the motor drive; see Fig. 1.9. The speed loop bandwidth is about 4 Hz. In practice, we are interested in rejecting low frequency tension disturbances in the range of 0 to 2 Hz. Most tension disturbances are in this range and anything beyond this range is

filtered by the web tension dynamics as the web is transported on rollers from span to span. The speed loop bandwidth is adequate enough for tracking the corrections to the reference speed provided by the outer loop tension controller. The initial estimates of the filter frequency λ and adaptation gain γ are obtained by performing model simulations and tuned online. The following values are chosen: $\lambda = 3000$ and $\gamma = 0.1$. Several amplitudes of sinusoidal speed disturbances are injected at the driven roller R9 to evaluate the robustness of the output regulator; the true values and initial values of the estimates at different web speeds are given in Table 4.1.

Operating Speed	True Parameters		Initial Values	
	θ_{1ref}	θ_{2ref}	θ_{10}	θ_{20}
0.51 m/s (100 fpm)	0.013	0.004	0.004	0.013
0.76 m/s (150 fpm)	0.012	0.005	0.008	0.012
1.02 m/s (200 fpm)	0.003	0.015	0.011	0.005

Table 4.1: True and initial estimates of disturbance parameters

The output regulation scheme with integral feedback is implemented in the rewind and pull roll sections of the R2R machine. The tension control law for these sections is given by (4.42)

$$u = u_f - K_{tp}(t_i - t_f) - K_{ti} \int (t_i - t_f) \tag{4.64}$$

where K_{tp} is the proportional gain, K_{ti} is the integral gain, t_i is the web tension in the i^{th} span, and t_f is the web tension when only feedforward control u_f is applied.

The output regulator with integral feedback is implemented at web speed of 100 FPM and tension reference of 20 lbf. In output regulator design, the initial estimates of the filter frequency λ and adaptation gain γ are obtained by performing model simulations and tuned online. The following values are chosen: $\lambda = 6000$ and $\gamma = 0.5$.

In another set of experiments, multiple frequency components which are present in the tension signal are targeted. The output regulator is tested for robustness in terms of rejecting more than one frequency components. The experiment is performed at 100 FPM and 20 lbf reference web tension in the pull roll section.

The drive system in the rewind section has an adjustable backlash (indicated as BL in the Figure 4.4), which can be used to insert a known backlash between the driving sprocket (labeled "1" in Figure 4.4) and the rewind shaft. In the current experiments, backlash of 1.55 mm is introduced in the transmission system, in addition to the existing backlash in the gear box. The disturbance frequency generated due to this

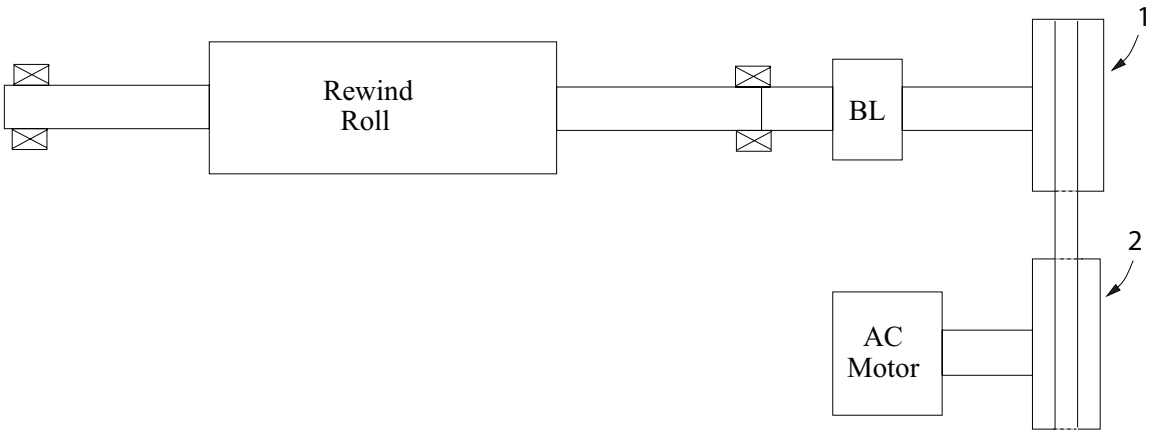

Figure 4.4: Rewind drive system in R2R web line

introduced backlash is targeted for attenuation in this set of experiments performed at 150 FPM and 20 lbf reference web tension. The output regulator is applied to the pull roll to attenuate the disturbances.

The web tension observer is implemented in the pull roll section and used as web tension feedback to regulate tension response in the pull roll section.

4.8 Experimental Results

The tension regulation and disturbance rejection capability of the proposed output regulation scheme and a well tuned industrial PI control scheme for polyester and Tyvek web materials for web transport speed of 100 FPM, 150 FPM, and 250 FPM are shown in Figures 4.5 and 4.6, respectively. The annotation in the plots correspond to the performance of the following controllers with and without the presence of disturbance:

- AB: PI controller with disturbance,
- BC: PI controller without disturbance,
- CD: Nonlinear tension regulator without disturbance,
- DE: Nonlinear tension regulator with disturbance.

The PI controller gains are tuned online for each material separately and different PI gains are used for each material to obtain the best performance with and without disturbance. For the output feedback scheme the same controller and parameter estimation gains are used for both materials. It is clear from the tension response plot (AB zone) that the PI scheme is not able to reject tension oscillations whereas the output feedback scheme is able to largely attenuate the tension disturbances after initial transients. The estimates of the disturbance parameters are also shown in the Figures 4.5 and 4.6; the parameter estimates converge to the true values. The average value of web tension with both the well-tuned PI and the output regulator are around the the reference value of 89 N (20 lbf) with different line speeds. However, the PI controller fails to attenuate the disturbance. The performance of the fixed gain PI controller is expected since there is no separate mechanism to compensate

for the disturbance. On the other hand, with the accurate estimation of disturbance parameters, the output regulator is able to reject the partially known disturbance (known frequency). It is noted that the two web materials (polyester and Tyvek) have substantially different mechanical properties, that is, the modulus of polyester is about 5 times that of Tyvek. The output regulation scheme with the same gains is able to provide similar performance for both materials; this is not the case with the PI scheme.

The tension regulation and disturbance rejection capability of the proposed output regulation scheme with proportional and integral feedback are shown in Figures 4.7(a) and 4.7(b), for the pull roll and rewind sections, respectively. The web tension is regulated at 20 lbf at transport speed of 100 FPM for Tyvek web material.

The annotation in the plot (given in Figures 4.7(a) and 4.7(b)) correspond to the performance of the following controllers with and without the presence of disturbance:

- FG: Nonlinear tension regulator with only proportional action and without disturbance,
- GH: Nonlinear tension regulator with proportional and integral action and without disturbance,
- HI: Nonlinear tension regulator with proportional and integral action and with disturbance,
- IJ: PI controller without disturbance,
- JK: PI controller with disturbance.

The plot shown in Figure 4.8(a) is the FFT of web tension and 100 FPM at reference tension of 20 lbf and the frequency components seen in the plot are due to

nominal machine elements. The high amplitude frequencies are targeted by the output regulator. The plot shown in Figure 4.8(b) indicates first high amplitude frequency (0.53 Hz) is mitigated by output regulator. While, the plot shown in Figure 4.8(c) attenuates two components, i.e. fundamental frequency and fourth harmonics (0.53 Hz and 2.12 Hz). The result indicates that output regulator is capable of rejecting multiple frequencies.

The plot shown in Figure 4.9(a) is the FFT of web tension due to backlash of 1.55 mm that is introduced through the backlash device in the rewind transmission. The plot shown in Figure 4.9(b) indicates the frequency at 3.17 Hz is generated by introduction of backlash at 150 FPM. This high amplitude frequency was targeted by the output regulator. The plot shown in Figure 4.9(c) indicates attenuation of frequency amplitude at 3.17 Hz. Similar, results can be seen in Figure 4.10 through the FFT of web tension at 250 FPM and reference tension of 20 lbf. The output regulator is able to attenuate disturbances at 5.3 Hz. Note that the disturbance frequency and amplitude change with speed and the same output regulator is capable of attenuating the disturbances.

The plot shown in Figure 4.11 are the results of utilizing web tension observer estimation in feedforward control action. The observer estimation used in replacement of measurement. The tension estimate gives desired performance in (i) control scheme with feedforward action by rejecting disturbance (BC zone) (ii) with only feedback action it reflects the presence of disturbance (AB zone).

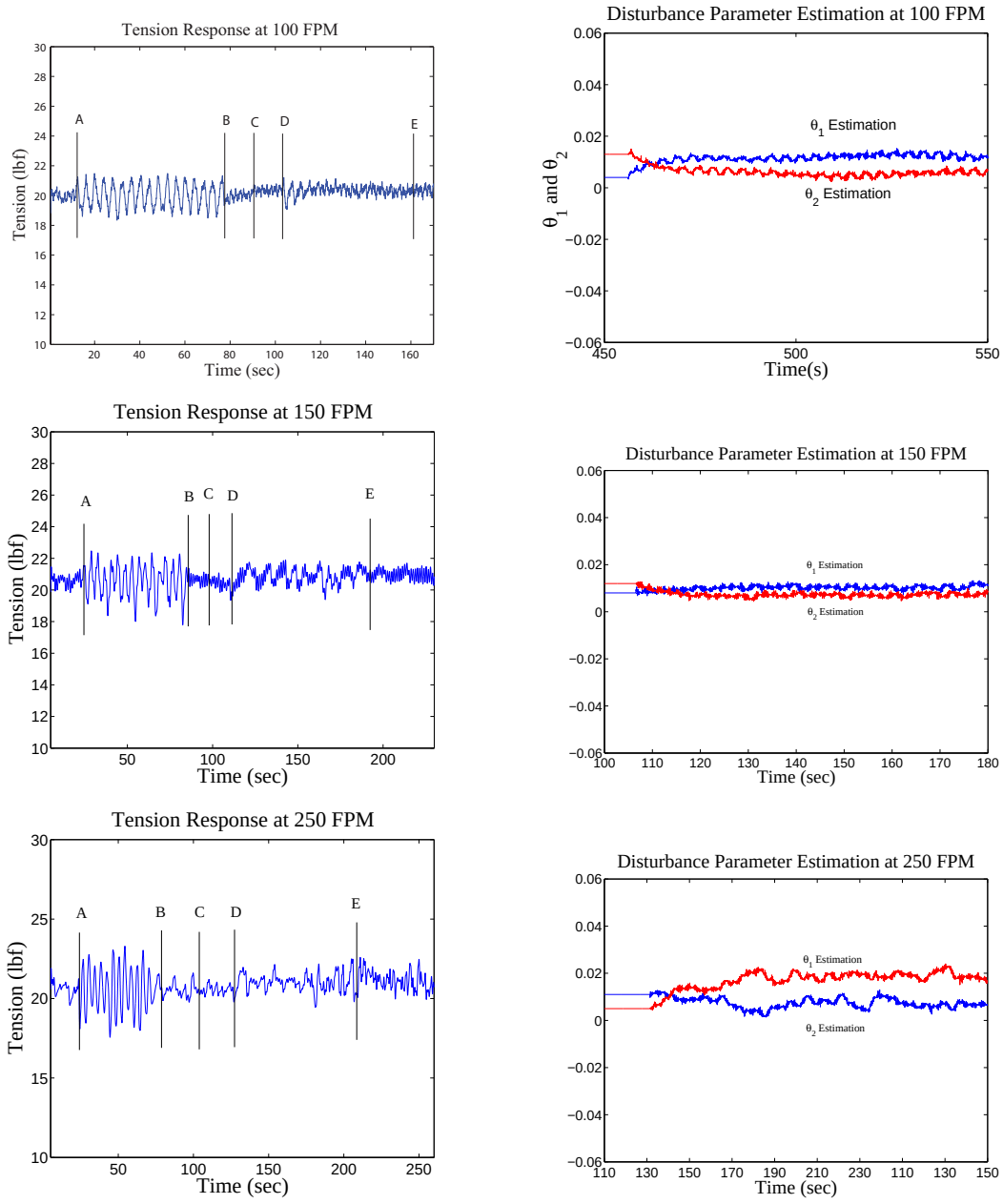

Figure 4.5: Disturbance rejection and parameter estimation: polyester

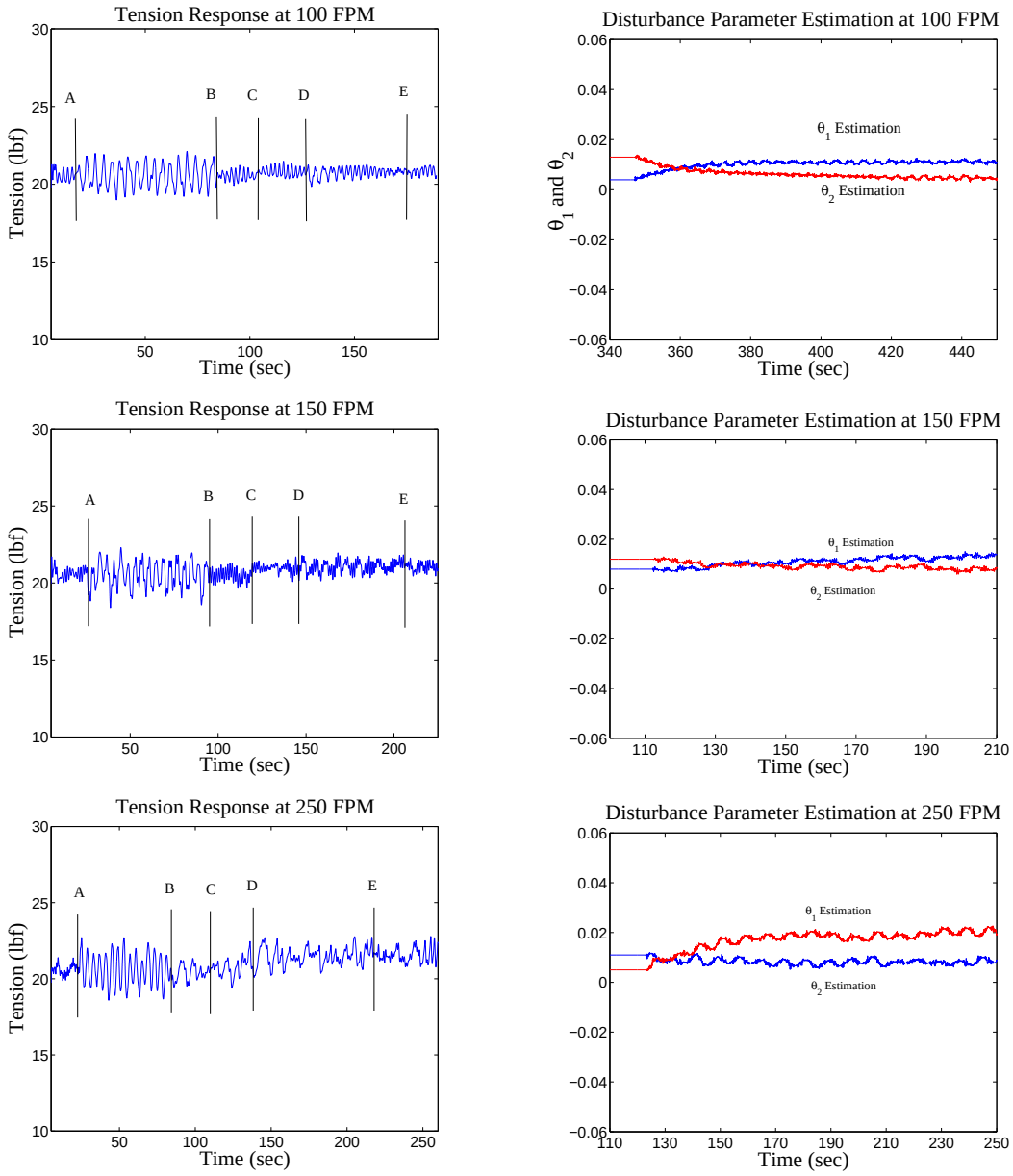

Figure 4.6: Disturbance rejection and parameter estimation: Tyvek

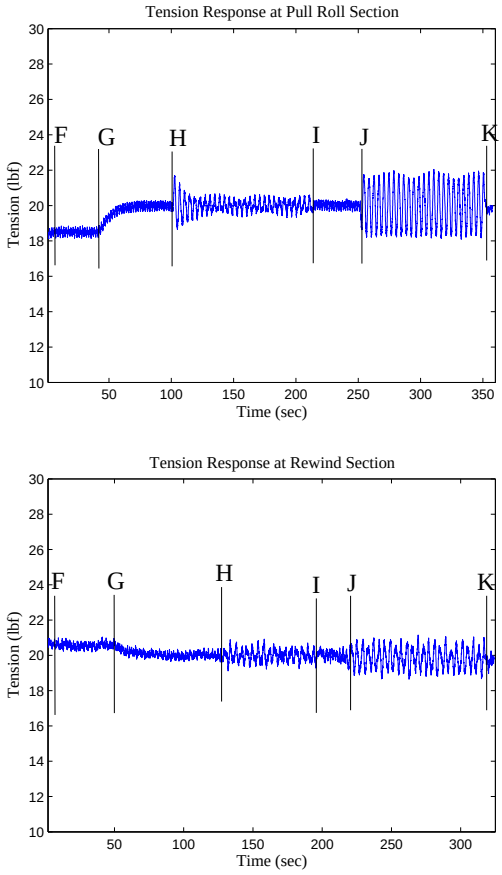

Figure 4.7: Tension response at 100 FPM for Tyvek material; Top: Pull roll section, Bottom: Rewind section

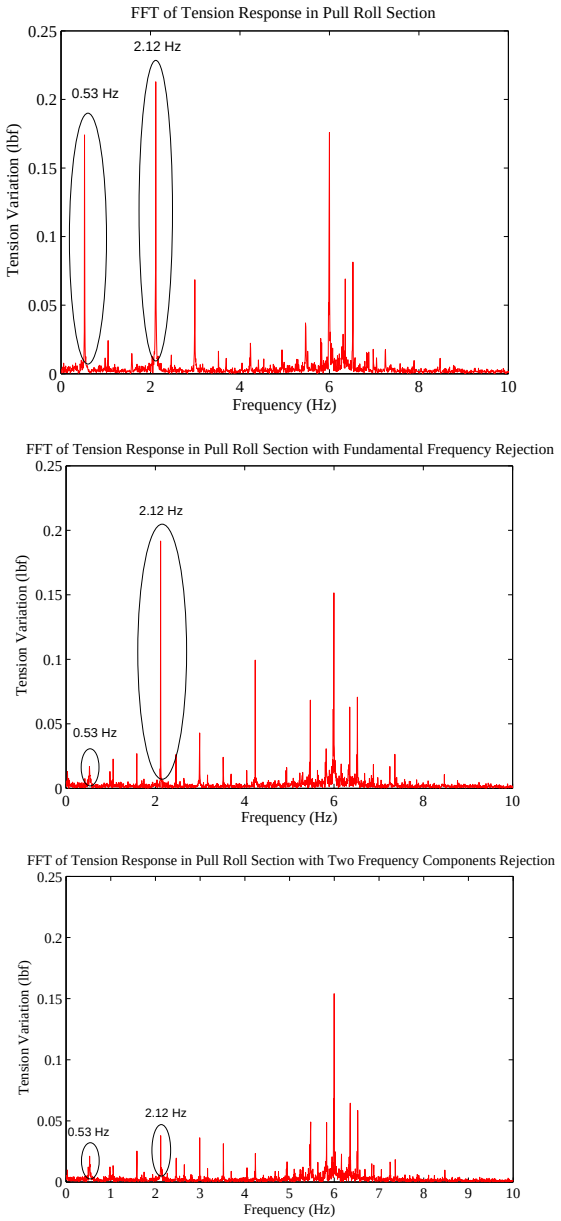

Figure 4.8: FFT of web tension response at 100 FPM at Reference Tension 20 lbf with Tyvek Web with; Top: PI control, Middle: output regulator rejected fundamental frequency, Bottom: output regulator rejected two frequency components

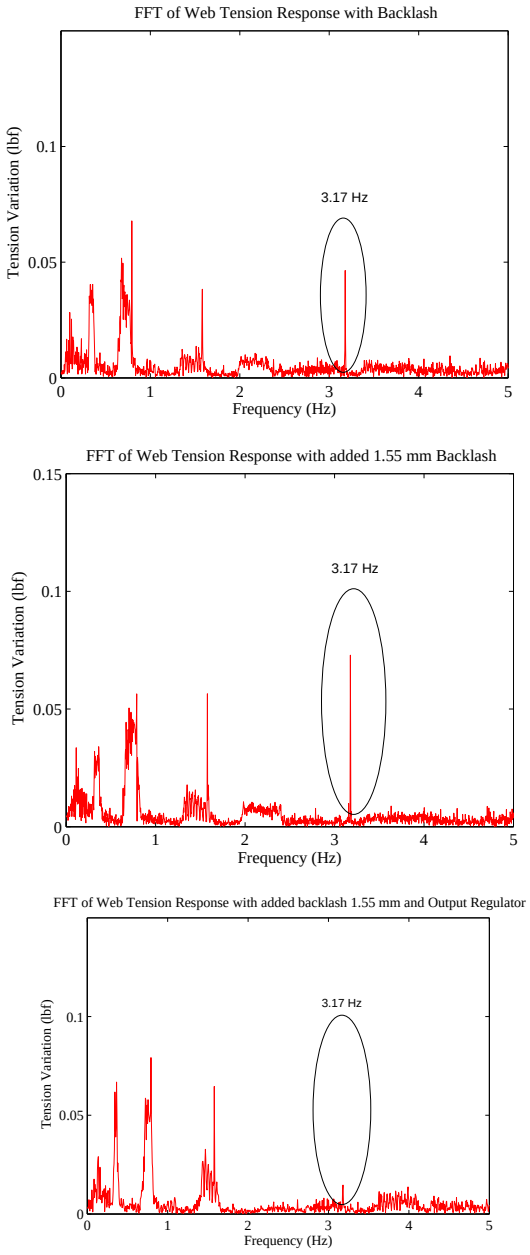

Figure 4.9: FFT of web tension response at 150 FPM and 20 lbf with ; Top: PI control and backlash, Middle: PI control and added backlash introduced, Bottom: Output regulator and added backlash.

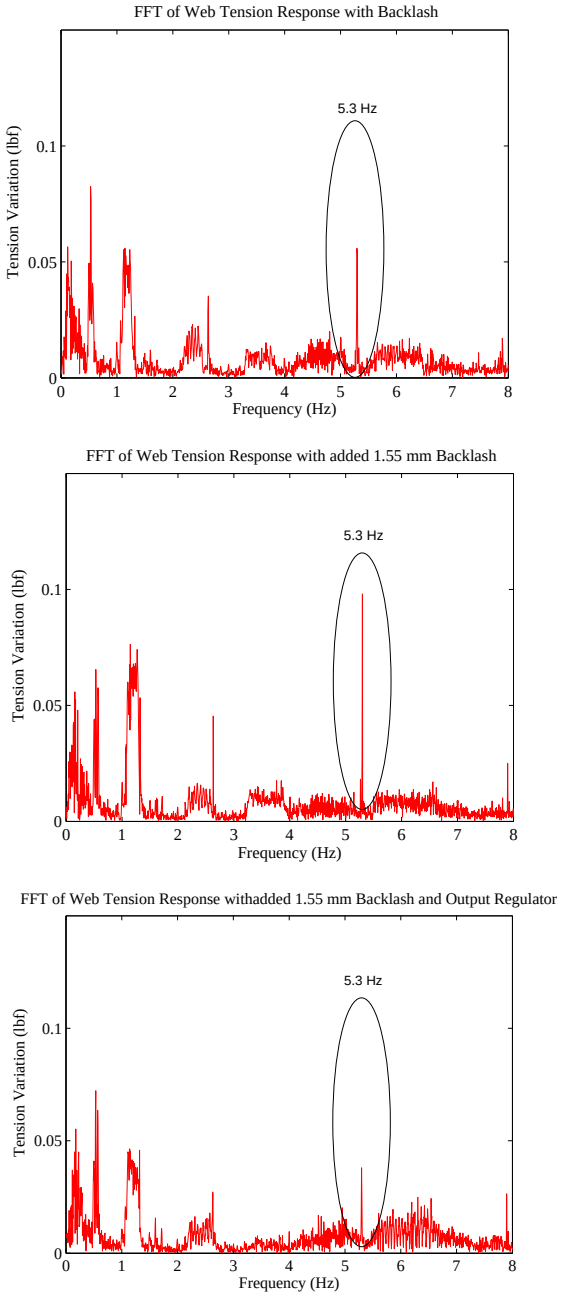

Figure 4.10: FFT of web tension response at 250 FPM and 20 lbf with ; Top: PI control and backlash, Middle: PI control and added backlash, Bottom: Output regulator and added backlash.

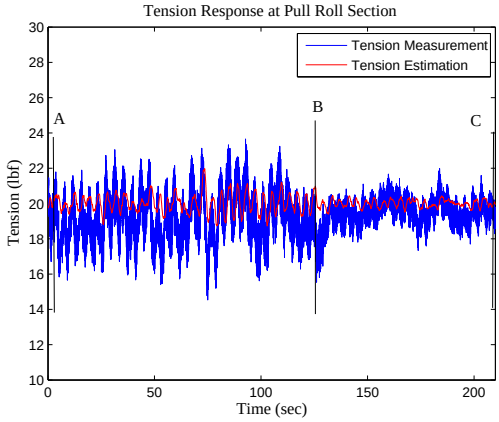

Figure 4.11: Web tension response in pull roll section with observer feedback

CHAPTER 5

Minimization of Interaction and Disturbance Propagation

In R2R systems, decentralized controllers are often employed because of the structure of the system and their ease of implementation. Since the material is transported from the unwind to the rewind through the process sections, the entire machine is divided into several sections and decentralized controllers are utilized for each section or subsystem. It is important to understand the mechanisms for transport behavior from each section to other downstream sections, i.e., interaction between subsystems, and how disturbances are propagated. Design of controllers that minimize disturbance propagation will aid in improving the processing of the material in the process sections.

In this chapter, we will first investigate minimization of interaction between subsystems of R2R systems when decentralized feedback and feedforward controllers are employed. In particular, we will consider a new interaction metric which is based on the Perron root of an irreducible matrix. We will also investigate control strategies that minimize disturbance propagation. To evaluate the proposed designs and recommendation, we will show results of extensive experiments conducted on a large R2R experimental platform.

The remainder of the chapter is organized as follows. The interaction minimization procedure is discussed in Section 5.1. The feedforward control action to improve performance and minimize disturbance propagation is discussed in Section 5.2. The implementation strategy of feedforward action is discussed in Section 5.3. Experi-

mental setup, application of the feedforward control action to the R2R system, and experimental procedure are discussed in Section 5.4. Experimental results are presented and discussed in Section 5.5.

5.1 Interaction Minimization

In this section, we will first provide some mathematical preliminaries that will aid in quantifying interaction between different sections of an R2R system and discuss methods to minimize interaction by improving performance of each decentralized control system using model-based feedback and feedforward algorithms such as the output regulator discussed in the preceding chapter.

An $n \times n$ matrix A is said to be reducible when there exists a permutation matrix P such that

$$P^T A P = \begin{bmatrix} X & Y \\ 0 & Z \end{bmatrix}$$

where X and Z are square matrices. A matrix that is not reducible is said to be irreducible.

Given a number $p \in [1, \infty]$ and a diagonal matrix $D \triangleq \text{diag}[d_1, d_2, \ldots, d_n] \in \mathcal{C}^{n \times n}$ with $d_i \neq 0$ for all $i = 1, \ldots, n$, the D-weighted Hölder l_p norm on $\mathcal{C}^n$ is given by

$$||x||_{pD} \triangleq ||Dx||_p \triangleq \left(\sum_{i=1}^{n} |d_i x_i|^p \right)^{1/p} \quad \text{for all } x \in \mathcal{C}^n. \tag{5.1}$$

The subordinate bound norm induced in $\mathcal{C}^{n \times n}$ by the l_p-norm on $\mathcal{C}^n$ is given by

$$||A||_{pD} \triangleq \sup_{x \neq 0} \frac{||Ax||_{pD}}{||x||_{pD}} \text{ for all } A \in \mathcal{C}^{n \times n}. \tag{5.2}$$

The p-norm weighted D_p^* is optimal for $p = 1$ and $p = \infty$ in the sense that

$$||A(j\omega)||_{pD_p^*} = \inf_D ||\langle A(j\omega) \rangle||_{pD} = p_A(\omega) \tag{5.3}$$

Let $\rho(A)$ denote the spectral radius of A, $\sigma(A)$ denote the set of eigenvalues of A, for a vector x let $x > 0$ imply that all the elements of x are positive, and $\| x \|_1$ denote the one-norm of vector x. The following is the Perron-Frobenius theorem.

Theorem 5.1.1 (Perron-Frobenius Theorem [64]) *If $A \geq 0$ is irreducible, then the following statements are true.*

1. *$r = \rho(A)$ and $r > 0$ (r is called the Perron root)*

2. *r is a simple eigenvalue*

3. *There exists a vector $x > 0$ such that $Ax = rx$*

4. *The Perron vector is the unique vector defined by*

$$Ap = rp, \quad p > 0, \quad \text{and} \quad ||p||_1 = 1, \tag{5.4}$$

   and, except for positive multiples of p, there are no other nonnegative eigenvector of A, regardless of the eigenvalue.

5. *The Collatz-Wielandt formula holds, i.e., $r = \max_{x \in \mathcal{N}} f(x)$, where*

$$f(x) = \min_{1 \leq i \leq n,\ x_i \neq 0} \frac{[Ax]_i}{x_i} \text{ and}$$
$$\mathcal{N} = \{x | x \geq 0 \text{ with } x \neq 0\}.$$

Let the R2R system dynamics be represented by the input-output relationship: $y(s) = G(s)u(s)$, where u is the input vector and y is the output vector. The off-diagonal elements of the transfer function matrix $G(s)$ specify the interaction between subsystems. The goal is to design a decentralized controller for each subsystem such that interaction is minimized in the closed-loop transfer function matrix. Let G be represented as $G = \overline{G} + \widetilde{G}$ where $\overline{G}$ contains the diagonal part of G and $\widetilde{G}$ contains

the off- diagonal part of G. The size of $\widetilde{G}$ may be used to quantify interaction. In particular, the effect of the off-diagonal elements and corresponding inputs on a particular output may be evaluated by the size of the relative error matrix $L_H \triangleq \widetilde{G}\overline{G}^{-1}$. Interaction may be quantified by the size of relative error matrix L_H. A D-weighted induced Hölder l_∞ norm of L_H is used to quantify interaction. This norm is equal to the Perron root and the Perron root based interaction metric (PRIM) for the system G is defined as [58]

$$p_{L_H}(\omega) \triangleq \mathcal{P}(\langle L_H(j\omega)\rangle) \tag{5.5}$$

where $\mathcal{P}(\langle L_H(j\omega)\rangle)$ is the Perron root of the irreducible matrix $\langle L_H(j\omega)\rangle$ at the frequency ω. A smaller value of PRIM means less interaction. Note that PRIM provides a form of the overall interaction in the multivariable system and does not provide information about interaction between any two subsystems in the system. In [58] it is discussed that if $\sup_\omega p_{L_H}(\omega) < 1$, then there exists a decentralized pre-filter that would ensure diagonal dominance (minimize interaction) at all frequencies of the closed-loop system transfer matrix. The pre-filters are designed by fitting transfer functions to the right Perron eigenvector of $L_H(\omega)$.

The stabilization criteria for multivariable systems employing decentralized controllers based on the size of the interaction measure and the diagonal part of the closed-loop system transfer matrix can be found in [65]. Suppose for a rational transfer function matrix $G(s)$ the decentralized controller K stabilizes the diagonal part of the transfer function matrix, $\overline{G}$, i.e., the diagonal part of the closed-loop system $\overline{H}$ is stable where $\overline{H} = \overline{G}K(I + \overline{G}K)^{-1}$, then condition for stability of the overall system can be obtained from the following theorem.

Theorem 5.1.2 *Assume G and $\overline{G}$ have the same number of unstable poles and $\overline{H}$ is*

stable. Then the closed-loop system $H = GK(I + GK)^{-1}$ *is stable if and only if*

$$\det[I + L_H \overline{H}\ ] \neq 0 \quad \forall s \in \mathcal{D}_{\mathcal{R}} \tag{5.6}$$

where $\mathcal{D}_{\mathcal{R}}$ is the Nyquist contour (with appropriate indentations to avoid any open-loop poles on the imaginary axis).

By using the small gain theorem, a sufficient condition for stability of the overall system based on the above theorem is given by

$$||L_H(j\omega)\overline{H}(j\omega)|| < 1 \ \forall \omega \tag{5.7}$$

where $||(\cdot)||$ is any compatible induced norm of $(\cdot)$. The stability constraint based on the Perron root of L_H and the diagonal structure of $\overline{H}$ is given by

$$|\overline{h}_i(j\omega)| < \frac{1}{p_{L_H}(\omega)} \ \forall i, \omega. \tag{5.8}$$

In the following two sections, we will show how performance of the decentralized control system can be improved by utilizing model-based feedforward and the particular structure of feedforward compensation in tension control systems.

5.2 Performance Improvement of Decentralized Control Systems

The linearized governing equations for each section of the R2R system shown in Figure 5.1 is given in the following equations which utilize the notation: J_i: driven roller moment of inertia, R_i: driven roller radius, V_i: web velocity at the driven roller, T_i: web span tensions, n_i: gear ratio, U_i: torque input, b_{f_i}: viscous friction coefficient, L_i: span length, t_0: wound on tension, v_{r_i}: velocity reference, t_{r_i}: tension reference, A_w: the cross-sectional area of the web and E: the Young's modulus of the web material.

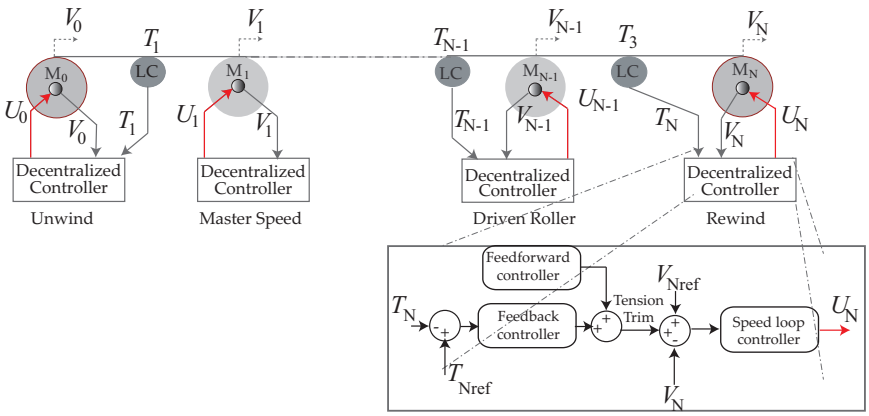

Figure 5.1: Decentralized tension control structure for roll-to-roll systems with an inner velocity loop and an outer tension loop

Unwind Section:

$$\frac{J_0}{R_0}\dot{V}_0 = T_1 R_0 - n_0 U_0 - \frac{b_{f0}}{R_0} V_0 \tag{5.9a}$$

$$L_1 \dot{T}_1 = -T_1 v_{r_1} + \left[A_w E - t_{r_1}\right] V_1 + \left[t_0 - A_w E\right] V_0 \tag{5.9b}$$

Lead and Follower Section:

$$\frac{J_1}{R_1}\dot{V}_1 = \left(T_2 - T_1\right) R_1 + n_1 U_1 - \frac{b_{f1}}{R_1} V_1 \tag{5.10}$$

Pull Roll Section:

$$\frac{J_2}{R_2}\dot{V}_2 = \left(T_3 - T_2\right) R_2 + n_2 U_2 - \frac{b_{f2}}{R_2} V_2 \tag{5.11a}$$

$$L_2 \dot{T}_2 = -T_2 v_{r_2} + \left[A_w E - t_{r_2}\right] V_2 - \left[A_w E - t_{r_1}\right] V_1 + T_1 v_{r_1} \tag{5.11b}$$

Rewind Section:

$$\frac{J_3}{R_3}\dot{V}_3 = -T_3 R_3 + n_3 U_3 - \frac{b_{f3}}{R_3} V_3 \tag{5.12a}$$

$$L_3 \dot{T}_3 = -T_3 v_{r_3} + \left[A_w E - t_{r_3}\right] V_3 - \left[A_w E - t_{r_2}\right] V_2 + T_2 v_{r_2} \tag{5.12b}$$

The coupling between tension zones is evident from Equations (5.9)–(5.12) which leads to interaction between tension zones. It can be seen through Theorem 5.1.2

that when the interaction term $L_H = 0$, any controller structure $\bar{H}$ will satisfy the stability criteria. It is shown in [58] that using the Perron vector the interaction in the system can be minimized. When the interaction is small, the decentralized controller should be designed such that the diagonal closed-loop system transfer function matrix $\bar{H}$ must be close to identity and should assure stability of the overall system. The feedback and feedforward control structure aids in this regard which is discussed below.

Consider one of the decentralized subsystems shown in Figure 5.2. Let y_f denote

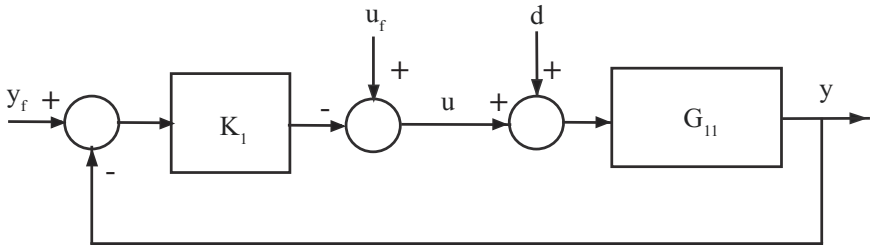

Figure 5.2: A subsystem with decentralized controller

the desired output, d denote the disturbance in the system, and $u = (y_f - y)K_1$ with $u_f = 0$ denote the feedback control input. The system output y is expressed as

$$y = \frac{K_1 G_{11}}{1 + K_1 G_{11}} y_f + \frac{G_{11}}{1 + K_1 G_{11}} d \tag{5.13}$$

Consider the control input $u = u_f - (y_f - y)K_1$, where u_f is the feedforward input that gives desired output y_f when applied to a known system model.

$$y_f = G_{11m}(u_f + \hat{d}) \tag{5.14}$$

where G_{1m} is the system model and $\hat{d}$ is the disturbance estimate. With the feedback and feedforward control input, the system output y can be expressed as

$$y = \frac{-K_1 G_{11}}{1 - K_1 G_{11}} y_f + \frac{G_{11}}{1 - K_1 G_{11}} u_f + \frac{G_{11}}{1 - K_1 G_{11}} d \tag{5.15}$$

Substituting equation (5.14) into equation (5.15) we get

$$y = \frac{-K_1 G_{11}}{1 - K_1 G_{11}} y_f + \frac{G_{11}}{G_{11m}(1 - K_1 G_{11})} y_f - \frac{G_{11}}{1 - K_1 G_{11}} \hat{d} + \frac{G_{11}}{1 - K_1 G_{11}} d \qquad (5.16)$$

This indicates that if $G_{11} \approx G_{11m}$ the system output tracks the desired reference and with perfect estimation the effect of the disturbance is reduced. Therefore, the feedback and feedforward controller together with the prefilter designed using the Perron interaction measure discussed in the preceding section will aid in improving the performance of decentralized control systems and minimizing interaction between subsystems.

5.3 Feedforward Implementation to Avoid Disturbance Propagation

In general, control schemes in R2R systems are implemented in the process sections with feedback from the upstream zone as shown in Figure 5.1. The feedforward action u_f given by equation (5.14) contains disturbance estimation and is used to attenuate the disturbance in a particular subsystem. However, this feedforward control action u_f also generates a disturbance in the neighboring downstream subsystem, that is, if the feedforward action is implemented with tension measurement from the upstream tension zone, it generates an estimate of disturbance in the downstream section and as a result there is a possibility of disturbance propagation into the downstream sections.

The existing decentralized control scheme in the process sections is implemented as shown in Fig. 5.3; the driven roller is controlled through feedback from upstream span web tension t_2. This feedback strategy is able to reject the disturbance and regulate the tension in the upstream tension zone. However, the control action generated by the driven roller induces disturbances into the downstream tension zone. Hence, although the strategy is able to mitigate disturbances in the upstream tension zone, it acts as a disturbance source to the adjoining downstream tension zone. This can

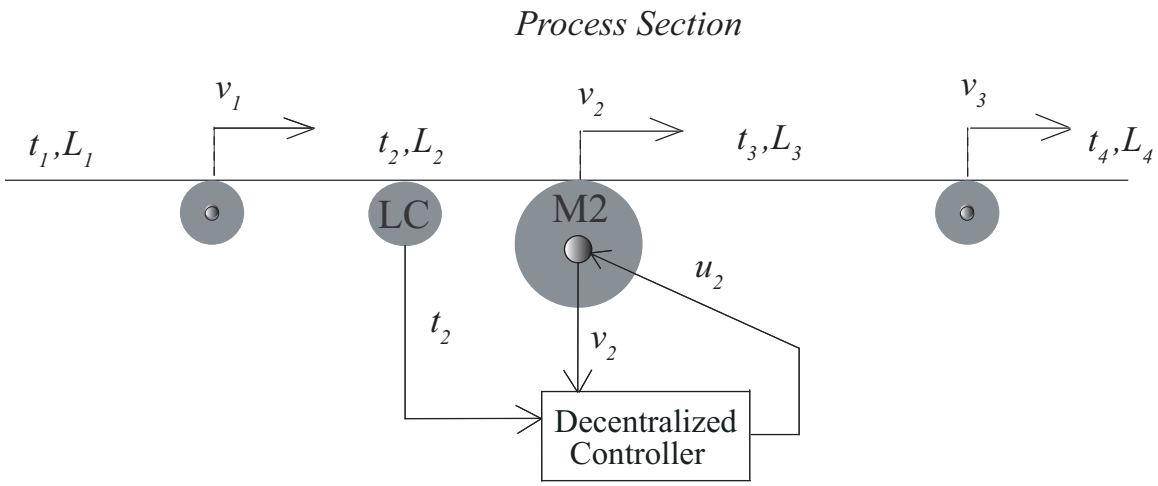

Figure 5.3: Decentralized control with upstream tension feedback

be deduced from the tension and velocity dynamics corresponding to the section of the web shown in Fig. 5.3 given by the following equations:

$$\dot{v}_1 = \frac{R_1^2}{J_1}(t_2 - t_1) - \frac{b_{f1}}{J_1}v_1 + \frac{R_1}{J_1}n_1u_1, \tag{5.17}$$

$$\dot{v}_2 = \frac{R_2^2}{J_2}(t_3 - t_2) - \frac{b_{f2}}{J_2}v_2 + \frac{R_2}{J_2}n_2u_2, \tag{5.18}$$

$$\dot{t}_2 = \frac{EA_w}{L_2}(v_2 - v_1) + \frac{1}{L_2}(t_1v_1 - t_2v_2), \tag{5.19}$$

$$\dot{v}_3 = -\frac{R_3^2}{J_3}t_3 - \frac{b_{f3}}{J_3}v_3 + \frac{R_3}{J_3}n_3u_3, \tag{5.20}$$

$$\dot{t}_3 = \frac{EA_w}{L_3}(v_3 - v_2) + \frac{1}{L_3}(t_2v_2 - t_3v_3). \tag{5.21}$$

Now consider the disturbance generated at the roller with web velocity v_1 as shown. The feedback and feedforward control action is applied at driven roller M2 with web velocity v_2. The control action u_2 has feedforward action u_{f2} in order to reject periodic disturbances. The feedforward action is synthesized with the plant model and disturbance estimation $\hat{d}$. With tension feedback from upstream span t_2, the control action u_2 can reject the disturbance by correcting the velocity v_2. Since the

velocity v_2 is also input to the downstream span tension, the corrective action u_2 generates disturbance in the downstream span tension t_3. The interaction between different subsystems propagates the disturbance further downstream affecting the other processes.

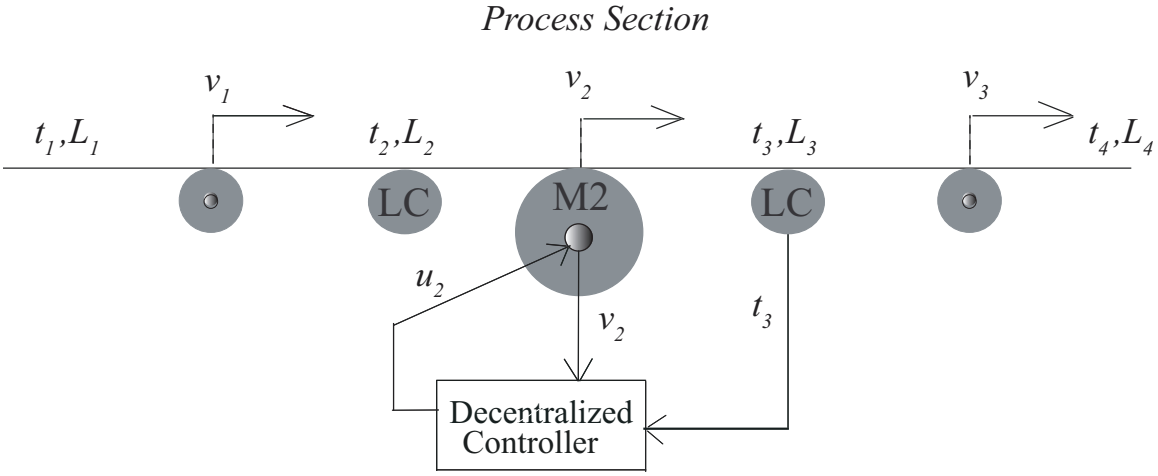

Figure 5.4: Decentralized control with downstream tension feedback

The proposed implementation of feedforward control action is shown in Figure 5.4. In the proposed scheme, web tension feedback is obtained from the downstream span. Although this strategy creates disturbance in the upstream span (within acceptable limits), it is capable of mitigating the interaction and reducing propagation of disturbances into downstream spans. This strategy is useful in reducing tension disturbance propagation into critical downstream process sections.

5.4 Experimental Setup and Procedure

The same experimental platform shown in Figure 2.1 is utilized for experimentation to verify the strategies discussed in the preceding sections. Web tension at its reference value is maintained by regulating the speed of the driven roller in that zone. The velocity correction provided by the outer tension loops influences the web tension

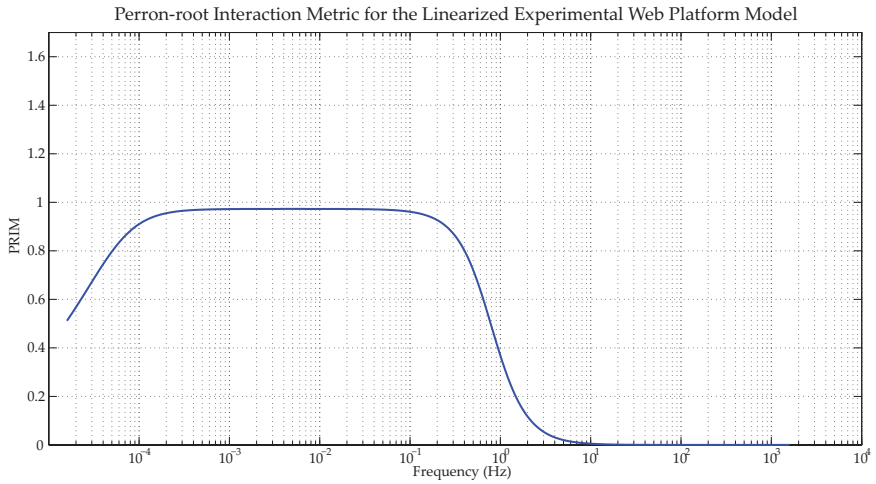

Figure 5.5: Perron root interaction metric for the linearized model of the roll-to-roll system

in the adjacent zone. Fig. 5.5 shows the PRIM with the three tension loop velocity corrections as the inputs and the web tensions in the three zones as the outputs. From the PRIM plot it is evident that interaction is dominant in the range of frequencies between 10^{-4} Hz to 1 Hz and is minimal above 1 Hz. The magnitude of interaction is close to 1 indicating that the velocity correction provided by the tension loop will have almost the same influence on one other tension zone. Note that the PRIM provides the worst case scenario for all the three tension zones and provides no information about the effect of any particular input-output pair.

Experiments were conducted on the experimental R2R system to compare three scenarios: (i) characterize the interaction in the actual system with feedback control action, (ii) utilize Perron root based filters to minimize the interaction, and (iii) use Perron root based filters and feedforward action to avoid propagation of disturbances. To illustrate the effect of these strategies, velocity disturbances at the S-wrap section were introduced to create tension disturbances in the unwind and pull roll tension zones and the effect of these disturbances in the rewind section were observed to

evaluate the interaction between these two zones. In the experiments, a six inch wide polymer web (called Tyvek) was transported with a web speed of 150 feet per minute (fpm) under a reference web tension of 20 pounds (lbf). A sinusoidal speed disturbance of magnitude 5 fpm was introduced at the S-wrap driven rollers for a duration of one minute; six distinct frequencies were considered from 0.01 to 1 Hz. The feedforward control action was applied to the pull roll with both upstream and downstream web tension feedback to evaluate the different strategies.

5.5 Experimental Results

Figure 5.6 shows the tension signals in the three tension zones when the web is transported in the forward direction (that is from the unwind to the rewind) and represents scenario (i) stated in the preceding section. Note that the tension disturbances observed in the unwind and the pull roll tension zones are due to the direct effect of the S-wrap velocity disturbance. The interaction of the different zones and disturbance propagation into downstream sections is evident from the tension signal measured in the rewind tension zone. From the plots it is evident that the magnitude of interaction is small above 0.25 Hz and increases with decreasing frequency. At low frequencies the tension disturbance observed at the rewind section is as high as the tension disturbances observed in the unwind and the pull roll sections as predicted by the PRIM (see Fig. 5.5).

Figure 5.7 shows the experimental results with pre-filters and feedback control action only; this represents scenario (ii). The results with the pre-filter show reduction of interaction between zones and minimization of disturbance propagation into the downstream tension zones.

Figure 5.8 shows the experimental results with pre-filters and feedforward action

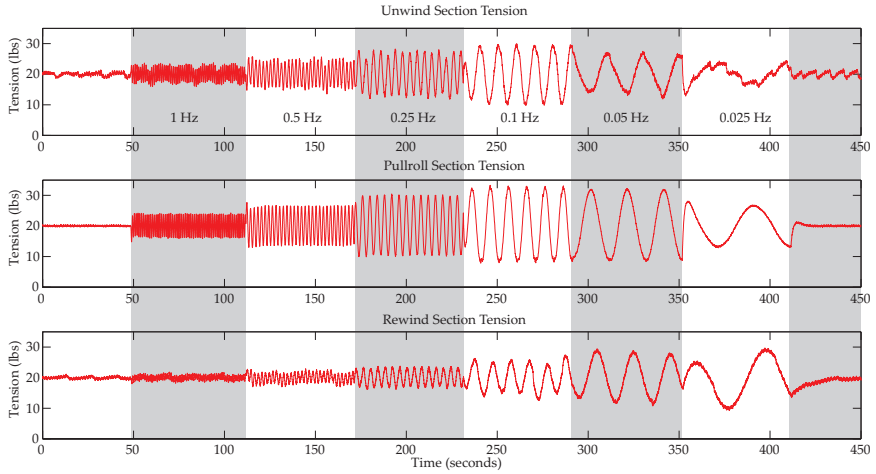

Figure 5.6: Tension measurement at the unwind, pull roll and rewind section with sinusoidal velocity disturbances at the S-wrap section.

obtained by upstream zone tension measurement; this represents scenario (iii). Although, the results with this strategy indicate rejection of disturbance in pull roll section but it generates disturbance into the downstream rewind tension zone.

Figure 5.9 shows the experimental results with pre-filters and feedforward action obtained by downstream zone tension measurement; this represents scenario (iii). The results with this strategy indicate significant interaction reduction as well as minimization of disturbance propagation into the downstream rewind tension zone.

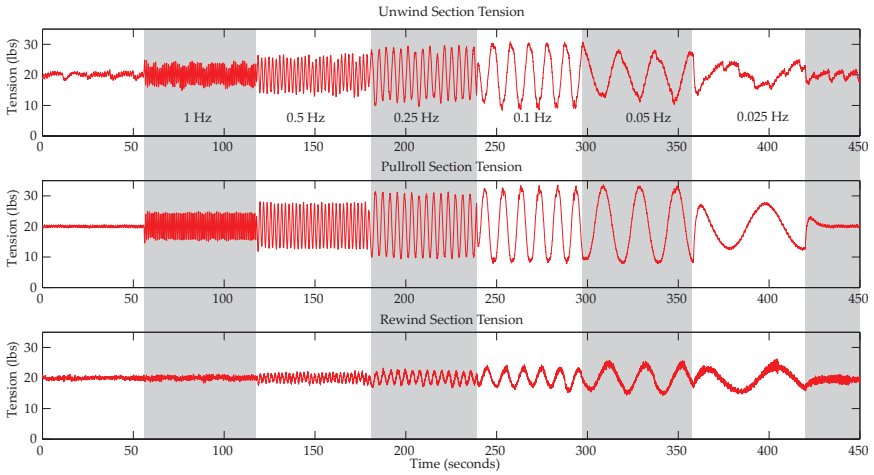

Figure 5.7: Interaction in the experimental platform with pre-filter; tension measurement at the unwind, pull roll and rewind section.

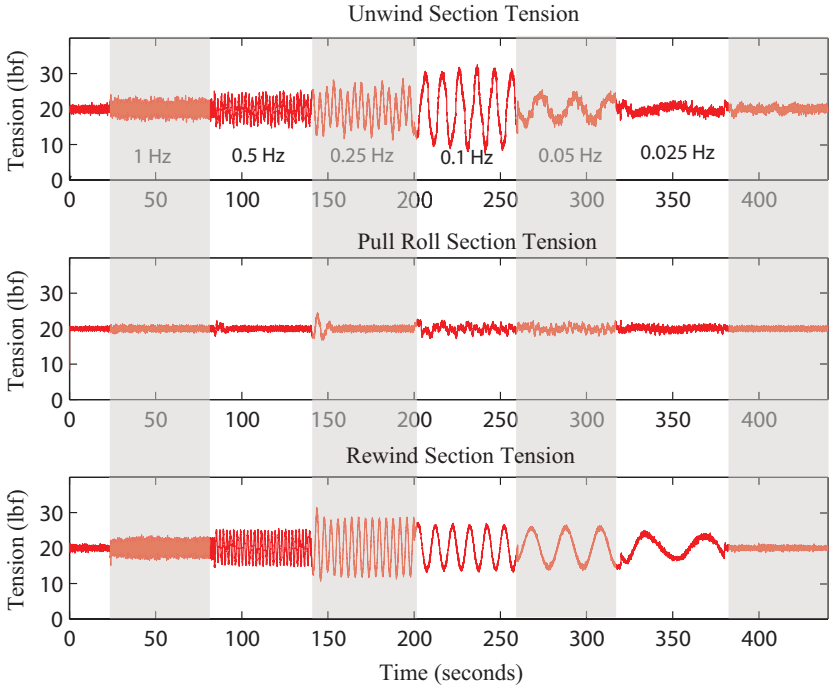

Figure 5.8: Interaction in the experimental platform with pre-filter and feedforward action obtained by upstream zone tension feedback; tension measurement at the unwind, pull roll and rewind section.

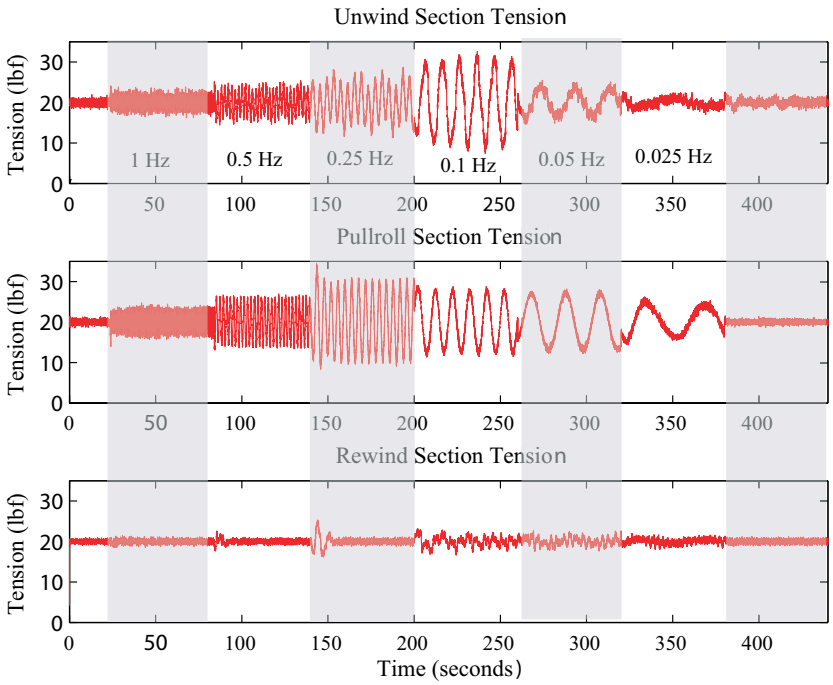

Figure 5.9: Interaction in the experimental platform with pre-filter and feedforward action obtained by downstream zone tension feedback; tension measurement at the unwind, pull roll and rewind section.

CHAPTER 6

Summary and Future Work

Design and analysis of efficient feedback and feedforward control strategies for controlling web speed and tension was the focus of the research presented in the report. A key objective of the research was also to select those control algorithms that are easy to implement on commercial real-time hardware, provide significant improvement in web speed and tension regulation performance, and provide the ability to minimize propagation of disturbances. Typical control algorithms for web tension regulation are described in Chapter 1 together with a discussion of various design strategies that were developed in this research.

Fixed gain PI control schemes are often employed in industrial R2R systems which typically do not provide adequate performance in the presence of plant uncertainties and changes in process parameters, for example, changes in web material or web speed. A model reference adaptive control scheme has been known to provide good performance under a wide variety of plant and process uncertainties. However, the implementation of an MRAC for the full system dynamic model is often cumbersome from an implementation point of view as many parameters are estimated. Utilizing the tools of the MRAC scheme, this dissertation focused on the design of a model reference adaptive PI (MRA-PI) control schemes for web tension regulation which is discussed in Chapter 2. The MRA-PI control scheme is simple in design and implementation since it requires estimation of only two parameters, the proportional and integral gains of the controller. The tuning effort required for obtaining the

gains of the fixed gain PI controller are considerably reduced by using the proposed MRA-PI controller. The parametric space for the two estimated gains in the MRA-PI scheme can be obtained by requiring the closed-loop system to be stable; initial parameter estimate values are chosen to satisfy the stability constraints.

Another adaptive PI control scheme based on an automatic initialization technique is designed in the second part of Chapter 2. Relay feedback technique is used for automatic initialization via determination of the ultimate frequency of the plant. The ultimate frequency is estimated using the relay feedback technique and then used to initialize the two adaptive PI controller parameter estimates. The ultimate frequency is further estimated online to account for changes in the plant parameters. Based on these estimations, the adaptive PI estimates are updated automatically. The advantage of the adaptive PI over conventional fixed gain PI is that it does not require knowledge of plant parameters and extensive tuning.

The problem of regulating the roll speed when the roll is connected to the motor shaft via a compliant mechanical transmission system was considered in Chapter 3. Since both web speed and tension are coupled, precise regulation of roll speed improves tension regulation performance. This problem is important in many industries where such transmission systems are employed, and practicing engineers often grapple with the question of which strategy is better, that is, either use motor speed feedback or roll speed feedback to regulate the roll speed. This problem was investigated in Chapter 3 via singular perturbation analysis and the associated small parameter is selected as the square of the inverse of the coefficient of compliance in the transmission. It is shown that pure load speed feedback is not stable and must be avoided. To directly control the load speed, we have also considered a stable scheme that utilizes both motor and load speed feedback. Since the feedback control action is not sufficient to reject periodic load disturbances, we have also considered a suit-

able adaptive feedforward algorithm that utilizes estimation of the disturbance and provides compensation to reject the disturbance. Experiments were conducted on an industrial grade transmission system to evaluate the control schemes and compare their performance. Although we have used only belt compliance as the compliant element in the transmission system, torsional compliance due to long shafts can also be included and the analysis conclusions will remain the same. The scheme is also applied for web transport and simultaneous regulation of roll speed and web tension. The scheme provides desired web tension performance by rejecting disturbances in the rewind section.

In Chapter 4, we have considered a solution to the nonlinear servomechanism problem and its successful application to the regulation of web tension in R2R manufacturing systems. The existing methods require the solution of a constrained partial differential equation, such as the one given in [47]. This method circumvents the need to solve a constrained partial differential equation. The method of solving a system of differential algebraic equations numerically provides a simple and implementable alternative that is quite attractive for R2R manufacturing. Although the solution to the system of differential algebraic systems might not be unique, from an engineering point of view, any solution which could get the desired output is all that is needed. We have corroborated the method by conducting a variety of experiments on the R2R experimental platform with different web materials and different web speeds. The output regulator was effective in rejecting periodic disturbances in tension. The output regulator also provides robust performance in terms of rejecting multiple frequency components. Further, when web tension measurement is noisy or it is not possible to obtain tension measurement, a simple web tension observer is also designed and shown to provide satisfactory results.

The use of feedforward control action along with interaction minimizing filters is

proposed with feedback from downstream tension zone in Chapter 5. The proposed strategy was able to minimize the interaction as well reduce disturbance propagation into downstream tension zones.

The work in this discussion focused on analysis and design of feedback and feedforward control schemes for web tension regulation in R2R manufacturing systems. The following topics provide opportunities for expanding this work in the future:

- In the tension output regulator problem, the feedback action is based on fixed gains in the controller and adaptive gains for feedforward action that estimates disturbances. Adaptation of gains that are used in both feedback and feedforward actions which generates a stable closed-loop system may provide improved results and can be considered as part of the future work.

- The tension output regulator was designed for each subsystem of the roll-to-roll system by considering each subsystem as a single input single output nonlinear system. Extending the approach to multivariable system employing decentralized controllers is an important generalization and can be considered as a part of the future work.

- The strategies discussed in the dissertation considered webs that are elastic and with large modulus. Application of this work to low modulus webs that are typically transported with large strains in the nonlinear regions of the stress strain curve would be very useful as many consumer products are currently being made with very thin materials.

- An important primitive element in almost all continuous R2R systems is the accumulator or the festoon. The strategies developed in this work can be extended to unwinds and rewinds that employ a festoon.

BIBLIOGRAPHY

[1] D. P. Campbell, *Dynamic Behavior of the Production Process, Process Dynamics*. John Wiley and Sons Inc., New York, first ed., 1958.

[2] D. King, "The mathematical model of a newspaper press," *Newspaper Techniques*, pp. 3–7, December 1969.

[3] G. Brandenberg, "New mathematical models for web tension and register error," *International IFAC Conference on Instrumentation and Automation in the Paper Rubber and Plastics Industry*, vol. 1, pp. 411–438, December 1977.

[4] J. J. Shelton, "Dynamics of web tension control with velocity or torque control," *Proceedings of the American Control Conference*, pp. 1423–1427, June 1986.

[5] G. E. Young and K. N. Reid, "Lateral and longitudinal dynamic behavior and control of moving webs," *ASME Journal of Dynamics Systems, Measurement, and Control*, vol. 115, pp. 309–317, June 1993.

[6] P. R. Pagilla, N. B. Siraskar, and R. V. Dwivedula, "Decentralized control of web proceesing lines," *IEEE Transactions on Control Systems Technology*, vol. 15, pp. 106–117, January 2007.

[7] W. Wolfermann, "Tension control of webs, a review of the problems and solutions in the present and future," *Proceedings of the Third International conference on Web Handling*, pp. 198–229, June 1995.

[8] D. Schroder and W. Wolfermann, "Application of decoupling and state space control in processing machines with continuous moving webs," *Proceedings International federation of Automatic Control*, pp. 198–229, June 1987.

[9] K. Shin, *Distributed control of tension in multi-span web transport systems*. PhD thesis, Oklahoma State University, Stillwater, May 1991.

[10] K. J. Astrom and B. Wittenmark, *Adaptive control*. Pearson Education Inc., 2nd ed., 2003.

[11] P. Ioannou, "Decentralized adaptive control of interconnected systems," *IEEE Transactions on Automatic Control*, vol. AC-31, pp. 291–298, April 1986.

[12] P. R. Raul, "Frequency repsonse of web systems containing load cells and dancers, dimensional analysis, and model reference adaptive schemes for tension control," Master's thesis, Mechanical and Aerospace Engineering, Oklahoma State University, July 2010.

[13] H. Koc, D. Knittel, M. Mathelin, and G. Abba, "Modeling and robust control of winding systems for elastic webs," *IEEE Transactions on Control Systems Ttechnology*, vol. 10, pp. 197–208, March 2002.

[14] W. Liu and E. J. Davison, "Servomechanism controller design of web handling systems," *IEEE Transactions on Control Systems Technology*, vol. 11, pp. 555 – 564, July 2003.

[15] P. R. Pagilla, K. N. Reid, and J. Newton, "Modeling of laminated webs," *Proceedings of the ninth International Conference on Web Handling*, vol. 9, June 2007.

[16] P. R. Pagilla, R. V. Dwivedula, and N. B. Siraskar, "A decentralized model reference adaptive controller for large-scale systems," *IEEE/ASME Transactions on Mechatronics*, vol. 12, pp. 154–163, April 2007.

[17] C. Branca, P. R. Pagilla, and K. N. Reid, "Governing equations for web tension and web velocity in the presence of non-ideal rollers," vol. 135, January 2013.

[18] B. T. Boulter and Z. Gao, "A real-time self tuning web tension regulation scheme," *Real-time Systems*, vol. 11, pp. 265–287, 1996.

[19] D. Knittel, E. Laroche, D. Gigan, and H. Koc, "Tension control for winding systems with two degrees of freedom h_∞ controller," *IEEE Transactions on Control System Technology*, vol. 39, no. 1, pp. 113–120, 2003.

[20] H. Noura, D. Sauter, F. Hamelin, and D. Theilliol, "Fault-tolerant control in dynamic systems: Application to a winding machine," *IEEE Control Systems Magazine*, vol. 20, pp. 33–49, February 2000.

[21] P. R. Pagilla, E. O. King, L. H. Dreinhoefer, and S. S. Garimella, "Robust observer-based control of an aluminum strip processing line," *IEEE Transactions on Industry Applications*, vol. 36, pp. 865–870, May 2000.

[22] D. Kuhm, D. Knittel, and M. A. Bueno, "Robust control strategies for an electic motor driven accumulator with elastic webs," *ISA Transactions*, vol. 51, pp. 732–742, November 2012.

[23] K. J. Astrom and T. Hagglund, "Automatic tuning of simple regulators with specifications on phase and amplitude margins," *Automatica*, vol. 20, no. 5, pp. 645–651, 1984.

[24] K. J. Astrom and T. Hagglund, "Automatic tuning of PID controllers," *Instrument Society of America*, NC, USA, 1988.

[25] T. Hagglund and K. J. Astrom, "Industrial adaptive controllers based on frequency response techniques," *Automatica*, vol. 27, no. 4, pp. 599–609, 1991.

[26] M. Lundh and K. J. Astrom, "Automatic initialization of a robust self-tuning controller," *Automatica*, vol. 11, pp. 1649–1662, 1994.

[27] T. Hagglund and A. Tengvall, "An automatic tuning procedure for unsymetrical processes," *Internal report, Department of Automatic control, Lund Institute of technology*, Lund, Sweden, 1994.

[28] K. J. Astrom and T. Hagglund, "A new auto-tuning design," *IFAC Int. Synmposium on adaptive control of chemical processes*, pp. 141–146, Lyngby, Denmark, 1988.

[29] J. Yang, C. S. Chen, and Y. Xu, "Automatic tuning of phase-lead and phase-lag compensator," *Int. J. control*, vol. 60, no. 4, pp. 631–640, 1994.

[30] W. Li, E. Eskinat, and W. L. Luybeb, "An improved autotune identification method," *Ind. Eng. Chem. Res.*, vol. 30, pp. 1530–1541, 1991.

[31] R. C. Chiang, S. H. Shen, and C. C. Yu, "Derivation of transfer function from relay feedback systems," *Ind. Eng. Chem. Res.*, vol. 31, pp. 855–860, 1992.

[32] Z. J. Palmor and M. Blau, "An autotuner for smith dead-time compensator," *Int. J. Control*, vol. 60, no. 1, pp. 117–135, 1994.

[33] K. J. Astrom, J. J. Anton, and K. E. Arzen, "Expert control," *Automatica*, vol. 22, no. 3, pp. 227–286, 1986.

[34] J. Balchen and B. Lie, "An adaptive controller based upon continuous estimation of the closed loop frequency response," *Journal of Modeling, Identification and Control*, vol. 8, no. 4, pp. 223–240, 1987.

[35] Y. Hori, H. Iseki, and K. Sigiura, "Basic consideration of vibration supression and disturbance rejection control of multi-inertia system using state feedback and load acceleration control," *IEEE Transactions on Industry Applications*, vol. 30 (4), 1994.

[36] R. V. Dwivedula, *Modeling the effects of belt compliance, backlash, and slip on web tension and new methods for decentralized control of web processing lines.* PhD thesis, Oklahoma State University, Stillwater, December 2005.

[37] G. Bradenburg, H. Unger, and A. Wagenpfeil, "Stability problems of a speed controlled drive in an elastic sysetm with backlash and corrctive measures by a load observer," in *Proc. Int. Conf. on Electrical Machines*, (Munich, Germany), pp. 523–527, 1986.

[38] G. Bradenburg and U. Schafer, "Design and performance of different types of observers for industrial speed and position controlled electromechanical systems," in *Proc. Int. Conf. of Electrical Drives and Power Electronics*, (Slovakia), pp. 1–10, 1990.

[39] E. A. Freeman, "The stabilization of control systems with backlash using a high-frequency on-off loop," *The institute of Electrical Engineers*, vol. 356 M, pp. 150–157, Feb. 1960.

[40] M. EI-Sharkawi and Y. Guo, "Adative fuzzy control of a belt-driven precision positioning table," in *In Proceedings of the IEEE International Electric Machines and Drives Conference*, vol. 3, pp. 1504–1506, June 2003.

[41] A. Hace, K. Jezernik, and M. Terbuc, "Robust motion control algorithm for belt-driven servomechanism," in *In Proceedings of the IEEE International Symposium on Industrial Electronics*, (Bled, Slovenia), pp. 893–898, 1999.

[42] Y. S. Lee and K. C. Hsu, "Shaft torsional oscillation of induction machine including saturation and hysteresis of magnetizing branch with an inertia load," in *In Proceedings of International Conference on Energy, Management and Power Delivery*, vol. 1, pp. 134–139, November 1995.

[43] S. P. Bhattacharyya and J. B. Pearson, "On the linear servomechanism problem," *International Journal of Control*, vol. 12, no. 5, pp. 795–806, 1970.

[44] B. A. Francis and W. M. Wonham, "The internal model principle of control theroy," *Automatica*, vol. 12, pp. 457–465, 1976.

[45] B. A. Francis, "The linear multivariable regulator problem," *SIAM Journal of Control and Optimization*, vol. 15, pp. 486–505, May 1977.

[46] H. W. Smith and E. J. Davison, "Design of industrial regulators: Integral feedback and feedforward control," *Proceedings of IEE*, vol. 119, pp. 1210–1216, August 1972.

[47] A. Isidori and C. I. Byrnes, "Output regulation of nonlinear systems," *IEEE Transactions on Automatic Control*, vol. 35, pp. 131–140, February 1990.

[48] J. Huang and J. Rugh, "An approximation method for the nonlinear servomechanism problem," *IEEE Transactions on Automatic Control*, vol. 37, pp. 1395–1398, September 1992.

[49] S. Devasia and B. Paden, "Nonlinear inversion-based output tracking," *IEEE Transactions on Automatic Control*, vol. 41, pp. 930–942, July 1996.

[50] S. Gopalswamy and J. K. Hedrick, "Tracking nonlinear non-minimum phase systems using sliding control," *International Journal of Control*, vol. 57, pp. 1141–1158, May 1993.

[51] D. V. Wissel, *DAE control of dynamical systems: Example of a riderless bicycle*. PhD thesis, Ecole Des Mines De Paris, 1996.

[52] S. Darbha, K. Nakshatrala, and K. R. Rajagopal, "On the vibrations of lumped parameter systems governed by differential-algebraic equations," *Journal of Franklin Institute*, vol. 347, pp. 87–101, February 2010.

[53] S. G. Manyam, S. Darbha, and K. R. Rajagopal, "Output regulation of a class of nonlinear systems using differential-algebraic equations," in *Proceedings of the ASME 2012 5th Annual Dynamic Systems and Control Conference*, vol. 2, (Fort Lauderdale, FL), October 2012.

[54] Y. Zhang and J. Wang, "Recurrent neural networks for nonlinear output regulation," *Automatica*, vol. 37, pp. 1161 – 1173, 2001.

[55] J. Carr, *Applications of Centre Manifold Theory*. Springer New York, 1981.

[56] M. Bando and A. Ichikawa, "Adaptive output regulation of nonlinear systems described by multiple linear models," in *Proceedings of the 9th IFAC Workshop on Adaptation and Learning in Control and Signal Processing*, vol. 9, (Imperial Anichkov Palace, Russia), 2007.

[57] H. W. Smith and E. J. Davison, "Design of industrial regulators: Integral feedback and feedforward control," *Proceedings of IEE*, vol. 119 (8), pp. 1210–1216, August 1972.

[58] A. Seshadri, P. R. Raul, and P. R. Pagilla, "Analysis and minimization of interaction in decentrlaized control systems with applicaiton to roll-to-roll manufacturing," *IEEE Transactions on Control Systems Technology*, vol. 22, pp. 520–530, March 2014.

[59] M. Bodson, "Rejection of periodic disturbances of unknown and time-varying frequency," *International Journal of Adaptive Control and Signal Processing*, vol. 19, pp. 67–88, 2005.

[60] P. Kokotovic, H. K. Khalil, and J. O'Reilly, *Singular Perturbation Methods in Control: Analysis and Design*. Society for Industrial and Applied Mathematics edition, Academic Press, London, first ed., 1986.

[61] S. Dubowsky and F. Freudenstein, "Dynamic analysis of mechanical systems with clearance: Part 1: Formulation of dynamic model," *ASME Journal of Engineering for Industry*, vol. 93, pp. 305–309, February 1971.

[62] S. Sastry and M. Bodson, *Adaptive Control: Stability, Convergence and Robustness*. Prentice-Hall Information and System Sciences Series, Prentice Hall, Englewood Cliffs, N.J., first ed., 1989.

[63] P. R. Raul, S. G. Manyam, P. R. Pagilla, and S. Darbha, "Output regulation of nonlinear systems with application to roll-to-roll manufacturing systems," *IEEE/ASME Transactions on Mechatronics, November, 2014*.

[64] C. D. Meyer, "Matrix analysis and applied linear algebra," *Society of Industrial and Applied Mathematics*, 2000.

[65] P. Grosdidier and M. Morari, "Interaction measures for systems under decentralized control," *Automatica*, vol. 22, no. 3, pp. 309–320, 1986.

[66] K. N. Reid and K. C. Lin, "Control of longitudinal tension in multi-span web transport systems during start-up and shut-down," *Proceedings of the Second International Conference on web handling*, pp. 77–95, June 1993.

[67] Y. Diao, "Resonant frequencies in web lines and filtering of web tension," Master's thesis, Mechanical and Aerospace Engineering, Oklahoma State University, December 2008.

[68] P. R. Pagilla and Y. Diao, "Resonant frequencies in web process lines due to idle rollers and spans," *ASME Journal of Dynamic Systems, Measurement and Control*, vol. 133, November 2011.

[69] J. J. Shelton, "Limitations to sensing of web tension by means of roller reaction forces," *in proceedings of the Fifth International Conference on Web handling*, June 1999.

[70] P. R. Pagilla, S. S. Garimella, L. H. Dreinhoefer, and E. O. King, "Dynamics and control of accumulators in continuous strip processing lines," *IEEE Transactions on Industry Applications*, vol. 37, pp. 934–940, June 2001.

[71] D. Knittel, "Robust control design using H_∞ methods in large scale web handling systems," *7th International Conference on Web Handling*, pp. 3–11, Stillwater, OK, USA, 2003.

[72] H. Koc, D. Knittel, M. de Mathelin, and G. Abba, "Modeling and robust control of winding systems for elastic webs," *IEEE Transactions on Control System Technology*, vol. 10, no. 2, pp. 197–208, 2002.

[73] D. Knittel, D. Gigan, and E. Laroche, "Robust decentrlized overlapping control of large scale winding systems," *Proceedings of the American Control Conference*, pp. 1805–1810, may 2002.

[74] P. R. Pagilla, R. V. Dwivedula, and N. B. Siraskar, "A decentralized model reference adaptive controller for large-scale systems," *IEEE Transactions on Mechatronics*, vol. 12, pp. 154–163, April 2007.

[75] R. V. Monopoli, "Model reference adaptive control with an augmented error signal," *IEEE transactions on automatic control*, vol. 19, pp. 474–484, 1974.

[76] A. Feuer and A. S. Morse, "Adaptive control of single-input, single-output linear systems," *IEEE transactions on automatic control*, vol. 23, pp. 557–569, 1978.

[77] M. Aoki, "On feedback stabilizability of decentralized dynamics system," *Automatica, Pergamon press*, vol. 8, pp. 163–173, June 1972.

[78] D. D. Siljak, *Large-scale dynamic systems*. JElsevier North-Holland,Inc., 1978.

[79] D. T. Gavel and D. D. Siljak, "Decentralized adaptive control: Structural conditions for stability," *IEEE Transactions on Automatic Control*, vol. 34, pp. 413–426, April 1989.

[80] K. S. Narendra and N. O. Oleng, "Exact output tracking in decentralized adaptive control systems," *IEEE Transactions on Automatic Control*, vol. 47, pp. 390–395, February 2002.

[81] K. S. Narendra, *Stable adaptive systems*. Englewood cliffs, N.J., 1989.

[82] S. Manyam, S. Darbha, and K. R. Rajagopal, "An adaptive controller based upon continuous estimation of the closed loop frequency response," *Fifth Annual*

Dynamic Systems and Control Conference, Ft. Lauderdale, FL, USA, October 2012.

[83] A. Isidori and C. Byrnes, "Output regulation of nonlinear systems," *IEEE Transactions on Automatic Control*, vol. 35, February 1990.

[84] B. A. Francis, "The linear multivariable regulator problem," *SIAM Journal on Control Optimization*, vol. 15, pp. 486–505, 1977.

[85] B. A. Francis and W. M. Wonham, "The internal model principle for linear multivariable regulators," *Journal on Applied Mathematics Optimization*, vol. 2, pp. 170–194, 1975.

[86] J. S. A. Hepburn and W. M. Wonham, "Error feedback and internal models on differentiable manifolds," *IEEE Transaction on Automation Control*, vol. AC-29, pp. 397–403, 1984.

[87] H. Frahm, "Device for damping vibrations of bodies, us patent 989958," 1911.

[88] J. Huang, *Nonlinear Output Regulation: Theory and Applications*. Advances in Design and Control, SIAM, Philadelphia, first ed., 2004.

[89] L. Liu, Z. Chen, and J. Huang, "Parameter convergence and minimal internal model with an adaptive output regulation problem," *Automatica*, vol. 45, no. 5, pp. 1306 – 1311, 2009.

[90] J. Huang, "Asymptotic tracking and disturbance rejection in uncertain nonlinear systems," *IEEE Transactions on Automatic Control*, vol. 40, pp. 1118 – 1122, 1995.

[91] M. Bodson, A. Sacks, and P. Khosla, "Harmonic generation in adaptive feedforward cancellation schemes," *IEEE Transactions on Automatic Control*, vol. 39 (9), September 1994.

[92] M. Nordin and P. O. Gutman, "Controlling mechanical systems with backlash-a survey," *Automatica*, vol. 38 (10), pp. 1633–1649, 2002.

[93] M. A. Mohan, "A new compensation technique for backlash in position control systems with elasticity," in *39th Southeastern Symposium on System Theory*, (Macon, GA), March 2007.

[94] R. Boneh and O. Yaniv, "Reduction of limit cycle amplitude in the presensce of backlash," *Journal of dynamci systems, measurement and control*, vol. 12 (2), pp. 278–284, 1999.

[95] M. Nordin and P. O. Gutman, "Digital qft-design for the benchmark problem," *European Journal of Control*, vol. 1 (2), pp. 97–103, 1996.

[96] C. Lin, T. Yu, and X. Feng, "Fuzzy control of a nonlinear pointing testbed with backalsh and friction," in *In Proceedings of the 35th Conference on Decision and Control*, (Kobe, Japan), pp. 4363–4368, December 1996.

[97] D. Chen and B. Paden, "Nonlinear adative torque-ripple cancellation for step motors," in *In Proceedings of the 29th IEEE Conference on Decision and Control*, vol. 6, pp. 3319–3324, December 1990.

[98] D. G. Luenberger, "An introduction to observer," *IEEE Transactions on Automatic Control*, vol. AC-16 (6), December 1971.

APPENDIX A

Speed Correction Based Simultaneous Motor and Load Speed Feedback Control Scheme-appendix

The control scheme that utilizes both motor and load speed feedback discussed in Section 3.4 considers the output of the load speed and motor speed controllers as torque correction. There is also another control scheme that is employed in practice where the outer load speed loop provides a speed reference correction to the inner motor speed which is shown in Fig. A.1. In the following we show that such a control scheme results in an unstable system, and thus must be avoided. For this analysis, we employ a simple proportional control action for the load speed controller and a PI controller for the motor speed loop. The closed-loop transfer function from ω_{rL} to

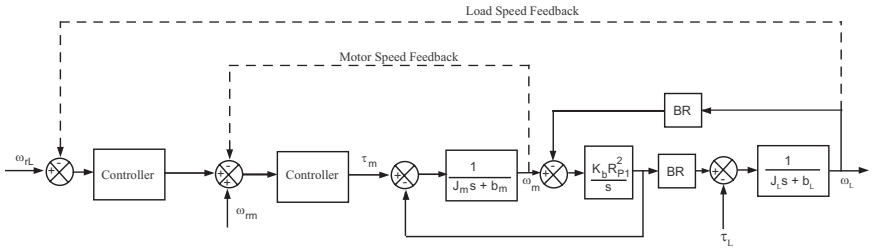

Figure A.1: Simultaneous motor and load speed feedback scheme: Speed mode

ω_L for this strategy is obtained as

$$\frac{\omega_L(s)}{\omega_{rL}(s)} = \frac{(G_R R_{P1} R_{P2} K_b / J_m J_L)\alpha_{mLs}}{\psi_{mLs}(s)} \tag{A.1}$$

where

$$\alpha_{mLs}(s) = K_{pm} K_{pL} s + K_{im} K_{pL} \tag{A.2}$$

$$
\begin{aligned}
\psi_{mLs}(s) &= s^4 + e_3 s^3 + e_2 s^2 + e_1 s + e_0, \\
e_3 &= \frac{(b_m J_L + J_m b_L + J_L K_{pm})}{J_m J_L}, \\
e_2 &= \frac{(K_b J_{eq} + b_m b_L + b_L K_{pm} + J_L K_{im})}{J_m J_L}, \\
e_1 &= \frac{(K_b b_{eq} + G_R^2 R_{P2}^2 K_b K_{pm} + b_L K_{im})}{J_m J_L} \\
&\quad + \frac{(G_R R_{P1} R_{P2} K_b K_{pm} K_{pL})}{J_m J_L}, \\
e_0 &= \frac{(G_R^2 R_{P2}^2 K_b K_{im} + G_R R_{P1} R_{P2} K_b K_{im} K_{pL})}{J_m J_L}.
\end{aligned}
\tag{A.3}
$$

Singular perturbation analysis results in the following slow and fast characteristic polynomials:

$$\psi_{ls}(s, \varepsilon) \approx s^2 + \delta_1 s + \delta_0 \tag{A.4a}$$

$$\psi_{lf}(p, \varepsilon) \approx p^2 - \delta_1' p + \delta_0' \tag{A.4b}$$

where

$$
\begin{aligned}
\delta_1 &= \frac{G_R^2 R_{P2}^2 b_m + R_{P1}^2 b_L + G_R^2 R_{P2}^2 K_{pm} + (G_R^2 R_{P2}^2 / R_{P1}) K_{pm} K_{pL}}{G_R^2 R_{P2}^2 J_m + R_{P1}^2 J_L} \\
\delta_0 &= \frac{G_R^2 R_{P2}^2 K_{im} + (G_R^2 R_{P2}^2 / R_{P1}) K_{im} K_{pL}}{G_R^2 R_{P2}^2 J_m + R_{P1}^2 J_L} \\
\delta_1' &= \frac{G_R^2 R_{P2}^2 b_m + R_{P1}^2 b_L + G_R^2 R_{P2}^2 K_{pL} K_{pm} + G_R^2 R_{P2}^2 K_{pm} (J_L / J_m)}{G_R^2 R_{P2}^2 J_m + R_{P1}^2 J_L} \varepsilon, \\
\delta_0' &= \frac{G_R^2 R_{P2}^2 J_L + R_{P1}^2 J_m}{J_m J_L}.
\end{aligned}
\tag{A.5}
$$

Note that the slow subsystem is stable for all K_{pm}, K_{im}, and K_{pL}. However, the fast subsystem is unstable for all $K_{pL} > 0$. The instability of the system is also evident from simple root locus analysis of the closed-loop characteristic with varying K_{pL}, which is shown in Figure A.2.

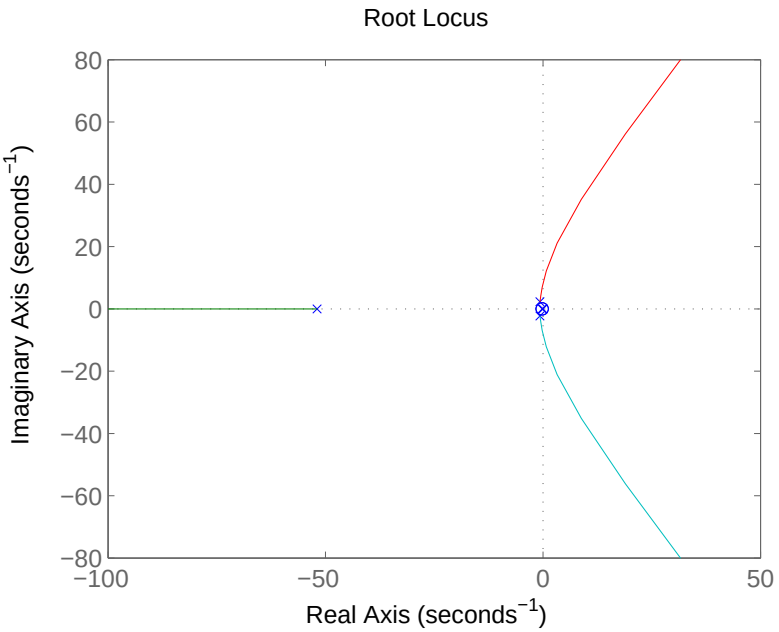

Figure A.2: Root locus plot with varying K_{pL} in speed mode

VITA

Pramod R. Raul

Candidate for the Degree of

Doctor of Philosophy

Thesis: DESIGN AND ANALYSIS OF FEEDBACK AND FEEDFORWARD CONTROL SYSTEMS FOR WEB TENSION IN ROLL-TO-ROLL MANUFACTURING

Major Field: Mechanical and Aerospace Engineering

Biographical:

Education:

Completed the requirements for the Doctor of Philosophy degree with a major in Mechanical and Aerospace Engineering at Oklahoma State University in May, 2015.

Received the M.S. degree from Oklahoma State University, Stillwater, Oklahoma, USA, 2010, in Mechanical and Aerospace Engineering.

Received the B.E. degree from Government College of Engineering, Pune, Maharashtra, India, in 2002, in Mechanical Engineering.

Experience:

Research Assistant at Oklahoma State University from January 2008-Present.

Apprentice Engineering Trainee at Mahindra & Mahindra Ltd., Nashik, India from June 2002 to August 2003.

Assistant Manager at Tata Motors Ltd., Pune, India from December 2003 to June 2007.